Charles University

Faculty of Science

Molecular and Cellular Biology, Genetics and Virology

4XMGVP

Ing. Kristýna Poncová

The role of eIF3 and Rps3 in stop codon readthrough

Úloha eIF3 a Rps3 v pročítání stop kodonu

Doctoral thesis

Supervisor: Mgr. Leoš Valášek, PhD.

Prague, 2020

Prohlášení:

Prohlašuji, že jsem závěrečnou práci zpracovala samostatně a že jsem uvedla všechny použité informační zdroje a literaturu. Tato práce ani její podstatná část nebyla předložena k získání jiného nebo stejného akademického titulu.

V Praze, 20.02.2020

Podpis

Acknowledgments

I would like to express my gratitude to my supervisor Leoš Valášek for letting me pursuit my Ph.D. studies in his laboratory and for his supervision and support over the years. I would also like to thank my colleagues, both past and present, from the team for a pleasant working environment and inspiring discussions, especially to Anička, the guardian angel of our lab, and to Slávka, my fellow bench neighbour for her patience, critical thinking and friendship that evolved during the years.

I extend my thanks to colleagues in the campus, with whom we share regular Friday seminars - Libor Krásný, David Staněk, and Petr Svoboda and their teams for valuable suggestions and stimulating environment.

My deepest thanks belong to my dear parents for their unconditional emotional and financial support during my long studies. I am also grateful to my partner and my close friends for being there for me anytime.

Thank you, everybody, for contributing to this work and for making me who I am now. I dedicate this Thesis to You.

ABSTRACT

Translation represents a highly regulated, interconnected process of protein synthesis in the cell. It could be divided into 4 phases: initiation, elongation, termination, and ribosomal recycling.

Our laboratory is involved in in-depth studies of a complex eukaryotic initiation factor 3 protein (eIF3). We are interested not only in revealing its molecular roles in the translational cycle in general but also in specific mechanisms that allow translational regulation according to specific cellular needs.

In the budding yeast, the eIF3 is composed of five essential subunits (a/Tif32, b/Prt1, c/Nip1, g/Tif35 and i/Tif34). In mammals, the protein is even more complex, comprising of 12 subunits (a-i, k-m).

eIF3 is a key player not only in translation initiation but also in ribosomal recycling and, surprisingly, in translation termination and stop codon readthrough as well. The latter process harbors important clinical potential, as approximately 1/3 of genetically inherited diseases is caused by the presence of a premature termination codon in the protein-coding region. Therefore, understanding the molecular mechanism underlying this phenomenon provides important tools for the targeted and less toxic drug development approaches needed for patient therapy.

In this Ph.D. Thesis, I uncovered the role of yeast small subunit ribosomal protein Rps3 in the control of stop codon recognition efficiency. I identified Rps3 residues involved in maintaining the termination fidelity and proved that eIF3 and Rps3 co-operate during the mechanism of the programmed stop codon readthrough. Precisely, I identified that the fine-tunning of the termination fidelity occurs by a minimum of three different contacts that the C-terminal domain of a/Tif32 subunit of eIF3 establishes with the Rps3 protein.

Additionally, I participated in two other eIF3-oriented projects in mammals. One dealt with the gene-specific mechanism of translational control called the reinitiation (REI) and its conservation between yeast and higher eukaryotes. We found out that the eIF3´s role in REI is indeed very well conserved, however, in mammals the eIF3h subunit is specifically involved instead of the a/Tif32 subunit, which has been demonstrated in yeast.

The second project focused on the fundamental role of mammalian eIF3 subunits in the 43S and 48S pre-initiation complex assembly. We proved the key role of the eIF3d

subunit in the recruitment of the 40S subunit to eIF3 and defined the roles of eIF3c, eIF3k and eIF3l subunits in the recruitment of the mRNA to the 43S pre-initiation complex.

As a whole, this Ph.D. Thesis extends the knowledge concerning the involvement of ribosomal proteins in translational control and reveals molecular details about translation stages influenced by eIF3 not only in yeast but also in mammalian cells.

ABSTRAKT

Translace představuje složitě regulovaný a vysoce provázaný proces výroby proteinů v buňce. Má několik základních fází-iniciaci, elongaci, terminaci a recyklaci ribosomů. Naše laboratoř se zabývá studiem multifaktoriálního komplexu eukaryotického iniciačního faktoru 3 (eIF3). Zajímá nás nejen odhalování jeho molekulárních rolí v průběhu translačního cyklu, ale také jeho úloha při specifických mechanismech, které se podílí na regulování translace v závislosti na buněčných potřebách.

eIF3 se skládá v kvasinkách z pěti esenciálních podjednotek (a/Tif32, b/Prt1, c/Nip1, g/Tif35 a i/Tif34). V savcích je jeho složení komplexnější s 12 podjednotkami (a-i, k-m).

eIF3 je klíčový hráč nejen v iniciaci translace, ale také ve fázi recyklace ribosomů a překvapivě i v translační terminaci a pročítání stop kodonu. Posledně zmiňovaný proces má velký klinický potenciál, jelikož téměř 1/3 geneticky podmíněných onemocnění je způsobena přítomností předčasného terminačního kodonu v protein kódující oblasti. Porozumění molekulárním detailům pročítání stop kodonu a translačně terminační mašinérie je důležité pro další vývoj selektivních a méně toxických léčiv vhodných k terapii. V této disertační práci jsem popsala jak protein malé ribosomální podjednotky Rps3 řídí efektivitu rozpoznávání stop kodonu. Identifikovala jsem konkrétní residua v Rps3 zodpovědná za udržení terminační přesnosti a prokázala jsem, že Rps3 ovlivňuje pročítání stop kodonu díky interakci s eIF3. Konktétně jsem prokázala, že k ovlivňování terminační fidelity jsou důležité minimálně tři různé kontakty, které vznikají mezi C-terminální doménou a/Tif32 podjednotky eIF3 a Rps3.

Navíc jsem se podílela na dvou projektech zaměřených na savčí eIF3. První projekt se zabýval genově specifickým mechanismem translační reiniciace a jeho konzervací mezi kvasinkami a vyššími eukaryoty. Zjistili jsme, že úloha eIF3 podporovat reiniciaci je zachována i v savčích buňkách, jen se na ni nepodílí a/Tif32 jako v kvasinkách, ale eIF3h podjednotka. Druhý projekt byl zaměřený na klíčovou a základní úlohu eukaryotického iniciačního faktoru 3- a to na zajištění správného složení 43S a 48S preiniciačního komplexu v savčích buňkách. Prokázali jsme důležitou úlohu eIF3d podjetnotky v rekrutaci 40S podjednotky k eIF3 a popsali jsme úlohu podjednotek eIF3c, eIF3k a eIF3l v rekrutaci mRNA k 43S preiniciačnímu komplexu.

Předkládaná disertační práce rozšiřuje znalosti o zapojení ribosomálních proteinů do translační regulace a dále odhaluje molekulární detaily translačních procesů ovlivňovaných eIF3 nejen v kvasinkách, ale i v savčích buňkách.

List of contents

List of abbreviations

5-FOA	5-fluoroorotic acid
18S NRD	18S non-functional rRNA decay pathway
aa	amino-acid
Å	Ångstrom, $1x10^{-10}$ m
A-site	aminoacyl tRNA binding site
Amp	ampicillin
Asc1	Absence of growth Suppressor of Cyp1; ribosomal protein of the 40S ribosomal subunit
Atf4	Activating transcription factor 4
β-ME	β-mercaptoethanol
BSA	bovine serum albumin
CTD	C-terminal domain
ddH_2O	double distilled water
dH_2O	distilled water
dsDNA	double-stranded DNA
E-site	exit site
E. coli	*Escherichia coli*
EDTA	ethylenediaminetetraacetic acid
eIF	eukaryotic initiation factor
es	expansion segment
ETS	external transcribed spacer
Gcn4	General control nonderepressible 4; an amino acid biosynthetic transcription factor
GDP	guanosine diphosphate
GST	glutathione S-transferase
GTP	guanosine triphosphate
h	helix
hc	high copy
HEPES	N-(2-hydroxyethyl) piperazine-N-2-ethan sulfonic acid
HLD	Hcr1 like domain
IGEPAL	(octyl phenoxy)polyethoxyethanol

ITS	internal transcribed spacer
Kan	kanamycin
KH	K-homology
LSU	large ribosomal subunit
NMD	nonsense-mediated decay
NTD	N-terminal domain
nts	nucleotides
m^7GpppN	7-methylguanosine cap
MDFF	Molecular dynamics flexible fitting
Met-$tRNA_i^{Met}$	initiator methionyl -tRNA
MFC	multi-factor complex
miRNA	micro RNA
mRNA	messenger RNA
nc tRNA	near cognate tRNA
NTC	normal termination codon
OD_{600}	optical density at 600 nm
P-site	peptidyl-tRNA binding site
PABP	poly-A binding protein
PBS	phosphate-buffered saline
PCI	Proteasome, COP9, Initiation factor 3
Pde2	phosphodiesterase 2
PEG	polyethylene glycol
Pi	inorganic phosphate
PIC	pre-initiation complex
PMSF	phenylmethylsulfonyl fluoride
pre-TC	pre-termination complex
PTC	premature termination codon
REI	reinitiation
RF	release factor
RP	ribosomal protein
RPE	reinitiation promoting elements
Rpg1	Required for passage through G1, a/Tif32 subunit of eIF3
RPL	ribosomal protein of the large subunit

RPS	ribosomal protein of the small subunit
RRM	RNA recognition motif
RT	readthrough
rti-tRNA	readthrough inducing tRNA
S	Svedberg
S. cerevisiae	*Saccharomyces cerevisiae*
SDS	sodium dodecyl sulfate
Slg^-	slow growth
sno-RNA	small nucleolar RNA
ssRNA	single stranded RNA
SSU	small ribosomal subunit
TBE	Tris-borate-EDTA
TBS	Tris-buffered saline
TC	ternary complex
TE	Tris-EDTA
TG	Tris-glycine
TMV	tobacco mosaic virus
Tris	Tris(hydroxymethyl)-aminomethane
UTR	untranslated region
Xrn1	exoribonuclease 1
YLC	Yeast-like core

List of publications

Poncová Kristýna, Wagner Susan, Jansen Myrte Esmeralda, Beznosková Petra, Gunišová Stanislava, Herrmannová Anna, Zeman Jakub, Dong Jinsheng, and Valášek Leoš S (2019) uS3/Rps3 controls fidelity of translation termination and programmed stop codon readthrough in co-operation with eIF3. *Nucleic Acids Res.* **47:** 11326–11343

This Thesis is based mainly upon my first-author paper. In this study, we analyzed the molecular mechanism that controls the efficiency of translational termination in yeast cells. Specifically, I described the involvement of two specific residues, the K108 and R116, of the small ribosomal subunit protein Rps3 in regulation of termination. Using dual-luciferase reporter system I demonstrated that mutations of these residues, (*rps3-K108E* and *rps3-R116D*) had opposite effects on the accuracy of stop codon recognition manifested as decrease or increase of stop codon readthrough, respectively. In addition, I revealed that the C-terminal domain of eIF3 subunit a/Tif32 plays a significant role in this process as a mutation of the region encompassing amino acid residues 955-964 (*box33* mutation) also decreased the frequency of stop codon readthrough. Combining these mutations either suppressed (*tif32-box33 – rps3- R116D*) or exacerbated (*tif32-box33 – rps3- K108E*) the readthrough phenotypes of individual single mutants, indicating for different types of genetic interactions. These observations I further supported by discovering a mutual web of interactions between the Rps3 and a/Tif32-CTD proteins *in vitro* with the help of GST-pull down experiments. Altogether, I identified 4 distinct binding sites between the interacting proteins, with three of them located within the a/Tif32-CTD region.

Furthermore, I described that Rps3-K108 affects the efficiency of termination in stop codon context-specific manner by promoting the incorporation of readthrough-inducing tRNAs and that this stimulatory effect on the readthrough requires proper conformation of the decoding center, as was proposed for eIF3 before, too.

In addition, the 80S re-sedimentation analysis revealed that the *rps3-R116D* mutation increases overall levels of eIF3 and termination factors in the terminating ribosomes, whereas the *rps3-K108E* mutation has the opposite effect. These results strongly suggest that Rps3 and eIF3 closely co-operate together to control translation termination and stop codon readthrough and a possible molecular mechanism is proposed.

Hronová Vladislava, Mohammad Mahabub P, Wagner Susan, Pánek Josef, Gunišová Stanislava, Zeman Jakub, **Poncová Kristýna**, and Valášek Leoš S (2017) Does eIF3 promote reinitiation after translation of short upstream ORFs also in mammalian cells? *RNA Biol.* **14:** 1660–1667

In this Point of View article, we broaden our current knowledge of translational reinitiation in mammalian cells using *ATF4* mRNA as a model. Strikingly, similarities were found with yeast *GCN4* mRNA regulation. Both mRNAs contain REI-permissive uORF1 and *cis*-acting sequence determinants of its activity were found to be conserved, specifically the 5' triple-circle hairpin and a 3' stem-loop of *ATF4* resemble similar structures of *GCN4*-RPEs ii. and iv. Furthermore, the role of eIF3 in promoting reinitiation appears to be also conserved between yeast and humans although different subunits were found to be responsible for this effect: in mammals eIF3h subunit and in yeast a/Tif32 subunit. This difference probably reflects the more complex nature of mammalian eIF3 compared to the yeast factor. I contributed to manuscript preparations of this Point of View article.

Herrmannová Anna, Prilepskaja Terezie, Wagner Susan, Šikrová Darina, Zeman Jakub, **Poncová Kristýna**, and Valášek Leoš S (2019) Adapted formaldehyde gradient cross-linking protocol implicates human eIF3d and eIF3c, k and l subunits in the 43S and 48S pre-initiation complex assembly, respectively. *Nucleic Acids Res.* **48:** 1969-1984

In this study, we optimized our previously established formaldehyde crosslinking protocol to one more suitable for translational studies in mammalian cells by allowing more efficient cell lysis and reducing the heterogeneity of the cross-linked material among samples. In the new protocol, the formaldehyde cross-linking is occurring directly in the sucrose gradient by using gradually increasing formaldehyde concentration whereas before, the cells were cross-linked before lysis in the dish. This way, a more accurate reflection of the differences in the composition of the 43S and 48S pre-initiation compexes in knockdowns of various eIF3 subunits is achieved.

We found that both, eIF3g and eIF3i subunits, are dispensable for assembly of pre-initiation complexes and that the roles of eIF3k and eIF3l proteins are also only minor in this process. On the other hand, the a-c-e subunits were identified as a major binding force of eIF3 to the 40S. In addition, the eIF3d subunit was revealed to act as an important intermolecular bridge between the eIF3 and the 40S, also with a role in promoting 43S PIC

assembly. Interestingly, the eIF3c was identified as a new factor stimulating mRNA recruitment to the 43S PICs. In this study, apart from being involved in manuscript preparations, I purified GST-tagged proteins and performed GST-pull down experiments to monitor *in vitro* interactions between investigated eIF3 subunits.

Introduction

Gene expression, the process of transformation of genetic information encoded in the DNA to mRNA and then to proteins, represents the central dogma of molecular biology and was postulated almost 62 years ago by Francis Crick (Crick, 1958).

Each step of this process from transcription (DNA->RNA), RNA processing to translation (mRNA->protein) is tightly regulated. In order to survive and thrive, cells need to adapt rapidly to changing environmental conditions. Compared to transcription and RNA processing, translational control of already existing mRNAs represents the fastest way to alter gene expression thus providing the immediate response.

To make a protein, a concerted effort of several factors is needed. Those include: the mRNAs, the tRNAs, various initiation, elongation, termination and recycling factors, and, importantly, the ribosome.

Literary review

1. Eukaryotic ribosome

One of the first hints about the existence of those ribonuclear particles came in the middle of the last century, roughly in 1955 when so-called Pallade particles were observed (Palade, 1955). The name ribosome was then first used in the 1958 meeting of Biophysical society at the Massachusetts Institute of Technology in Boston by Richard B.Roberts. However, it took almost another half a century until the first high-resolution structure of the ribosome emerged (Schluenzen et al., 2000) and this effort was honored in 2009 by awarding a Nobel prize to three researchers essentially involved: Venkatraman Ramakrishnan, Thomas A. Steitz, and Ada E. Yonath.

Since then extensive research into the nature of those highly complex, asymmetric molecular machines took place. Although amazing progress has been made in the field, the ribosome still has not revealed all of its secrets and there is certainly still room for further fascinating discoveries. Eukaryotic ribosomes consist of two subunits, small ribosomal subunit (the 40S, SSU) and large subunit (60S, LSU), together forming a complete 80S ribosome (**Figure 1**); (S stands for Svedberg, unit of the velocity of sedimentation, $1S=10^{-13}s$) (Chao and Schachman, 1956). The reason why the Svedberg units are not additive (e.g

40S with 60S adds up to 80S) is that the sedimentation coefficient is counted as the molecular weight of the particle normalized to its friction coefficient - it depends also on the shape of the particle.

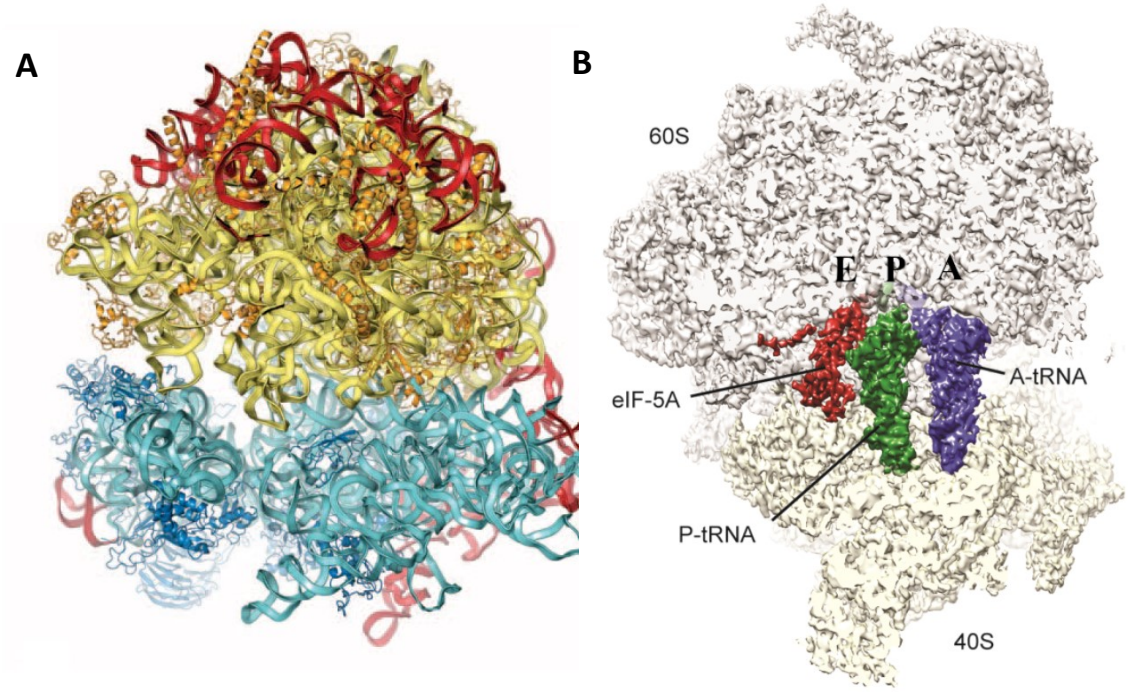

Figure 1 Schematic structure of yeast 80S ribosome. (A) Proteins and rRNA in the 40S are colored dark and light blue, respectively, and dark and pale yellow, respectively, in the 60S subunit. Expansion segments new to eukaryotes are in red. Adapted from Adam Ben-Shem et al., (2010)**. (B) Yeast 80S ribosome with highlighted A- (amino-acyl), P- (peptidyl), E- (exit) sites.** Binding of P-tRNA (green) and A-tRNA (blue) and eIF-5A (dark red) is shown. eIF5A can rescue stalled ribosomes on mRNA during the synthesis of polyproline stretches. Adapted from Schmidt et al., (2016).

However, eukaryotic ribosomes existing as 80S particles may not always hold as general true, even some eukaryotic ribosomes have been described to sediment with the same velocity as bacterial 70S (Arisue et al., 2004).

The molecular mass of an average eukaryotic ribosome ranges from 3.5 MDa for lower eukarya to 4 MDa for higher eukarya and their molecular diameter is around 250-300 Å (Yusupova and Yusupov, 2017).

The 40S ribosomal subunit is responsible for mRNA codon decoding and houses the tRNA binding sites: A, P, and E (the A-site is the acceptor site for amino-acyl tRNA; the P-site is the peptidyl-tRNA site that accommodates the nascent polypeptide chain and the E-site is the exit site for the discharged tRNA) as well as the mRNA entry and exit channels **(Figure 1).**

The 60S subunit houses peptidyltransferase center that catalyzes peptide bond formation, polypeptide exit tunnel and GTPase binding site. All these sites are essential for ribosomal function and are evolutionarily conserved across all kingdoms of life, although there might be some variation (Melnikov et al., 2012).

Prokaryotic or eukaryotic ribosomes should be able to synthesize proteins from any provided mRNA templates universally. However, the existence of specialized ribosomes has been already described in the past in mitochondria, where special membrane-bound ribosomes are able to synthesize only a specific subset of proteins needed for the catalytic activity of the respiratory chain and no others (Gruschke and Ott, 2010). Specialized cytoplasmic ribosomes have been also identified recently (Genuth and Barna, 2018).

To efficiently cover all cellular needs, translation is usually a very fast process: it has been counted that there occur as much as 13 000 translation initiation and termination events *per* yeast cell *per* second and speed of elongation is on average around 2.63 amino-acids *per* second (von der Haar, 2008; Riba et al., 2019).

1.1. Briefly on ribosome biogenesis

In eukaryotes, ribosomes are made in the nucleolus, a non-membrane organelle of a much larger nucleus. In yeast, the nucleolus is formed around dense chromatin of chromosome XII (**Figure 2**), where all the genes for rRNA are located and transcribed by RNA polymerases I and III (Woolford and Baserga, 2013).

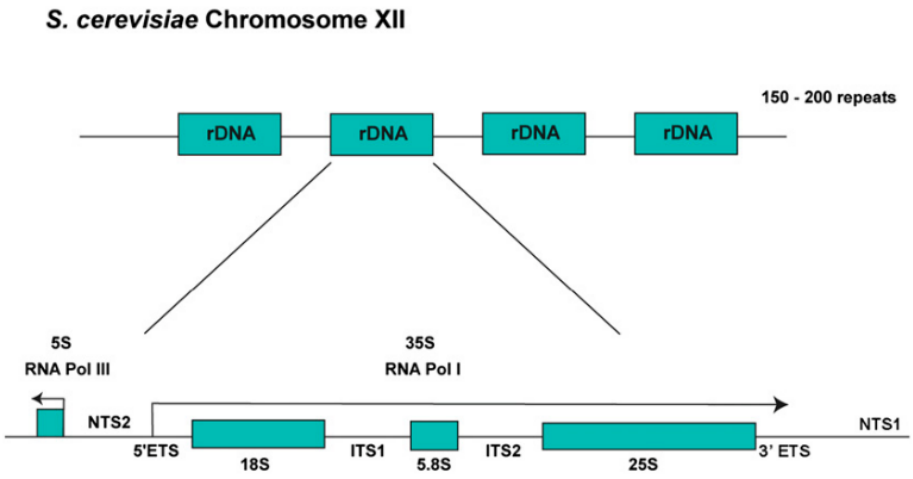

Figure 2 Organization of the rDNA locus in *S. cerevisiae*. The 150-200 rDNA repeats are located on chromosome XII. Next, a single transcription unit is transcribed by RNA polymerase I (RNA pol I) to synthesize the 35S primary pre-rRNA transcript, which is then processed to produce the mature 18S, 5.8S, and 25S rRNAs (right part of the scheme). The 5S rRNA is transcribed by RNA polymerase III (RNA pol III) (left part of the scheme). NTS, non-transcribed spacer; ETS, external transcribed spacer; ITS, internal transcribed spacer. Adapted from Woolford and Baserga, (2013).

Ribosomal biogenesis *per se* is an extremely energy-consuming process. There are approximately 200 000 ribosomes *per* yeast cell and the dividing yeasts have been reported to produce no less than 2000 ribosomes *per* minute (Warner, 1999). Moreover, ribosomal RNA accounts for as much as 85% of all RNA in the cell and ribosomal proteins represent up to 15 % of cellular proteins (Mager, 1988). Nascent rRNA assembles with most ribosomal proteins co-transcriptionally in a consequent and partly self-organized manner. Therefore the absence of individual ribosomal proteins results in distinct defects in the pre-rRNA processing steps. Defects were also found to be correlated with the particular locations of the corresponding ribosomal protein within the ribosome. Proteins in the body of SSU are important for early steps in pre-rRNA processing, on the other hand, proteins important for later phases are mostly located in the head of the 40S, bound to 3´ domains of 18S rRNA (**Figure 3**) (Woolford and Baserga, 2013). The latter is the case also of here studied protein Rps3. This protein is located in the head region of the 40S subunit and is incorporated into the mature subunit late in the cytoplasm with the help of its associated chaperones, Yar1 and Ltv1 (Mitterer et al., 2016; Pertschy, 2017).

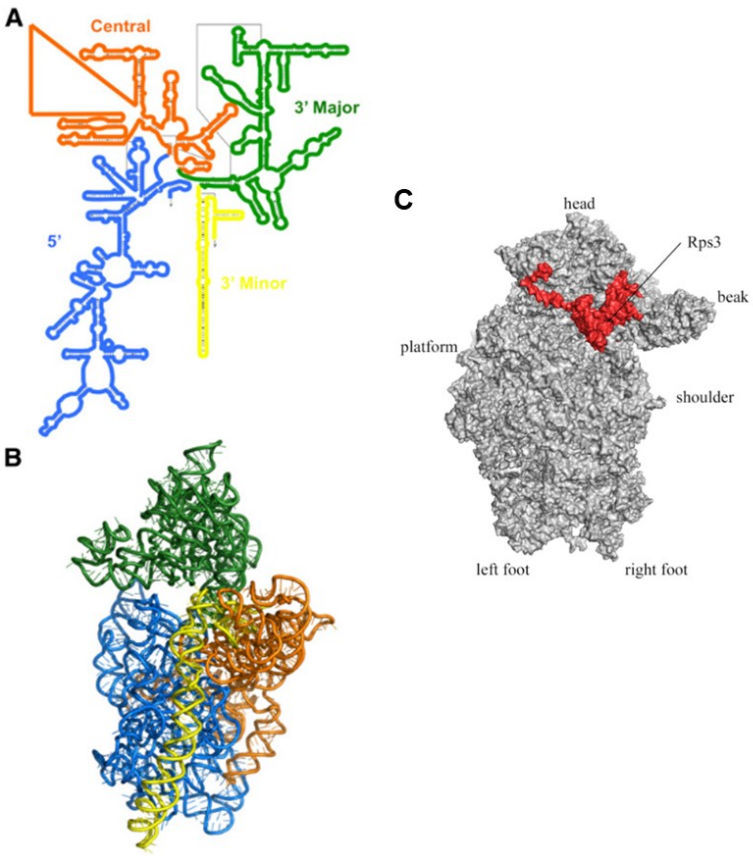

Figure 3 (A) Secondary structure of S. cerevisiae 18S rRNA. 4 evolutionary conserved domains of 18S rRNA: orange central, blue 5′end rRNA, green 3′ major and yellow 3′ minor rRNA ends. **(B) The tertiary structure of 18S rRNA from the crystal structure of yeast ribosomes.** Adapted from Woolford and Baserga, (2013). **(C) Solvent surface representation of 40S subunit with highlighted Rps3 (red) and specific 40S features: right and left foot, shoulder, platform, head and its protrusion - beak.** Prepared using PDB ID 3J81.

1.2. Structure of yeast ribosome

Eukaryotic ribosome is much more complex and larger (approximately by 40 %) then the prokaryotic one. It contains 46 additional ribosomal proteins (RP) and its rRNA has more variable regions and contains 30 so-called expansion segments (**Figure 1**), (Yusupova and Yusupov, 2017). Expansion segments are regions of variable size that interrupt the universal, core secondary structure of ribosomal RNA in eukaryotes (Gebri, 1996).

Compared to prokaryotes, the higher degree of complexity of the eukaryotic ribosome reflects more complicated procedures of ribosomal biogenesis and assembly as well as their further sophisticated function in translation and translational regulation (Warner and Mcintosh, 2009; Jackson et al., 2010; Armache et al., 2010).

The complete, 80S eukaryotic ribosome can be split into two unequal parts with a mass ratio of 2:1 corresponding to 60S and 40S subunits. This was firstly observed by

Nonomura already in 1971 and can be induced either by sufficiently low Mg^{2+} concentration or by the presence of Li^{+}, Na^{+} or urea. The dissociation is reversible (Nonomura et al., 1971).

The yeast 40S subunit consists of 1 single 18S rRNA chain with length of 1800 nucleotides (nts) and 33 ribosomal proteins. On the other hand, the larger 60S subunit bears 3 rRNA molecules: 25S (3396 nts), 5.8S (158 nts) and 5S (121 nts), and 46 ribosomal proteins (Adam Ben-Shem et al., 2010).

In the further sections mostly the small subunit and its Rps3 will be described in more detail as they have been the primary focus of this study.

1.2.1. **40S subunit structure**

The secondary structure of 40S subunit 18S rRNA is organized into four phylogenetically conserved structural domains: the 5′, central, 3′ major and 3′ minor (**Figure 3B**). These domains are further constructed into tertiary structures together with ribosomal proteins: the body, which contains the 5′ domain of 18S rRNA; the platform, which contains the central domain; and the head, which contains the 3′ major domain of 18S (Woolford and Baserga, 2013). Several more features can be morphologically described in the 40S subunit: beak, shoulder and right and left foot (**Figure 3C**) (Laletina et al., 2006).

1.3. Ribosomal proteins

In the budding yeast genome, the genes coding for ribosomal proteins are often encoded by two paralogous genes. This is probably the result of a whole-genome duplication event that occurred about 150 million years ago before *Saccharomyces* and *Kluyveromyces* lineages diverged from each other (Langkjær et al., 2003). Precisely, all 79 yeast ribosomal proteins are encoded by together 138 genes, meaning that 59 RPs are duplicated (Simoff et al., 2009). Such extensive degree of duplication did not occur in other organisms, for example, slime mold *Dictyostelium discoideum* has all ribosomal genes present in single copies (Steel and Jacobson, 1986) and also *Drosophila sp.* has most of them as single-copied, only a few of them (9) have more copies, however, these are expressed only in small number of tissues or at low levels (Marygold et al., 2007).

Most duplicated ribosomal proteins are differentially expressed and exhibit high variation in both, upstream and downstream regulatory sequences. However, there is almost

a 95 % sequence identity between all the paralogs (Parenteau et al., 2015) and 21 ribosomal protein paralogs are even wholly identical (Steffen et al., 2012).

Interestingly, the deletion of one of the yeast paralogous proteins often leads to a qualitatively different phenotype than the deletion of the other. This provides opportunities for assembling ribosomes that have slightly different properties, which might be beneficial for the cell (Woolford and Baserga, 2013). This phenomenon is also exploited by cancer cells, which have often disrupted RP stoichiometry and can then use various ribosomal populations to drive oncogenic translational program (Kulkarni et al., 2017). Recently, it has also been proved that even ribosomes lacking particular ribosomal protein (e. g. Rps26) specifically translate a different group of mRNAs then cells with the complete ribosomal protein set, which suggests the existence of cellular pathways involved in translational regulation by the ribosome components themselves. (Ferretti et al., 2017; Genuth and Barna, 2018). Rps3 protein does not have any paralogue and is encoded by a single gene in *S. cerevisiae*.

Interestingly, most of the yeast RP encoding genes (81 %) are split by an intron. This is very unique because most of the genes in the yeast genome are intron-less. None of the intron deletions has an effect on cell growth under yeast standard cultivation conditions. However, there is usually a drastic effect on the expression of both of the duplicated RP genes (both, increase and decrease were observed), and also the sensitivity to various drugs is altered upon intron deletion. Introns thus probably represent another tool for the cell how to fine-tune intra- and inter-dependent gene expression of RP genes to increase the survival of yeast cells under stress (Parenteau et al., 2011). In addition, mRNA of small ribosomal protein Asc1 carries an intron that has been described to encode U24 sno-RNA important for ribosomal biogenesis (Li et al., 2009). Rps3 gene contains no intron.

Most of the ribosomal proteins are essential for the cell. Extensive analysis of all yeast ribosomal proteins revealed that only 15 out of 79 proteins were non-essential for yeast viability. 5 of them are single-copy genes (**Rps12**, **Asc1,** Rpl29, Rpl38, Rpl39) and 10 are duplicated ribosomal proteins (from the 40S: **Rps7**, **Rps25**). More details can be found in Steffen et al., (2012) and de la Cruz et al., (2015). Rps3 represents an essential protein.

1.3.1. **General properties of ribosomal proteins**

Ribosomal proteins are usually relatively small with a high percentage of basic amino acids (for example, the smallest ribosomal protein, Rpl41 of LSU, has just 25 amino acids

with 10 arginines and 7 lysins). The reason for this unusually high basicity is that in the mature ribosome all ribosomal proteins interact with rRNA and those basic parts neutralize negatively charged rRNA (Klein et al., 2004). However, few acidic ribosomal proteins also exist and they are called P-proteins because they are often phosphorylated (proteins RplP0, Rp1P1 and RplP2 of the large subunit). They are unusual in other respect, too. RplP1 and Rplp assemble into the ribosome in the later, cytoplasmatic phase and even then they can cycle between ribosomes and the cytosolic pool, with only the phosphorylated forms found associated with ribosomes (Szick et al., 1998).

A lot of basic ribosomal proteins possess also a more acidic globular domain that is found on the ribosomal surface (Ramakrishnan and Moore, 2001; Meskauskas et al., 2008).

The intersubunit interface is largely free of any RPs. Most of them are located on the solvent-exposed sites and serve as a docking place for other factors and proteins (Ramakrishnan and Moore, 2001). This is also the case of Rps3, which is known to make multiple contacts with other ribosomal proteins and associated factors, which will be discussed later.

The copy number of ribosomal proteins

Normally, ribosomal proteins are present just in one copy *per* ribosome (Hardy, 1975). Again, exceptions to the rule are the previously mentioned acidic proteins of the large subunit. The eukaryotic RplP1/P2 proteins are present in 4 copies in the ribosome (Liljas, 2001). Rps3 is present only in 1 copy on the ribosome.

1.3.2. **Ribosomal proteins of the 40S**

In **Table 1**, there is a list of all yeast small ribosomal subunit proteins with some details provided. The list involves human and bacterial names as well as newly implemented universal names because, as of 2014, the new nomenclature of ribosomal proteins has been established to better describe and unify ribosomal protein classification (Ban et al., 2014). The universal name features the bacterial protein number, and in case that the protein is conserved, prefix u- (like universal) is added before the number. If the protein is eukaryote specific only, prefix e- is added. Also, contacts that the proteins make with other ribosomal proteins and ribosomal rRNA are noted as well as the information of whether the mutations in the corresponding genes have been linked to human disease. The yeast 40S subunit with depicted ribosomal proteins is in **Figure 4**.

Out of total 33 ribosomal proteins of the yeast 40S subunit, 15 have bacterial homologs and an additional 12 have homologs in archaea, with only 6 proteins found uniquely in the eukaryotes. The majority of the additional proteins is present on the solvent-exposed site of the 40S, although some extensions are involved in the formation of long-range contacts within the SSU (Rabl et al., 2011). The eukaryote-specific proteins widely interact with eukaryote-specific rRNA expansion segments and act to stabilize this additional rRNA architecture.

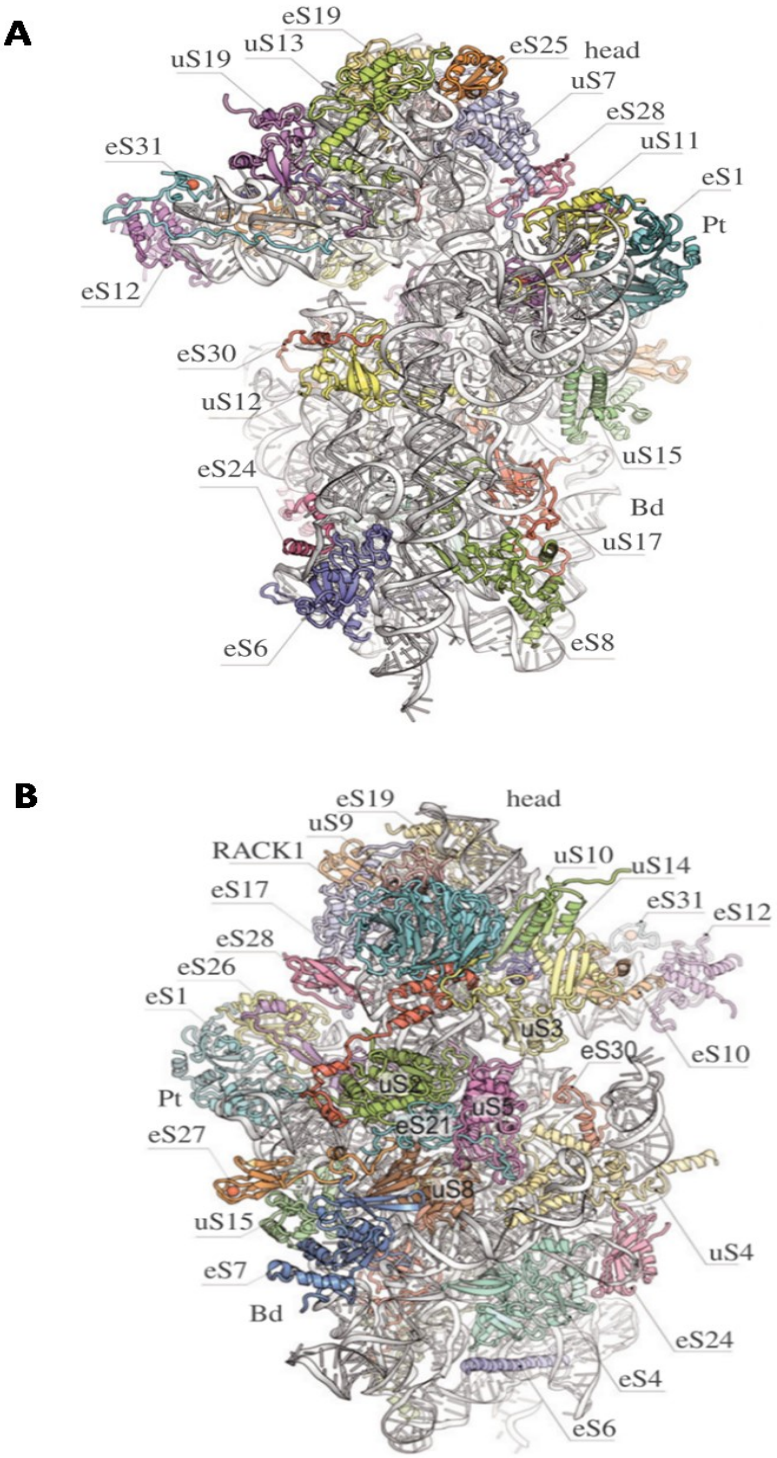

Figure 4 Schematics of ribosomal proteins of the 40S subunit. (A) Intersubunit side**. (B**) Solvent exposed side**.** Adapted from Yusupova and Yusupov, (2017).

Table 1 List of all yeast ribosomal proteins of 40S subunit and their bacterial and human orthologues. Universal name and taxonomic range are also provided. If the mutation in the protein was observed to be linked with a disease in the humans, it is noted. Abbreviations: CA, congenital asplenia, DBA, Diamond–Blackfan anemia; 5q−,5q− syndrome. N/A, no bacterial ortholog for these proteins. B-Bacteria, A-archea, E-eukaryotes. u-universal, e-eukaryotic,h-helix,es-expansion segment, j-junction. Rps3 is highlighted in blue. Ribosomal proteins highlighted in red denote severe Slg$^-$ defect upon deletion of the corresponding non-essential gene. The table was adapted from de la Cruz et al., (2015) and Ban et al., (2014).

Yeast RP name (nonesential)	human RP name	bact. RP na-me	Taxo-nomic range	univers-al name	RP contacts	rRNA main contacts
S0A(YGR214W) S0B(YLR048W)	SA	S2	B,A,E	uS2	S2,S17, S21	head:h35 platform: h26
S1A(YLR441C) S1B(YML063W)	S3A	N/A	A,E	eS1	S14,S26	platform:h23
S2(YGL123w)	S2	S5	B,A,E	uS5	S0,S9,S21,S22,S3 S30	body: h1, h2 head:h35,h36
S3(YNL178W)	**S3**	**S3**	**B,A,E**	**uS3**	**S10,S20, S29,S17, Asc1,S2**	**head:h34,h38,h41**
S4A(YJR145C) S4B(YHR203C)	S4	N/A	A,E	eS4	S6,S9,S24	body: h7,h9,h15
S5(YJR123W)	S5	S7	B,A,E	uS7	S16,S25, S28	head: h29, h40, h41a, j43/28
S6A(YPL090C) S6B(YBR181C)	S6	N/A	A,E	eS6	S4	body: h6, h7,h8, ES3B,h10
S7A(YOR096W) S7B(YNL096C)	S7	N/A	E	eS7	S13,S22, S27	platform: ES6A,ES6E
S8A(YBL072C) S8B(YER102W)	S8	N/A	A,E	eS8	S11	body: ES3A,h9,h11,h13, j6/7
S9A(YPL081W) S9B(YBR189W)	S9	S4	B,A,E	uS4	S2,S4,S24,S30	body: h3,h12,h17,es 6A,es6D
S10A(YOR293W) S10B(YMR230W)	S10	N/A	E	eS10	S3,S12	head:h33,j32/33, h34
S11A(YDR025W) S11B(YBR048W)	S11	S17	B,A,E	uS17	S4,S8,S13,S22, S23	body:h9,h11,h20,es 6c
S12(YOR369C)	S12	N/A	E	eS12	S10, S31	head: h33
S13(YDR064W)	S13	S15	B,A,E	uS15	S7,S27	platfrom:h20,h22
S14A(YCR031C) S14B(YJL191W)	S14	S11	B,A,E	uS11	S1,S26	platform: h23,h24,h45
S15(YOL040C)	S15	S19	B,A,E	uS19	S18	head:h33,h42, j30/31, j30/32
S16A(YMR143W) S16B(YDL083C)	S16	S9	B,A,E	uS9	S19,Asc1	head:h39,es9,h40,h4 1a,h43
S17A(YML024W) S17B(YDR447C)	S17	N/A	A,E	eS17	S0,S3,Asc1	head:h37,h38,h40

S18A(YDR450W) S18B(YML026C)	S18	S13	B,A,E	uS13	S15,S19, S25	head: h41a,h42
S19A(YOL121C) S19B(YNL302C)	S19	N/A	A,E	eS19	S16,S18	head: es9,h41
S20(YHL015W)	S20	S10	B,A,E	uS10	S3,S29	head:h31,h34,h39, h41
S21A(YKR057W) S21B(YJL136C)	S21	N/A	E	eS21	S0,S2,S22	platform:es6a,h27
S22A(YJL190C) S22B(YLR367W)	S15A	S8	B,A,E	uS8	S7,S11, S21,S23, S27	body:h12, platform:es6a,es6e, h25
S23A(YGR118W) S23B(YPR132W)	S23	S12	B,A,E	uS12	S11,S22, S30	body:h3,h5,h18, platform: h19,h44
S24A(YER047W) S24B(YIL069C)	S24	N/A	A,E	eS24	S4,S9	body:h6,h8,h15,h17 platform: es6d
S25A(YGR027C) S25B(YLR333C)	S25	N/A	A,E	eS25	none	head:h41a,j41/42, j42/29
S26(YGL189C) S26B(YER131W)	S26	N/A	E	eS26	S1	head:h26,h27,h28, platform:j23/22, h45,3´end
S27A(YKL156W) S27B(YHR021C)	S27	N/A	A,E	eS27	S7,S13, S22	platform: h22,h26
S28A(YOR267C) S28B(YLR264W)	S28	N/A	A,E	eS28	S5	h29,h43
S29A(YLR388W) S29B(YDL061C)	S29	S14	B,A,E	uS14	S3,S20	head:h31,h32,j31/32 h34
S30A (YLR287C-A) S30B(YOR182C)	S30	N/A	A,E	eS30	S9,S23	body:h16,h17,h18
S31(YLR167W)	S27A	N/A	A,E	eS31	S12	head: h33, long tail contacts h32,h34
Asc1(YMR116C)	RACK1	N/A	E	RACK1	S3, S16, S17	head: h39, h40

2. General overview of translation

In the current textbook view, the process of translation can be divided into 4 phases: initiation, elongation, termination and ribosomal recycling (**Figure 5**). Each of these steps is influenced by specific factors and will be briefly discussed in the following sections, with the main focus on initiation factor eIF3, translation termination, and their mutual inter-relationship.

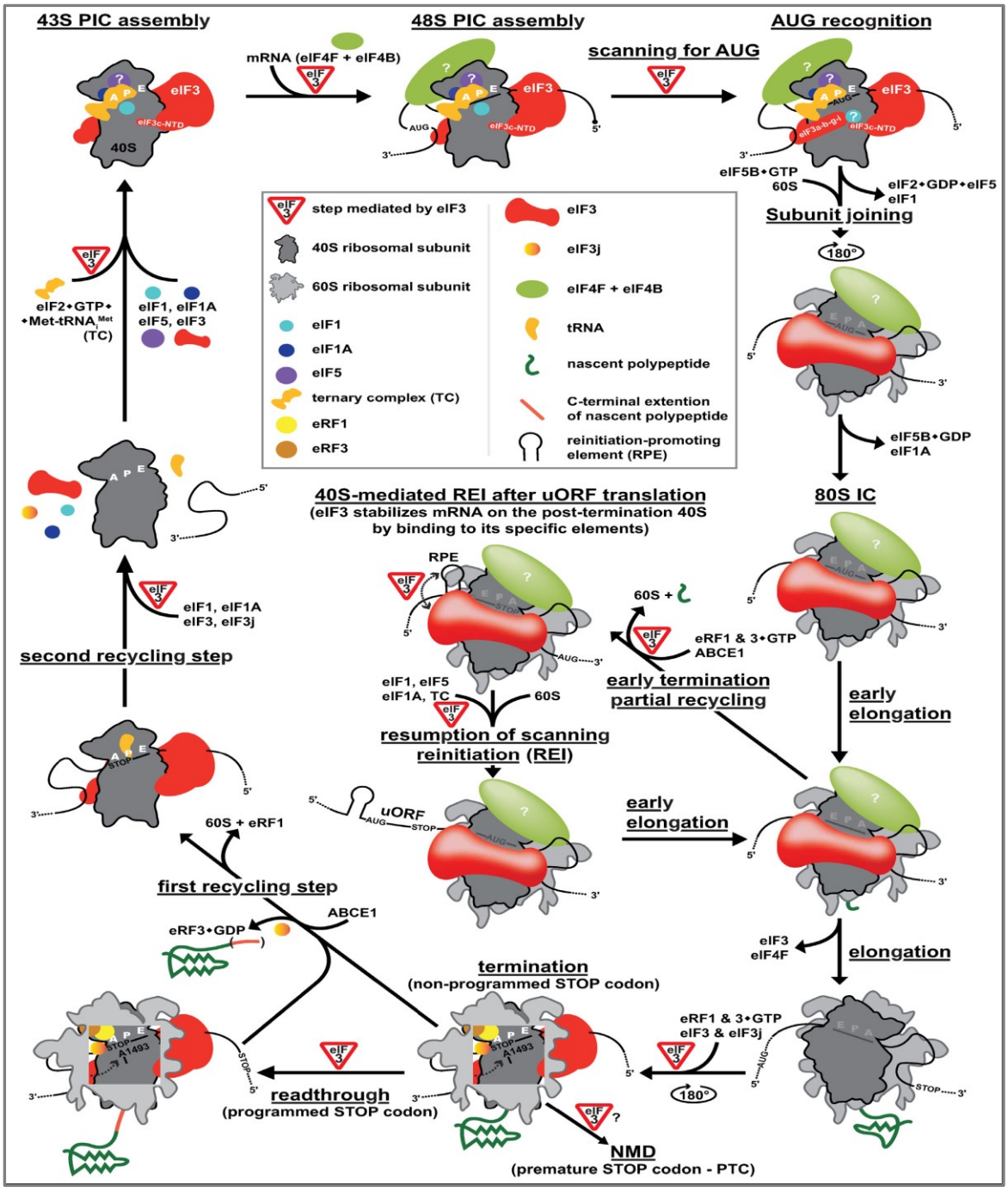

Figure 5 Schematics of the entire translational cycle with 'detours' for: (1) reinitiation (REI) (2) programmed stop codon readthrough (RT) and (3) the non-sense mediated decay pathway (NMD), highlighting the role of eIF3 at the individual steps. For details on selected steps, see the text. Adapted from Valášek et al., (2017).

2.1. Eukaryotic initiation

The initiation phase represents the most tightly regulated phase of the whole translation process. The eukaryotic initiation is also largely different from the prokaryotic one, as the regular eukaryotic mRNAs do not possess an equivalent of the bacterial Shine-Dalgarno sequence and therefore occurs through a scanning mechanism to actively locate the initiating start codon instead of direct recruitment of the SSU to the Shine-Dalgarno sequence.

Prior to binding the mRNA, the free 40S subunit associates with several initiation factors (eIFs): eIF1, eIF1A, eIF3, eIF5 and a ternary complex (TC) composed of initiator Met-tRNA$_i^{Met}$ and GTP-bound eIF2. Together, they form a 43S pre-initiation complex (43S PIC). This complex then interacts with the mRNA to form the 48S PIC (Valášek, 2012; Valášek et al., 2017; Hinnebusch, 2017).

Eukaryotic mRNA is directed for translation *via* binding of different specific proteins such as the poly(A)-binding protein (PABP) and the eIF4F factor complex, which consists of eIF4A, eIF4E, and eIF4G factors. The eIF4E associates with 7-methylguanosine (m7G) cap of the mRNA and also with a scaffolding protein eIF4G. eIF4A is a helicase involved ATP-dependent unwinding of secondary structures encountered during the scanning process (Pestova and Kolupaeva, 2002). eIF4G also associates with PABP and this is believed to form a typical, closed-loop structure of the mRNA (Marintchev and Wagner, 2004).

After 43S PIC recruitment to the mRNA, the 48S structure is formed and scanning for the initiator AUG begins. Recognition of the start codon is achieved by correct base-pairing between the Met-tRNA$_i^{Met}$ located in the P-site and the AUG. The recognition triggers a series of conformational changes in the complex. Namely, the GTP-bound eIF2 is hydrolyzed, releasing the phosphate, eIF1 factor is released or dislocated and the whole 40S subunit transits from the so-called open, scanning-conductive state (py48S-open state in **Figure 6**), to the closed, scanning-arrested state and clamps on the mRNA to await 60S subunit joining (py48S-closed state in **Figure 6**). In the closed state, a latch between helices h18 and h34 of the rRNA is formed (Llácer et al., 2015a).

Most of the initiation factors, apart from eIF3 (and probably eIF4F as well), leave upon 80S formation (Hinnebusch, 2017). The subunit joining step is catalyzed by the eIF5B protein and is performed at the expense of a second GTP hydrolysis that accompanies initiation. Ejection of eIF5B marks the end of the initiation phase, leaving the 80S initiation ribosome ready for subsequent elongation steps (Valášek et al., 2017).

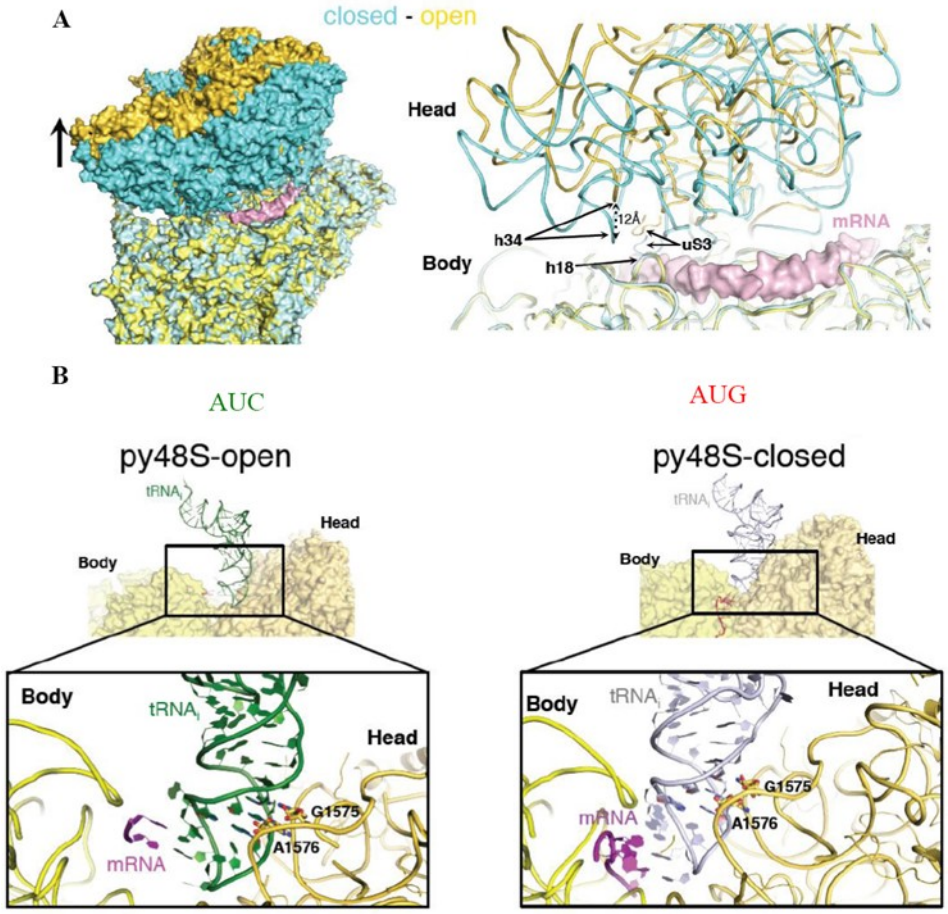

Figure 6 (A) Schematics of py48S-open (yellow) and py48S-closed (blue) conformations of the ribosome. Upon start codon recognition, a 12 Å closure of the latch between helices h18 and h34 of rRNA, accompanied by a downward movement of the head and constriction of the mRNA entry channel occurs**.**
(B) Rearrangement of the P-site from an open structure (py48S-open) to a constricted one (py48S-closed, right) is accompanied by the formation of contacts between tRNAi and the 40S body that are absent in the open state. Adapted from Llácer et al., (2015).

Nearly every step of the translation initiation is promoted and regulated by the eIF3 factor, however, its functions go well beyond that and will be described in more detail in subsequent Section 5. After successful initiation, translation proceeds with elongation phase creating successive peptide bonds between incorporated amino acids according to the message encoded in mRNA´s codons until a stop codon is encountered by the ribosome (this phase will be not described in details in this Thesis).

2.2. Eukaryotic termination and recycling

Termination of translation occurs when a non-sense (stop) codon (UAA, UGA or UAG) reaches ribosomal A-site. For those codons, there is no cognate tRNA that could decode them, so instead, a specific protein called release factor 1 (eRF1, known as Sup45 in yeast), recognizes the stop codon and binds to the ribosomal A-site in complex with another release factor, GTP-bound eRF3 (Sup35 in yeast) (Brown et al., 2015). There are again exceptions to the rule, and in some organisms like ciliate protists, diplomonads or green *algae* various stop codons are canonically decoded as sense ones (Swart et al., 2016; Keeling, 2016; Pánek et al., 2017).

The decoding of the stop codons by the eRF1 is achieved with the help of the fact that its structure mimics the structure of the tRNA and in complex with eRF3, it mimics the higher-order structure of the ternary complex of aminoacyl-tRNA, elongation factor 1 and GTP that together bind to the A-site during elongation cycle (Song et al., 2000).

After binding of the eRF1-eRF3 complex, GTP-bound eRF3 is hydrolyzed, which triggers a conformational change that leads to eRF3 dissociation from the complex. The dissociation is further promoted by the Hcr1 protein (Beznosková et al., 2013). However, some recent models argue that eRF3 stays bound even after GTP hydrolysis (Bulygin et al., 2017). Either way, in the next step, the still A-site bound eRF1 moves closer to P-site tRNA and with its universally conserved GGQ motif (this motif is required for the hydrolysis of the ester bond between the tRNA and nascent polypeptide) it stimulates peptide hydrolysis and release. This step is further promoted by the ATPase ABCE1 (Rli1 in yeast) which contributes to the peptide release. After ATP hydrolysis ABCE1 changes conformation to help the catalysis of splitting of the ribosomal subunits to make them available for next translation rounds (recycling) (Matheisl et al., 2015; Taylor et al., 2012). The recycling of the 60S subunit is *in vivo* further promoted by an accessory recycling factor Hcr1 (Young and Guydosh, 2019).

Subsequent dissociation of deacylated tRNA from the P-site and the release of the 40S subunit from the mRNA can be achieved either by the action of the initiation factors eIF3, eIF1 and eIF1A (priming the subunit directly for a new round of initiation) or by the action of non-canonical initiation factor eIF2D (known as Ligatin or Tma64 in yeast) or lastly, by the action of protein complex composed of DENR (density-regulated protein, Tma22 in yeast) and MCT-1 (multiple copies in T-cell lymphoma-1, Tma20 in yeast). Interestingly, this complex is formed by two proteins homologous to N- and C- terminal regions of the

eIF2D (Ligatin) (Pisarev et al., 2007; Skabkin et al., 2010; Gunišová et al., 2018). After the recycling is complete, the liberated ribosomal subunits together with mRNA are ready for the new translation cycle (**Figure 5**).

3. Specific mechanisms of translational regulation

3.1. Translational reinitiation

Reinitiation (REI) is a spectacular mechanism of specific translational regulation (**Figure 5)**. This mechanism occurs largely after translating mRNAs containing short uORFs (**u**pstream **O**pen **R**eading **F**rames). Short uORFs are *cis*-acting sequences, which appear in the 5′ leader of some main gene coding ORFs and regulate their expression. Recent data revealed that uORFs are quite widespread in the eukaryotic genome and regulate as much as ~ 13% of yeast and ~50% of mammalian transcripts (Lawless et al., 2009; Chew et al., 2016). They were found in a variety of mRNAs coding for different factors ranging from transcription and growth factors to development, cell cycle and stress response-related mRNAs (Janich et al., 2015; Hinnebusch et al., 2016; Gunišová et al., 2018).

Usually, uORFs were found to downregulate the main ORF expression, as full ribosomal recycling normally takes place at the stop codon of the uORF preceding the main gene and the ribosome gets discharged from the mRNA. However, in some specific cases, translation of uORF can be followed by incomplete ribosomal recycling (meaning that only the large 60S subunit and deacylated tRNA are recycled). In this case, the 40S subunit will stay bound to mRNA even after termination, resumes scanning and reinitiates translation on the next start codon. Those uORFs are called REI-permissive and features responsible for the incomplete ribosomal recycling and subsequent reinitiation have been described in great detail mostly on *GCN4* mRNA (Gunišová et al., 2018)

GCN4 mRNA encodes a transcription factor responsible for the activation of 600 stress-related genes activated upon e.g amino-acid starvation in yeast (Hinnebusch, 2005). It contains 4 uORFs, out of them two are REI-permissive (uORF1 and uORF2). The molecular mechanism that lies behind the uORF1 and uORF2 permissiveness was revealed in our laboratory. We described that sequences preceding those uORFs interact with the NTD of a/Tif32 (one of the subunits of yeast eIF3, see further) and this interaction is involved in stabilizing of the 40S subunit on the mRNA to promote reinitiation (Szamecz et

al., 2008; Gunišova and Valašek, 2014). Precisely, 4 specific elements in the 5′ leader of uORF1 were described and named reinitiation promoting elements (RPEs). Two of them are unstructured, RPE i. and RPE iii., and the structures of the other two represent a 22-nucleotides long hairpin of RPE ii. and a double-circle hairpin of RPE iv., respectively. RPEs i. and iv. were identified as those interacting with NTD of a/Tif32 (Munzarová et al., 2011).

Recently, we developed a novel *in vivo* RNA–protein pull down assay and showed that the short-lived retention of eIF3 on elongating ribosomes and its interaction with *cis*-acting features described above is the essential precondition that renders short uORFs highly REI-competent (Mohammad et al., 2017).

Atf4 is a mammalian functional homolog of Gcn4, serving also as a principal effector of the so-called integrated stress response by activating transcription of many genes that enable cell survival upon exposition to different stress situations. Because its mRNA bears two uORFs (one short and one longer and overlapping main ORF) it is of great interest to explore whether it shares similar regulatory features with uORFs in *GCN4* mRNA (Vattem and Wek, 2004).

3.2. Stop codon readthrough

The process of the stop codon decoding during canonical termination by eRF1 is generally very effective (the frequency of occasional readthrough (RT) is quite low, below ≤ 0.1%) (Schueren and Thoms, 2016). However, regulatory mechanisms exist that can cause the stop codon to be more prone to readthrough (discussed further below in Section 3.2.1). During readthrough, eRF1 is outcompeted at the A-site of the ribosome by a near-cognate tRNA (nc-tRNA) carrying its corresponding amino acid, which is then incorporated into the protein (see **Figure 7**). Near-cognate tRNAs are tRNAs that create a single mismatch upon pairing to a stop codon, usually at the position 3 or 1 of the stop codon (Dabrowski et al., 2018).

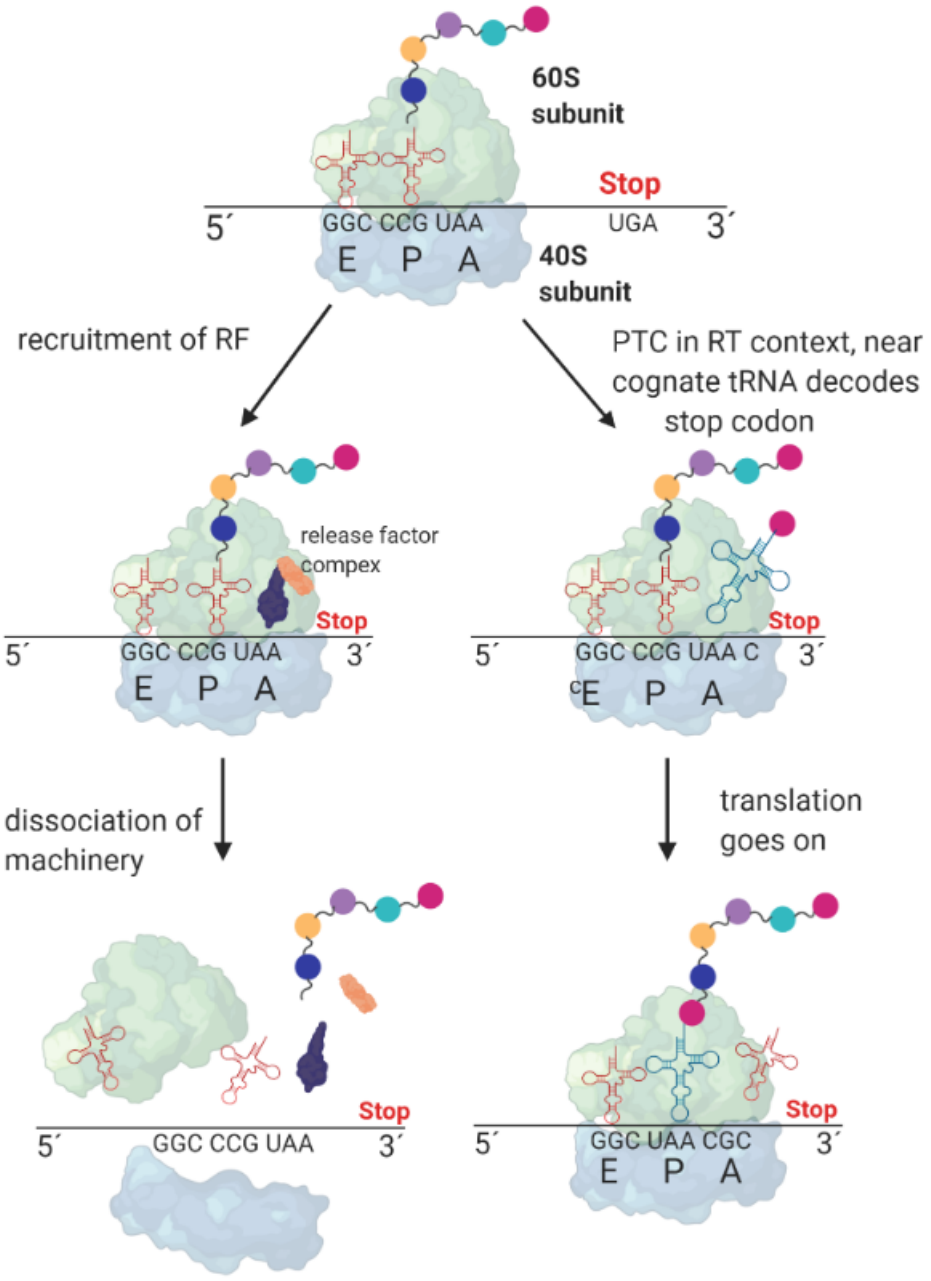

Figure 7 Schematic mechanism of translation termination and stop codon readthrough.
Translation termination can be regarded as a constant competition between stop codon recognition by release factors (left) and stop codon decoding by near-cognate tRNAs that results in stop codon readthrough (RT) (right). The likelihood of stop codon RT increases when the stop codon (UAA here) is followed by a cytosine residue. Ribosome thus continues translation in the same reading frame until the next stop codon (depicted as 'Stop') is encountered resulting in the synthesis of an extended polypeptide. A-site is the acceptor site for amino-acyl tRNA. P-site is the peptidyl-tRNA site that accommodates the nascent polypeptide chain. E-site is the exit site for discharged tRNA. RF-release factor, PTC-premature termination codon. Near-cognate tRNA is indicated in blue. Figure prepared using BioRender.

Relatively frequently incorporated nc-tRNA from the natural tRNA pool of *S.cerevisie,* are $tRNA^{Cys}$, $tRNA^{Trp}$ (both preferentially incorporated at UGA stop) and $tRNA^{Gln}$, $tRNA^{Tyr}$, $tRNA^{Lys}$ (for stop codons UAA and UAG) (Blanchet et al., 2014). In our previous research in yeast, we expanded the decoding rules to the +4th position of the stop

codon and showed that the identity of the +4 base determines the preferred selection of the particular nc-tRNAs on individual stop codons as well (Beznosková et al., 2016). Furthermore, this phenomenon is conserved in humans too (Xue et al., 2017).

In specific cases, stop codons can be also suppressed by the specialized fully-cognate tRNAs carrying non-canonical amino acids such as pyrrolysine (observed in *archaea*) or selenocysteine (found in all kingdoms of life). Those specialized tRNAs are brought to the ribosome by specific elongation factors and require special mRNA insertion sequences further downstream of the stop codon (selenocysteine insertion sequence (SECIS) for selenocysteine and putative pyrrolysine insertion sequence (PYLIS) for pyrrolysine) (Zinoni et al., 1990; Zhang et al., 2005).

Regarding the outcome of the readthrough, two situations can occur depending on the stop codon position in the mRNA:

1. The stop codon is located at the end of the protein-coding region (NTC, normal termination codon).

In case it is readthrough, a C-terminally extended protein is made. In the majority of circumstances, the elongated part of the protein probably has no obvious coding potential, what is more, it can even interfere with the functioning of the original protein. However, in some special cases, the C-terminal extension can provide some additional role to the protein than can be exploited when the conditions in the cell change: for example, it can carry a cellular localization signal, homo-/heterodimerization domain or alter the ligand-binding properties of the protein (Rodnina et al., 2020). The same strategy of stop codon RT is also widely used by many ssRNA viruses to expand their limited genome coding capacity (Beier, 2001).

2. The stop codon is located in the protein-coding region (PTC, premature termination codon).

Normally, the interruption of a coding region with a stop codon has to be avoided as termination at such PTC leads to truncated and therefore usually non-functional protein product (the probability of sustainment of the function is usually inversely correlated to the distance of the PTC to the NTC). However, when the PTC gets readthrough, the synthesis of complete protein is maintained. These findings have huge therapeutic potential (see Section 3.2.2). It is interesting to note that the basal RT level occurring on the PTCs has been reported to be much higher (even 10x) that RT level occurring on NTCs. The possible explanation is that for efficient termination, direct contact between RFs and PABP is needed (Cosson et al., 2002; Amrani et al., 2004). PTCs are usually located further away from the

mRNA poly(A) tail than NTCs and thus such interaction is limited. As a consequence, eRF3 activity would be less effective and results in the prolonged presence of the pre-termination 80S complex on the PTC. This prolonged presence can lead to aberrant termination, followed by the nonsense-mediated decay (NMD) and transcript degradation, or can increase the likelihood of RT (Dabrowski et al., 2018).

3.2.1. **Features controlling the efficiency of stop codon readthrough**

Not all stop codons have the same likelihood of being readthrough by the ribosome. Past research in this field has identified several factors that influence the probability of RT, and the list is still not complete.

Basically, it could be divided into factors acting in *cis* and in *trans*.

Cis-acting factors influencing the RT efficiency

a) The type of the stop codon. Not all stop codons have the same 'leakiness', the effectivity of RT decreases in this order UGA>UAG> UAA (Cridge et al., 2018).
b) The nucleotide context of the stop codon (both upstream and downstream of the stop codon). The biggest influence has the base immediately following the stop codon (+4). The highest readthrough is observed if the +4 base is a pyrimidine, especially a cytosine (Namy et al., 2001). Sequences as far as +9 from the stop codon have been described to modulate readthrough efficiency (Firth and Brierley, 2012). From the other side, -2 and -1 nucleotides from the stop codon required for the highest RT were found to be adenines (Tork et al., 2004).
c) The presence of specific mRNA secondary structures further downstream from the stop codon. In most cases, the secondary structures have been described to promote stop codon readthrough. Several possible explanations for the phenomenon range from steric clashes with the release factors, altered mRNA-ribosome interactions or ribosomal pausing at the stop codon due to the unwinding of the secondary structures by ribosomal helicase (Qu et al., 2011; Firth and Brierley, 2012).

d) The identity of tRNA in the ribosomal P-site and also the identity of the incorporated amino acid at position -2. In yeast, it was described that codons coding for a basic amino acid residue (like arginine) at - 2 position have higher RT efficiency (approx. two-fold) compared to codons coding for a non-basic amino acid at the same position. However, these results are opposite to what was reported in bacteria. The effect of different P-site tRNAs on the efficiency of RT could be caused by the presence of different tRNA modifications (Mottagui-Tabar et al., 1994, 1998).

Extensive analysis of the aforementioned factors revealed that the least termination efficient (therefore most readthrough-inducing) sequence to be: AA- UGA - CAA UUA (Firth & Brierley 2012; Namy et al. 2001). This specific variation (CAA UAA) of the general readthrough-inducing motif, which is referred to as the CARNBA sequence, was indeed found to be used by the TMV (Tobacco mosaic virus) virus to produce a C-terminally extended replicase (Skuzeski et al., 1991).

Readthrough occurring at stop codons in termination ineffective contexts, frequently also stimulated by specific *trans*-factors (see further below), is sometimes referred to as programmed stop codon readthrough.

***Trans*-acting factors modulating the RT efficiency**

Trans-acting factors are generally much less understood and described than the *cis*-acting ones. It is no surprise that loss of function mutations (or downregulations) of the key players of the termination process, such as the release factors, do have a direct effect on termination efficiency and increase the frequency of stop codon readthrough (Chauvin et al., 2005; Carnes et al., 2003). Similarly, downregulation of another termination and recycling player, Rli1, was found to alter the efficiency of termination (Khoshnevis et al., 2010).

Furthermore, proteins involved in targeting the PTC-containing mRNAs for the NMD have been also found to influence stop codon readthrough, although in an organism-specific manner. Precisely, deletions of key players of this pathway from the yeast genome, the Upf proteins, resulted in an increased stop codon readthrough (Wang et al., 2001; Salas-Marco and Bedwell, 2005). Conversely, when the *UPF* genes were downregulated by RNAi in mammalian cell lines, the effect on readthrough was the opposite (Jia et al., 2017). The observed inconsistency could be partly attributed to a probably slightly different mechanism

of action of the Upf1 protein in yeast and in mammals. In yeast, for the efficient termination on the PTC, the ATP hydrolysis mediated by Upf1 protein is required for the disassembly of the trimeric complex (ribosome with release factors bound, mRNA and Upf proteins) allowing Xrn1-mediated 5′→3′ exonucleolytic decay of the mRNA (Serdar et al., 2016). In the fully reconstituted translation termination system, human Upf1 protein had been shown to possess no direct influence over the process. However, for the other Upf proteins, the explanation of the different behavior is yet-to-be given (Neu-Yilik et al., 2017; Hellen, 2018).

Surprisingly, another *trans*-acting factor influencing the stop codon RT has been identified in our laboratory as the eukaryotic initiation factor 3. Mutants of different eIF3 subunits were found to decrease the frequency of stop codon RT on reporter mRNAs with programmed stop codon contexts (Beznosková et al., 2013). We also proposed a molecular mechanism; for its details see **Figure 8** (Beznosková et al., 2015).

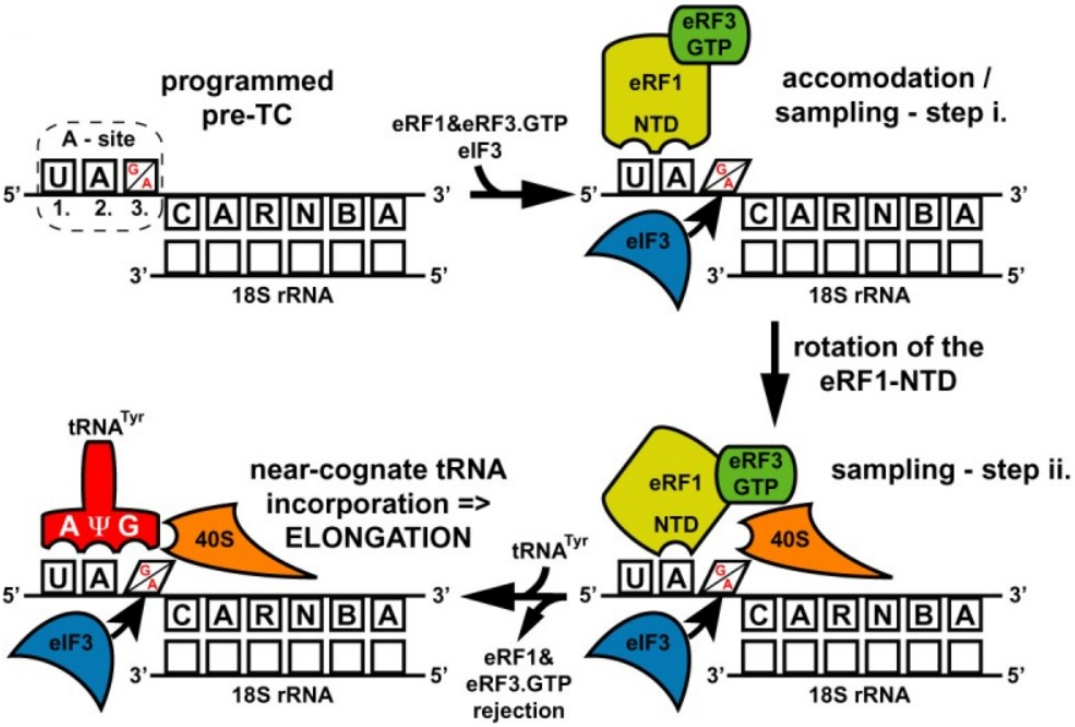

Figure 8 Schematics of programmed stop codon readthrough. Stop codon occurs in the unfavorable termination context bearing specific consensus sequences like CARNBA in its 3′ UTR (untranslated region) - in this particular case proposed to base-pair with 18S rRNA. The eIF3 presence in the pre-termination complexes alters the decoding property of the nucleotide at the third stop codon position. This prevents its proper decoding and subsequently, after the eRF1-eRF3-GTP complex rejection, allows the incorporation of near-cognate tRNAs with the mismatch at the third position to readthrough the stop codon. Adapted from Beznosková et al., (2015).

It may generally appear that more translation factors might be involved in the regulation of stop codon RT as previously thought. The specific elongation factor eIF5A was

also recently proposed as one of them. Cells lacking eIF5A were shown to have inefficient termination, with ribosomes found either stalled at stop codons or translating past them in the 3´ UTR (Schuller et al., 2017).

Another recently described protein influencing termination and RT is Pub1. Pub1 is an RNA binding protein involved in various cellular functions. It was shown to modulate the stability of transcripts containing uORFs (one prominent example is the GCN4) (Ruiz-Echevarría and Peltz, 2000) or stress granule formation (Buchan et al., 2008). Urakov and colleagues found that it interacts with the prion domain of eRF3 and that it can associate with the ribosomes during termination. *PUB1* deletants displayed decreased frequency of stop codon readthrough on the majority of tetranucleotide stop signals (Urakov et al., 2017).

Among other factors reported to influence the fidelity of termination, and therefore affecting the stop codon RT in yeast, were proteins of the small ribosomal subunit: Rps2, Rps9 and Rps23. This is not surprising since those proteins as integral parts of ribosomes represent a very ancient, over 2 billion years conserved, ribosomal ambiguity center responsible for controlling the fidelity of translation (Alksne et al., 1993).

Additionally, the involvement of ribosomal protein Rps25 in stop codon readthrough has also been described (Landry et al., 2009). It was proposed that Rps25 can alter termination efficiency through its conserved proline residue, which projects into the decoding center and is a site for hydroxylation. Upon the modification, various effects on termination in yeast and human cells were observed (Singleton et al., 2014; Hellen, 2018).

Recently, the role of the A-site neighboring C-terminal tail of Rps15 in maintaining termination fidelity was characterized. It was proposed to occur *via* direct interaction of the C-terminal tail of Rps15 with the release factors complex (Nguyen et al., 2020).

In this Thesis, Rps3 is presented as another ribosomal protein influencing the stop codon readthrough and termination in yeast (Poncová et al., 2019).

3.2.2. **Clinical importance of stop codon readthrough**

If we count all genetic mutations responsible for human diseases, those caused by a premature termination codon as a result of insertion, deletion, single point mutation or splicing error, account for approximately 30 % of them (Wittenstein et al., 2019). These types of mutations cause several million people worldwide suffering from diseases like Duschen muscular dystrophy, cystic fibrosis, hemophilia A and B (James et al., 2005), Pompe disease (Bellotti et al., 2019), inheritable cancer syndromes or β-thalassemia (Kar et

al., 2019). The strategy of increasing stop codon readthrough on those PTCs in a controllable manner and thus ensuring the corrective renewal of production of functional full-length proteins has great therapeutic potential, that is not still fully uncovered. Unfortunately, the currently used compounds are non-convenient for a long–term (life-long) therapy due to their high toxicity or a wide spectrum of negative side effects (for instance, one group of compounds called aminoglycoside antibiotics that worsen translational fidelity and non-specifically increase stop codon readthrough was found to be highly oto- and nephrotoxic) (Keeling and Bedwell, 2011).

As a new hope, novel therapeutics are starting to emerge - for example Atauren (TranslarnaTM), developed by PTC Therapeutics, is currently under clinical trials in the USA (https://www.ptcbio.com/our-pipeline/areas-of-interest/ataluren/).

Any new research that could describe more details about translational termination machinery and shed more light on the mechanism of stop codon readthrough thus represents an essential knowledge that might be beneficial for designing further strategies of new drug development and treatment of diseases caused by PTCs.

4. Ribosomal protein Rps3

Rps3 is located in the head region of the 40S subunit near the mRNA entry channel, and its basic residues protrude directly into the mRNA channel lumen. This position predestines Rps3 to perform important functions related not only to the elementary process of translation but also to different functions far beyond that, which makes Rps3 one of the most fascinating protein of the whole ribosome (Zhou et al., 2015).

In the budding yeast, Rps3 is encoded by a single gene and is composed of 240 amino acids. It is known to contain a KH (**K**-**h**omology) motif in its N-terminus (amino acids 1-88). This relatively widespread RNA-binding motif was first characterized in the K protein (mRNA binding protein involved in telomere maintenance) in 1993 and contains VIGXXGXXI consensus sequence repeats (where X could be any amino acid) (Siomi et al., 1993; Denisenko and Bomsztyk, 2002). The protein fold of the KH domain in the Rps3 protein is slightly different thus defining a new type of fold (type II). Importantly, the RNA-binding function is unaltered (Grishin, 2001).

The KH motif is followed by a nine-amino acid linker to a central RRM-like domain composed of a four-stranded β-sheet surrounded by two α-helices (amino acids 98–189)

(Limoncelli et al., 2017). This part of the protein forms the mRNA entry channel architecture adjacent to the ribosomal A-site. The last part of the Rps3 structure represents a 50 amino acid long C-terminal tail, which extends from the body of the Rps3 protein along the outer surface of the subunit. This part is known to make multiple contacts with the Asc1 ribosomal protein (Asc1 is an abbreviation of Absence of growth Suppressor of Cyp1 and it represents a non-essential ribosomal protein, especially required for the translation of short mRNAs) (Thompson et al., 2016; Limoncelli et al., 2017). Rps3 C-terminal tail is also subject to a wide range of post-translational modifications, as several of its residues were found to be sites of acetylation, phosphorylation, succinylation or ubiquitination (Peng et al., 2003; Albuquerque et al., 2008; Weinert et al., 2013; Fang et al., 2014; Limoncelli et al., 2017). The potential of these modifications for regulation remains unexplored.

Apart from contacting Asc1, Rps3 is known to make contacts with Rps17 (also *via* the long C-terminal tail) and neighboring proteins Rps2, Rps10, Rps20, Rps29 (de la Cruz et al., 2015). However, the functional significance of those interactions beyond their structural role remains also unclear. Also, Rps3 has been shown to interact with C-terminus of a/Tif32 (Chiu et al., 2010) and the functional importance of this contact for translational termination and stop codon readthrough has been investigated as a major part of this study.

Figure 9 displays sequences from Rps3 homologs across kingdoms of life. Generally, the KH and RRM domains are evolutionary very well conserved across all species whereas the C-terminal tail is significantly conserved only within eukaryotes. The only Rps3 residue remaining identical across all kingdoms of life is the R116 which makes it the prime candidate for important functions.

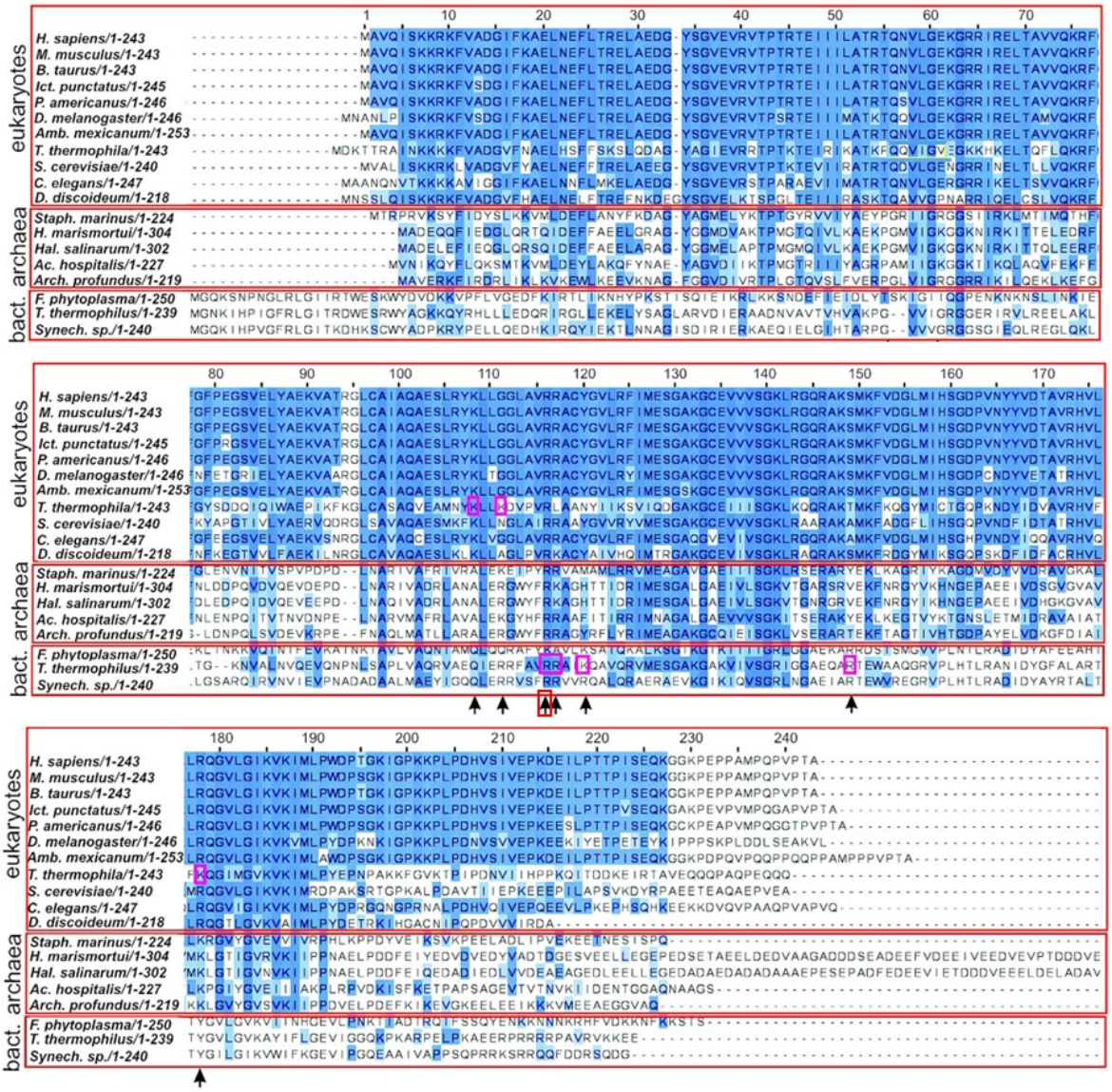

Figure 9 Alignment of amino acid sequences of eukaryotic, archaeal and bacterial proteins homologous to Rps3. The numbering corresponds to human Rps3. Conserved protein fragments are marked; darker color corresponds to the higher degree of conservation. The protein sequences and their codes are: *H. sapiens, Homo sapiens* (P23396); *M. musculus, Mus musculus* (P62908); *B. taurus, Bos_taurus* (Q3T169); *Ict. punctatus, Ictalurus punctatus* (Channel catfish) (Q90YS2); *P. americanus, Pseudopleuronectes americanus* (Q6QZI0); *D. melanogaster*, *Drosophila melanogaster* (Q06559); *Amb. mexicanum, Ambystoma mexicanum* (Axolotl) (P79891); *T. thermophila, Tetrahymena thermophila* (E6PBS1); *S. cerevisiae, Saccharomyces cerevisiae* (P05750); *C. elegans, Caenorhabditis elegans* (P48152); *D. discoideum, Dictyostelium discoideum* (P90526); *Staph. marinus, Staphylothermus marinus* (A3DNB3); *H. marismortui, Haloarcula marismortui* (P20281); *Hal. Salinarum, Halobacterium salinarum* (P15009); *Ac. Hospitalis, Acidianus hospitalis* (F4B8D7); *Arch. profundus, Archaeoglobus profundus* (D2RE60); *F. phytoplasma, Flavescence doree phytoplasma* (Q8VL42); *T. thermophilus, Thermus thermophilus* (P80372); *Synechocystis_sp*. (F7UN05). Basic residues correlated to the ribosomal helicase activity are shown in magenta boxes in the *T. thermophila* and *T. thermophilus* sequences; their positions are marked by arrows at the bottom of the respective alignment panels. The arrow pointing at the evolutionary conserved residue R116 is highlighted in red. Adapted from Graifer et al., (2014).

4.1. Rps3 in translation

Rps3 has been described to be involved in translation initiation *via* its participation in rearrangements of the 40S subunit induced by binding of translation initiation factors eIF1 and eIF1A (Passmore et al., 2007). Binding of the factors dissolves the so-called latch formed by the residues in helices h18 of 18S rRNA of the 40S body and h34 and Rps3 of the 40S head. This leads to the establishment of a new connection between Rps3 and h16 and opening of mRNA entry channel referred to as the 'scanning competent open conformation' of the 40S which allows the mRNA loading and scanning of its codons. Upon start codon recognition, reversal latch closure occurs and scanning 40S subunit rearranges back to its arrested state (Hinnebusch, 2017).

In addition, Rps3 has been also found to promote the 40S interaction with mRNA at the entry channel to enhance initiation accuracy as mutants in basic residues of Rps3 that are in contact with mRNA decreased initiation at near-cognate start codons (Dong et al. 2017).

In bacteria, uS3 (yeast Rps3) together with another ribosomal protein uS4 (yeast Rps9), has also been implicated in the intrinsic helicase activity of the ribosome. Taykar and colleagues (2005) described that the ribosome itself is capable to melt double-stranded RNA structures up to 27 bp in length and that mutants in the conserved basic residues of Rps3 abolished this helicase activity (Takyar et al., 2005).

Furthermore, some Rps3 mutations have been already demonstrated to suppress frameshift and nonsense mutations in some tested genes (Hendrick et al., 2001), whereas some others increased frameshifting at inhibitory CGA-CGA codon pairs (Wang et al., 2018). This points out the important regulatory function of Rps3 in translation, however, the molecular mechanism has still not been proposed.

Recently, Rps3 has also been identified as a crucial player in different RNA surveillance pathways. It was found to participate in releasing stalled ribosomes from mRNA *via* no-go decay (Simms et al., 2018) and also affecting the functionally related **n**on-functional 18S r**R**NA **d**ecay (18S NRD pathway), most probably based on the interaction between its C-terminal tail and Asc1 protein (Limoncelli et al., 2017).

4.2. Extraribosomal functions of Rps3

Ribosomal proteins are long known to exert functions related to ribosomal biogenesis and in the past decade, great progress in characterizing also the extraribosomal functions of these proteins has been made. Those include, but are not limited to: DNA repair, cell death, inflammation, tumorigenesis, or transcriptional regulation (Gao and Hardwidge, 2011; Zhou et al., 2015).

It is highly likely that the list of functions and the number of involved ribosomal proteins would be further growing as the ribosomal proteins are the prime candidates for those functions. They just have it all: they are abundant, ubiquitous and RNA-binding (Warner and Mcintosh, 2009). Most of the ribosomal proteins with attributed extraribosomal function usually have just one such function, however, the involvement of Rps3 in many different processes makes it one of the most versatile proteins known. The complete list and discussion of its extraribosomal functions would go far beyond the scope of this Thesis, which focuses on translation, therefore, only the most prominent will be mentioned here.

Rps3 has been described to influence the host-pathogen signaling pathways for both, viruses and bacteria, and it was shown to promote pro-inflammatory signaling upon bacterial infection (Gao and Hardwidge, 2011). Also, it seems to play a role in DNA repair, as it can cleave abasic sites in the DNA after damage (Seong et al., 2012). Besides, Rps3 can regulate apoptosis and its amino acids 15-26 represent the dead domain important for the onset of the process (Jang et al., 2004). Furthermore, Rps3 is differentially expressed in various cancers and can activate the p53 tumor suppressor signaling pathway (Gao and Hardwidge, 2011). Finally, Rps3 has been described to selectively modulate NF-κB target gene expression (Wan et al., 2007).

5. eIF3 complex

Translation initiation factor 3 represents the largest and most complex translation initiation factor with molecular weight reaching 360 kDa in yeast (Khoshnevis et al., 2012) and 800 kDa in mammals (Damoc et al., 2007). Despite recent progress in structural biology thanks to the development of different visualization techniques (like cryo-EM, cryo-electron microscopy etc.), the complete structure of eIF3 has still not been solved due to the presence of flexible domains.

5.1. Composition of yeast and mammalian eIF3

In yeast, eIF3 comprises five essential subunits (a/Tif32, b/Prt1, c/Nip1, i/Tif34, and g/Tif35) which are required for translation *in vivo*. In the past, it was believed that eIF3 also comprises one more subunit, termed j/Hcr1, but collected evidence strongly indicates that this represents only an eIF3 associated factor and not a *bona fide* subunit (Valášek et al., 2017).

The schematic structures of yeast and mammalian eIF3 proteins are depicted in **Figure 10**. One can observe that mammalian eIF3 is even more complex, comprising 12 subunits designated a-m (the eIF3j is not counted in the a to m list, as it was shown to be just an eIF3 associated factor, similarly as in yeast). Out of the eIF3 mammalian subunits, 5 represent orthologs of yeast subunits, and 7 are additional proteins (eIF3d, e, f, h, k, l, and m) (Damoc et al., 2007).

The central structural motif is composed of 8 subunits (a, c, e, f, h, l, k, m) creating an octamer and representing a typical five-lobed structure with additional appendages that can be also found in other proteins, which also constitute PCI domains like eIF3 (abbreviation stands for **P**roteasome-**C**op9 signalosome-e**I**F3 and is found in the listed proteins) (Pick et al., 2009; Wagner et al., 2016). With a little imagination, a homunculus configuration featuring head, right and left arm and feet can be distinguished in the structure (**Figure 10**). The octameric core is further interconnected with the so-called YLC (**Y**east **L**ike **C**ore) module composed of eIF3 a, b, g and i subunits. In the depicted model based on our previous research (Wagner et al., 2014; Wagner et al., 2016), the c/Nip1 subunit of eIF3 is not present in the mammalian YLC complex, even though it is present in the yeast eIF3.

Two studies I contributed to throughout my Ph.D. studies deal with the role of individual mammalian eIF3 subunits during initiation, as well as during reinitiation, details of which can be found in the List of publications.

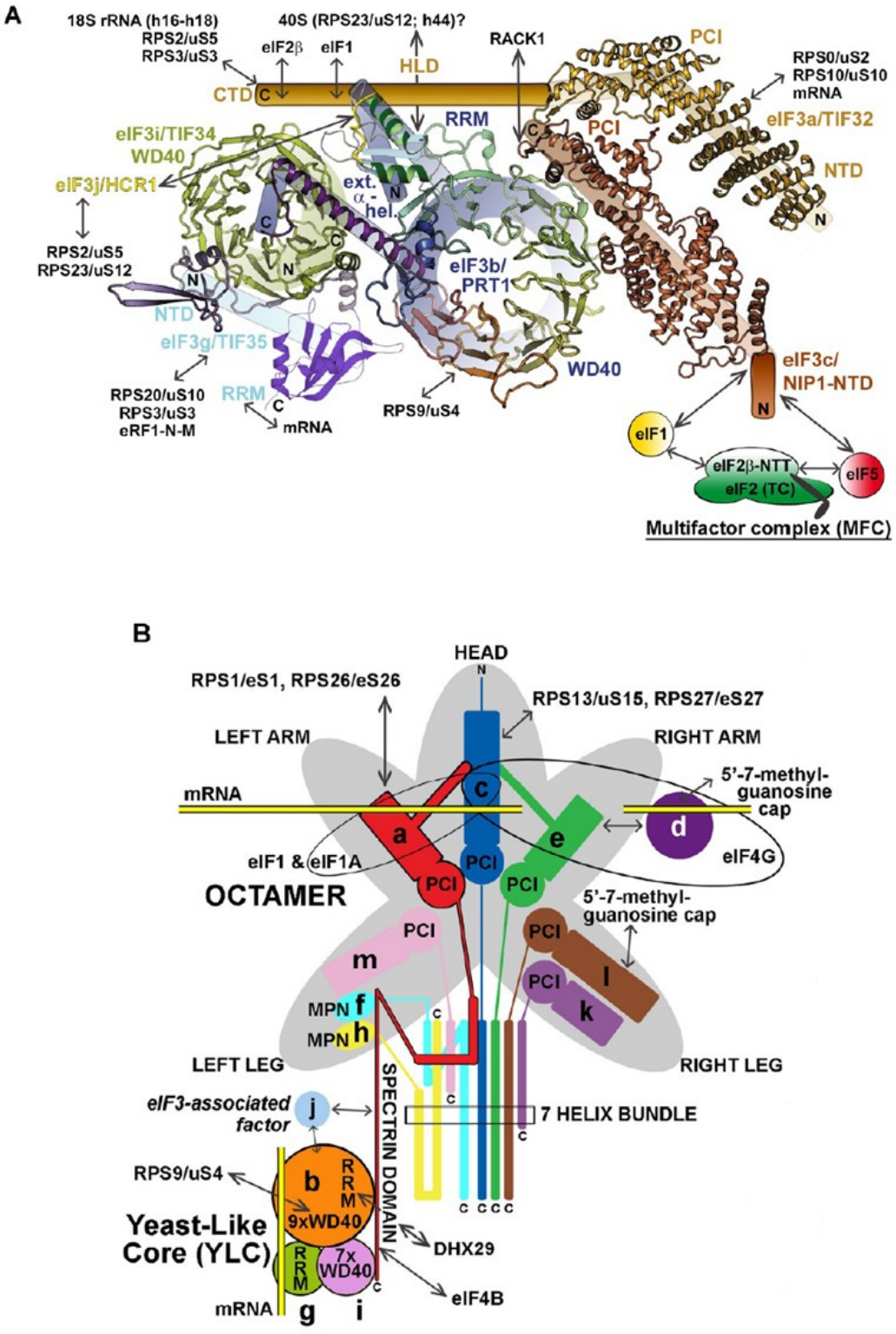

Figure 10 (A) Schematics of the yeast eIF3 complex. A best possible 3D model composed of all available structures of the eIF3 subunits and their domains. Arrows indicate all known interactions of eIF3 domains with other eIFs, ribosomal proteins and mRNA. NTD, N-terminal domain; CTD, C-terminal domain; HLD, HCR1-like domain; RRM, RNA recognition motif; PCI, PCI domain; WD40, WD40 domain; TC, ternary complex. Adapted from (Valášek et al., 2017). **(B) A schematic model of human eIF3.** Contacts of eIF3 with other proteins are depicted too. Adapted from Wagner et al., (2016).

5.2. Functional versatility of the eIF3 complex

eIF3 is one of the most versatile initiation factors. In addition to its multiple subunit composition, this also stems from the fact that eIF3, unlike other eIFs, interacts with the solvent-exposed side of the 40S subunit and its long extensions, represented in eIF3a-CTD and eIF3c-NTD, nearly encircle the whole 40S. They are thus able to contact both the mRNA entry and exit channels, and also reach nearly to the P-site of the ribosome (Cate, 2017; Llácer et al., 2015; Des Georges et al., 2015). This way, the entire 40S subunit is expansively occupied by eIF3, which then, in turn, can control not only the vast majority of translation initiation steps, but also different translational processes that follow (please note that as mentioned in Section 0, eIF3 does not dissociate from 40S immediately after initiation).

Briefly, eIF3 was found to stimulate the TC (ternary complex) and mRNA recruitment to the pre-initiation complex (Asano et al., 2000; Valášek et al., 2002). It has also a role in stabilizing the 48S PIC and subsequent control of scanning (Chiu et al., 2010; áet al., 2012; Obayashi et al., 2017). Additionally, it has a direct influence over the fidelity of the start codon selection (Valášek et al., 2004)

The eIF3 functions in steps following initiation are supported by our recent research in which we demonstrated its persistence on the 40S even during the first few steps of elongation after which it gradually drops off (Mohammad et al., 2017). The role of eIF3 in termination that was described above suggests for its *de novo* reassociation with the 80S ribosomes during termination to control even a broader scale of translation events (Beznosková et al., 2013, 2015).

The list of extra-initiation eIF3 functions can be completed by its role in the ribosomal recycling (Pisarev et al., 2007), nonsense-mediated decay pathway (Morris et al., 2007; Isken et al., 2008; Flury et al., 2014), translational reinitiation (Szamecz et al., 2008; Munzarová et al., 2011) as well as cell cycle dynamics (Kovařík et al., 1998).

5.3. The a/Tif32 subunit of yeast eIF3

The a/Tif32 subunit with molecular weight reaching 110.3 kDa represents the largest protein of the yeast eIF3 complex. Following its discovery in 1998, it was named Rpg1 (**R**equired for **P**assage through **G**1) and characterized as a factor required for passage through the G1 phase of the cell cycle (Kovařík et al., 1998). However, its role as an integral part of the eIF3 complex emerged soon (Valášek et al., 1998).

In *S. cerevisiae*, the *TIF32* gene encodes a protein product of 964 amino-acids in length. The protein contains several protein domains for different functional contacts. (**Figure 10**). In the N-terminal half, it is the previously mentioned PCI domain (amino acids 321-496), serving as a scaffold for other protein interactions (Khoshnevis et al., 2014). This part of the protein was characterized to bind to the Rps0A protein and also interacts with the C-terminal domain of c/Nip1 subunit (Valášek et al., 2002; Kouba et al., 2012; Khoshnevis et al., 2012). The Rps0A-a/Tif32-NTD contact represents an important intermolecular bridge between the eIF3 complex and the 40S subunit since the truncation of the first 200 a/Tif32 amino acids severely compromises their mutual association (Szamecz et al., 2008). Besides, regions responsible for interaction with specific structural features in mRNAs containing REI-permissive short uORFs (such as *GCN4* and *YAP1*) are also located in the N-terminus of the subunit. Those contacts are needed to promote the gene-specific translational control mechanism of reinitiation, which regulates the translation of the main open reading frame (Szamecz et al., 2008; Munzarová et al., 2011).

The C-terminal part of the a/Tif32 protein is slightly acidic and rich in prolines. It also harbors the so-called HLD (Hcr1-like) domain (amino acids 625-869, sharing 25 % identity with the Hcr1 protein) that mediates the interaction between the a/Tif32 subunit and j/Hcr1, b/Prt1 and eIF1 proteins (Valášek et al., 2002). Besides, the C-terminus of a/Tif32 interacts with eIF2 and also with the ribosomal region at the entry channel, formed by ribosomal proteins Rps2, Rps3, and the helices h16-18 of the 18S rRNA (**Figure 10**A) (Valášek et al., 2002; Valášek et al., 2003; Chiu et al., 2010).

Last, the proline-rich region at the C-terminus of a/Tif32 (amino acid 926-947) shows homology with so-called Microtubule-associated proteins (MAPs) and suggests another function of a/Tif32 protein in influencing microtubule dynamics in *S. cerevisiae*, most probably connected to its role in the cell cycle (Hašek et al., 2000).

6. Aims of the work

The main goal of this Thesis was to reveal and further describe molecular details of the role of the 40S ribosomal protein Rps3 and translation initiation factor eIF3 in the process of translational termination and regulation of stop codon readthrough in yeast. This Thesis also participates in further characterization of mammalian eIF3 complex and dissects its roles in general translational initiation as well as in the specific regulatory mechanism of translational reinitiation. However, main experimental work focused on the characterisation of the Rps3 protein in translation termination.

List of specific objectives:

- To identify Rps3 residues that influence the accuracy of stop codon recognition and provide a detailed characterization of their functional contributions using a multitude of different translational assays.
- To investigate the aspects of how Rps3 influences the stop codon readthrough on different stop codons and in various nucleotide contexts.
- To determine how Rps3 affects stop codon decoding by near-cognate tRNAs.
- To examine molecular details of the interaction between a/Tif32 and Rps3 *in vitro*.
- To analyze the composition of the pre-termination 80S ribosomal complexes in *rps3* mutants with defects in stop codon recognition.
- To examine in *vitro* interaction between mammalian eIF3a, eIF3g and eIF3i subunits.

7. Material and methods

7.1. Laboratory equipment

7.1.1. Centrifuges

Beckman Coulter Allegra® X-15R Centrifuge, rotor SX 4750A

Beckman Coulter optima^{TM}L-90K Ultracentrifuge, rotors SW 41 and SW 32 Ti

Biosan Centrifuge/vortex Multi Spin MSC-300

Eppendorf Centrifuge 5414D

7.1.2. Electrophoresis

Bio-Rad Criterion Cell

Bio-Rad Mini-Sub Cell GT Cell

Bio-Rad Wide-Sub Cell GT Cell

Bio-Rad PowerPac Basic power supply

Bio-Rad PowerPac HC power supply

Bio-Rad PowerPac Universal power supply

7.1.3. Other equipment

Beckman Coulter DU®530 Life Science UV/VIS Spectrophotometer

BioComp Gradient Master

Bio-Rad Gene Pulser Xcell Electroporation System

Biosan Bio RS-24 Rotator

Biosan Mini Rocker MR-1

Biosan Multi RS-60 Rotator

BMG Fluostar microplate reader

Brandel BR-188 Density Gradient Fractionation System

Eppendorf Mastercycler ep gradient S

Eppendorf Thermomixer Comfort

Syngene G:BOX iChemi – gel documentation and analysis system

Multitron INFORS HT shaker

Scientific Industries Vortex Genie 2

Thermo Scientific SGD2000 Slab Gel Dryer

7.2. Chemicals

10x TBE (Bio-Rad)

10x TBS (Bio-Rad)

10x TG (Bio-Rad)

10x PBS (prepared in IMG service facility)

Agar (Serva)

Bacto Peptone (Becton, Dickinson and Company)

Bacto Tryptone (Becton, Dickinson and Company)

Bacto Yeast Extract (Becton, Dickinson and Company)

Bio-Rad Protein Assay Kit (Bio-Rad)

Bromophenol Blue (Sigma)

β-Mercaptoethanol (Sigma)

Complete Protease Inhibitor Mix tablets, EDTA free (Roche)

Criterion Precast Gels, 4-20% Tris-HCl, 1mm, 12+2 Well Comb 45 µl and 18 Well Comb, 30 µl (Bio-Rad)

D-glucose (Lachner)

ECL™ Anti Rabbit IgG, HRP-linked whole antibody (from donkey) (GE Healthcare)

EDTA (Sigma)

EDTA-free Complete Protease Inhibitor Mix tablets (Roche)

Electroporation cuvettes (Eppendorf)

EP-MAX™ 10B Competent Cells (Bio-Rad)

Ethidium bromide (Serva)

Gel Code® Blue Stain Reagent (Thermo Scientific)

Glutathione Sepharose™ 4B (GE Healthcare)

HEPES (Serva)

Imidazole (Fluka)

Igepal CA-630 (Sigma)

Lithium acetate dihydrate (Sigma)

PEG (Fluka)

PMSF (Serva)

SDS solution 20% (Sigma)

SeaKem® LE Agarose (Lonza)

Sodium Floride (Fluka)

Subcloning Efficiency^{TM} DH5α^{TM} Competent Cells (Invitrogen)

Sucrose (Fluka)

SuperSignal West Femto Maximum Sensitivity Substrate (Thermo Scientific)

Tris (Serva)

Triton X-100 (Sigma)

Tween 20 (Sigma)

7.3. Solutions

B buffer for GST-pull downs: 20 mM HEPES (pH 7.5); 75 mM KCl; 0.1mM EDTA; 2.5mM $MgCl_2$; 0.05% IGEPAL, 1 % milk (wt % - percentage by mass)

Blotting buffer (1000 ml for 1 blotting): 700 ml dH_2O; 200 ml methanol; 100 ml 10xTG

GA solution: 20mM Tris-HCl (pH 7.5); 50 mM KCl; 10 mM $MgCl_2$

GB solution: 20mM Tris-HCl (pH 7.5); 50 mM KCl; 10 mM $MgCl_2$; 45% sucrose

GF buffer: 25 ml GA; 5 mM NaF; 1 mM DTT; 1 mM PMSF; 1 μg/ml Aprotinin; 1 μg/ml Leupeptin; 1 μg/ml Pepstatin; 1 tablet of Complete EDTA-free Protease Inhibitor Mix

LiAc solution: 0.1 M LiAc

Sample buffer for agarose gel electrophoresis 6x: 30 % glycerol; 0.25 % bromophenol blue

SDS-Loading Buffer 6x: 3.3 ml 1 M Tris (pH 7.5); 6 ml glycerol; 1.2 g SDS; heat up and add 150 μl β-ME and a little bit bromophenol blue

SDS-PAGE running buffer: 1xTG; 0.1% SDS

TBS-T buffer: 1x TBS; 0.1% Tween 20

TE buffer: 10 mM Tris-HCl pH 7.5, 1 mM EDTA

Transformation solution (1X LiAc/TE/PEG) : 40% PEG 4000, 0.1 M LiAc, 10 mM Tris-HCl pH 7.5, 1 mM EDTA

Saccharomyces cerevisiae strains

Strain	**Genotype**	**Source or reference**
H417	*MATa leu2-3,-112, ura 3-52, trp1*	Klaus Nielsen
H424	*MATα leu2-3,-112 ura3-52 trp1 Δ gcn2-del' tif32-del'*	Klaus Nielsen
ME538	*MATa leu2-3,-112, ura3-52, trp1Δ, rps3::KanMX [YCp-pRPS28-N-FLAG-RPS3-WT-LEU2]*	This study
ME540	*MATa leu2-3,-112, ura3-52, trp1Δ, rps3::KanMX [YCp-pRPS28-N-FLAG-RPS3-K108E-LEU2]*	This study
KPH28	*MATa leu2-3,-112, ura3-52, trp1Δ, rps3::KanMX [YCp-pRPS28-N-FLAG-RPS3-R116D-LEU2]*	This study
KPH31	*MATa trp1, leu2-3,-112, ura3-52, rps3Δ::kanMX+tif32Δ(hisG) [YCp-RPS3, LEU2 and pRS314-TIF32, URA3]*	This study
KPH46	*MATa trp1, leu2-3,-112, ura3-52, rps3Δ::kanMX+tif32Δ(hisG) [pRPS28-FLAG-RPS3-URA3 and pRS314-TIF32 WT, TRP1]*	This study
ME166	*MATa, trp1, leu2-3,-112, ura3-52, rps3Δ::kanMX [pRPS28-FLAG-RPS3-URA3]*	This study
KPH126	*MATa, trp1, leu2-3,-112, ura3-52, rps3Δ::TRP1 [pRPS28-N-FLAG-RPS3-WT-LEU2]*	This study
KPH127	*MATa, trp1, leu2-3,-112, ura3-52, rps3Δ::TRP1 [pRPS28-N-FLAG-RPS3-K108E-LEU2]*	This study
KPH128	*MATa, trp1, leu2-3,-112, ura3-52, rps3Δ::TRP1 [pRPS28-N-FLAG-RPS3-R116D-LEU2]*	This study

7.4. *E.coli* strains

Strain	Genotype	Source
DH5α	fhuA2 Δ(argF-lacZ)U169 phoA glnV44 Φ80 Δ(lacZ)M15 gyrA96 recA1 relA1 endA1 thi-1 hsdR17	Invitrogen
BL21	B F⁻ *ompT gal dcm lon* $hsdS_B(r_B^- m_B^-)$ $[malB^+]_{K\text{-}12}(\lambda^S)$	Stratagene

7.5. Plasmids

Plasmid	Description	Source or reference
KP26	pRS314 TIF32-WT	This study
KP27	pRS314 tif32-box32	This study
KP28	pRS314 tif32-box33	This study
B196	pRS315 TIF32-WT	(Valášek et al., 2002b)
PBB119	pRS315-tif32-box32	A. Hinnebusch
PBB120	pRS315-tif32-box33	A. Hinnebusch
ME102	YEplac195-RPS28promoter-N-FLAG-RPS3	(Ferreira-Cerca et al., 2007)
ME111	YEplac195-RPS28promoter-N-FLAG	P. Milkereit
ME112	YEplac181-RPS28promoter-N-FLAG	This study
ME113	YEplac181-RPS28promoter-N-FLAG-RPS3 WT	This study
ME231	YCPlac111-RPS28promoter-N-FLAG	This study
ME119	YCplac111-RPS28promoter-N-FLAG-rps3 K108A N111A R117A	This study
ME232	YCPlac111-RPS28promoter-N-FLAG-RPS3 WT	This study
ME233	YCPlac111-RPS28promoter-N-FLAG-rps3 R116A Y120A R124A Y125A E128A	This study

KP44	YCPlac111-RPS28promoter-N-FLAG-rps3 Y120A R124A Y125A E128A	This study
pDH12-24	YCPlac111-rps3-R117D	A. Hinnebusch
ME234	YCPlac111-RPS28promoter-N-FLAG-rps3 K108E	This study
KP15	YCPlac111-RPS28promoter-N-FLAG-rps3 R116D	This study
ME235	YCPlac111-RPS28promoter-N-FLAG-rps3 N111A	This study
ME215	YCPlac111-RPS28promoter-N-FLAG-rps3 R116A	M.Jansen
KP37	YCPlac111-RPS28promoter-N-FLAG-rps3 K108E R116D	This study
B596	high copy wt *SUI1* in *TRP1* plasmid from YEplac112	C. Fekete
pTH477	high copy PGK-Renilla-Firefly R/T cassette (stop codon of Renilla is UGA-C; for read-through measurements) in *URA3* plasmid from YEplac195	(Keeling et al., 2004a)
pTH460	high copy PGK-Renilla-Firefly R/T cassette (stop codon of Renilla is replaced with CAA-C [coding triplet]; for control read-through measurements) in *URA3* plasmid from YEplac195	(Keeling et al., 2004a)
PBB82- TMV	high copy PGK-Renilla-Firefly R/T cassette (stop codon of Renilla is UGA-CAAUUA; for read-through measurements) in *URA3* plasmid from YEplac195	(Beznosková et al., 2015)
PBB84- PDE2	high copy PGK-Renilla-Firefly R/T cassette (stop codon of Renilla is UGA-CAAGAA; for read-through	(Beznosková et al., 2015)

	measurements) in *URA3* plasmid from YEplac195	
PBB85-SUP45	high copy PGK-Renilla-Firefly R/T cassette (stop codon of Renilla is UGA-AUAAAU; for read-through measurements) in *URA3* plasmid from YEplac195	(Beznosková et al., 2015)
KP22	high copy PGK-Renilla-Firefly R/T cassette (stop codon of Renilla is UGA-C; for read-through measurements) in *TRP1* plasmid from YEplac112	This study
KP23	high copy PGK-Renilla-Firefly R/T cassette (stop codon of Renilla is replaced with CAA-C [coding triplet]; for control read-through measurements) in *TRP1* plasmid from YEplac112	This study
KP34	high copy PGK-Renilla-Firefly R/T cassette (stop codon of Renilla is UGA-A; for read-through measurements) in *TRP1* plasmid from YEplac112	This study
KP35	high copy PGK-Renilla-Firefly R/T cassette (stop codon of Renilla is UGA-G; for read-through measurements) in *TRP1* plasmid from YEplac112	This study
KP36	high copy PGK-Renilla-Firefly R/T cassette (stop codon of Renilla is UGA-U; for read-through measurements) in *TRP1* plasmid from YEplac112	This study
ZP40 YEp-R/T-UAGC-W	high copy PGK-Renilla-Firefly R/T cassette (stop codon of Renilla is UAG-C; for read-through measurements) in *TRP1* plasmid from YEplac112	This study

KP41	high copy PGK-Renilla-Firefly R/T cassette (stop codon of Renilla is UAA-C; for read-through measurements) in *TRP1* plasmid from YEplac112	This study
pTH477	high copy PGK-Renilla-Firefly R/T cassette (stop codon of Renilla is UGA-C; for read-through measurements) in *URA3* plasmid from YEplac195	(Keeling et al., 2004b)
pTH460	high copy PGK-Renilla-Firefly R/T cassette (stop codon of Renilla is replaced with CAA-C [coding triplet]; for control read-through measurements) in *URA3* plasmid from YEplac195	(Keeling et al., 2004b)
PBB75	high copy PGK-Renilla-Firefly R/T cassette (stop codon of Renilla is UGA-A; for read-through measurements) in *LEU2* plasmid from YEplac181	(Beznosková et al., 2015)
PBB76	high copy PGK-Renilla-Firefly R/T cassette (stop codon of Renilla is UGA-G; for read-through measurements) in *LEU2* plasmid from YEplac181	(Beznosková et al., 2015)
PBB77	high copy PGK-Renilla-Firefly R/T cassette (stop codon of Renilla is UGA-U; for read-through measurements) in *LEU2* plasmid from YEplac181	(Beznosková et al., 2015)
Yep-R/T-UAGC-L	high copy PGK-Renilla-Firefly R/T cassette (stop codon of Renilla is UAG-C; for read-through measurements) in *LEU2* plasmid from YEplac181	(Beznosková et al., 2015)
Yep-R/T-UAAC-L	high copy PGK-Renilla-Firefly R/T cassette (stop codon of Renilla is UAA-C; for read-through measurements) in *LEU2* plasmid from YEplac181	(Beznosková et al., 2015)

YEplac112	high copy cloning vector, *TRP1*	(Gietz and Akio, 1988)
YEplac195	high copy cloning vector, *URA3*	(Gietz and Akio, 1988)
YCplac111	single copy cloning vector, *LEU2*	(Gietz and Akio, 1988)
pRS314	low copy cloning vector, *TRP1*	(Sikorski and Hieter, 1989)
pTH335	high copy *URA3* vector (pRS426) containing genomic DNA surrounding the *tW(CCA)G1* gene	(Beznosková et al., 2015)
PBB97	high copy *tC(GCA)P1* in *URA3* plasmid from pRS426	(Beznosková et al., 2015)
PBB90	high copy *URA3* vector (pRS426) containing the *tY(GUA)J2* wild-type gene (*SUP4*)	(Beznosková et al., 2015)
PBB150	high copy *tQ(CUG)M* in *URA3* plasmid from pRS426	(Beznosková et al., 2015)
pGEX-5X-3	cloning vector for GST fusions	(Smith and Johnson, 1988)
B75-pGEX TIF32-CTD	GST-TIF32-CTD fusion plasmid from pGEX-5X-3	(Valášek et al., 2002b)
SW118-pGEX Tif32-CTD-box32	GST-TIF32-CTD-box32 fusion plasmid from pGEX-5X-3	A. Hinnebusch
SW119-pGEX TIF32-CTD-box33	GST-TIF32-CTD-box33 fusion plasmid from pGEX-5X-3	A. Hinnebusch
ME194-pT7-RPS3-WT	T7 promoter-based plasmid containing RPS3-WT	This study
ME229-pT7-rps3-K108E	T7 promoter-based plasmid containing rps3-K108E	This study
KP14-pT7-rps3-R116D	T7 promoter-based plasmid containing rps3-R116D	This study
KP19-pGEX-rps3 WT	GST-RPS3 fusion plasmid from pGEX-5X-3	This study

KP20-pGEX-rps3-K108E	GST-rps3-K108E fusion plasmid from pGEX-5X-3	This study
KP21-pGEX-rps3-R116D	GST-rps3-R116D fusion plasmid from pGEX-5X-3	This study
pGADT7-TIF32 1-200	T7 promoter-based plasmid containing TIF32 1-200	(Kouba et al., 2012a)
pGADT7-TIF32 200-396	T7 promoter-based plasmid containing TIF32 200-396	(Kouba et al., 2012a)
pT7-TIF32 490-790	T7 promoter-based plasmid containing TIF32 490-790	(Valášek et al., 2001)
pT7-TIF32	T7 promoter-based plasmid containing TIF32-WT	(Valášek et al., 2001)
pT7-tif32-box32	T7 promoter-based plasmid containing tif32-box32	A. Hinnebusch
pT7-tif32-box33	T7 promoter-based plasmid containing tif32-box33	A. Hinnebusch
B471	*kanMX::TRP1* disruptor	(Voth et al., 2003)
B897	pFA6a-KanMX4	(Wach et al., 1994)
ME148	YEplac181-RPS28promoter-N-FLAG-rps3-E28R	M.Jansen
ME149	YEplac181-RPS28promoter-N-FLAG-rps3-E31R	M.Jansen
ME150	YEplac181-RPS28promoter-N-FLAG-rps3-E32R	M.Jansen
ME122	YEplac181-RPS28promoter-N-FLAG-rps3-137	M.Jansen
ME147	YEplac181-RPS28promoter-N-FLAG-rps3-138	M.Jansen
ME123	YEplac181-RPS28promoter-N-FLAG-rps3-139	M.Jansen
ME114	YEplac181-RPS28promoter-N-FLAG-rps3-141	M.Jansen

ME115	YEplac181-RPS28promoter-N-FLAG-rps3-145	M.Jansen
ME116	YEplac181-RPS28promoter-N-FLAG-Rps3 F107A	M.Jansen
ME117	YEplac181-RPS28promoter-N-FLAG-Rps3-Δ205	M.Jansen
ME118	YEplac181-RPS28promoter-N-FLAG-Rps3-Δ190	M.Jansen

7.6. Oligonucleotides

Primer name	Primer sequence (5´to 3´)
KP19_R	CGTAAGCAGCTCTATCGATAGCCAAACCG
KP20_F	CGGTTTGGCTATCGATAGAGCTGCTTACG
KP21_BamHI	ACTGGATCCGAATGGTCGCTTTAATCTCT
KP22_SalI	AATGTCGACCTAAGCTTCAACTGGTTCAG
TK132_RPS3 UPTAG	AAACAAACTACAAAAATGGATGTCCACGAGGTCTCTTCACA GCAGTAAGCCTAATCCGTACGCTGCAGGTCGAC
TK133_RPS3 DOWNTAG	ATTTAATAATTAAATCTACGGTGTCGGTCTCGTAGCCTGTGC ATAAATGAAGCCAATCGATGAATTCGAGCTCG
TK105_RPS3 UP	TGTTTTGATAACTGAAAATAAAACAGCAAACAAACTACAAA AATG
TK106_RPS3 DOWN	ATTATTGTACTTATAGTTTATTTATGTATTTAATAATTAAATC TA
TK148	GAATCTATGAAATTCGCATTGTTGGCCGGTTTGGCTATCAGA GCAGCTGCTTACGGTGTCGTC
TK149	CCGGCCAACAATGCGAATTTCATAGATTC
TK150	GCTATCGCGAGAGCTGCTGCCGGTGTCGTCGCAGCAGTTATG GCATCTGGTGCTAAG
TK151	CGGCAGCAGCTCTCGCGATAGCCAAACCG
ME104	CTATGAAATTCGAGTTGTTGAACGG
ME105	CCGTTCAACAACTCGAATTTCATAG

ME106	CAAATTGTTGGCCGGTTTGGCTATCAG
ME107	CTGATAGCCAAACCGGCCAACAATTTG
GeneString Rps3	ATGGATTACAAGGATGACGACGATAAGGGTACCGGATCCAT GGTCGCTTTAATCTCTAAGAAAAGAAAGCTAGTCGCTGACG GTGTCTTCTACGCTGAATTGAACGAATTCTTCACCAGAGAAT TAGTGAAGAAGGTTACTCCGGTGTTGAAGTCCGTGTCACTCC AACCAAGACCGAAGTTATCATCAGAGCTACCAGAACTCAAG ATGTTTTGGGTGAAAACGGTAGAAGAATCAACGAATTAACT TTGTTGTTCAAAAGAGATTCAAGTACGCTCCAGGTACTATTG TCTTATATGCTGAAAGAGTTCAAGACCGTGGTTTGTCCGCTG TCGCTCAAGCTGAATCTATGAAATTCAAATTGTTGAACGGTT TGGCTATAGAAGAGCTGCTGCCGGTGTCGTCGCAGCAGTTAT GGCATCTGGTGCTAAGGGTTGTGAAGTTGTTGTTTCCGGTAA ACTAAGAGCTGCCAGAGCTAAGGCTATGAAATTTGCTGACG GTTTCTTGATCACTCTGGTCAACCAGTCAACGACTTCATTGA CACTGCTACTAGACACGTCTTGATGAGACAAGGTGTTTTGGG TATC

7.7. Cultivation media

7.7.1. Bacterial cultivation media and plates

LB medium: 10 g/l Bacto tryptone; 5 g/l Bacto yeast extract; 5 g/l NaCl (if needed add Ampicilin/Kanamycin to final concentration 150 mg/l (Amp) or 40 mg/l for Kanamycin).

LB/Amp plates: 10 g/l Bacto tryptone; 5 g/l Bacto yeast extract; 5 g/l NaCl; 25 g/l agar; Ampicilin to final concentration 150 mg/l.

LB/Kan plates: 10 g/l Bacto tryptone; 5 g/l Bacto yeast extract; 5 g/l NaCl; 25 g/l agar; Kanamycin to final concentration 40 mg/l.

SOC medium: 20 g/l Bacto tryptone; 5 g/l Bacto yeast extract; 0.6 g/l NaCl; 0.2 g/l KCl; 3.5 g/l glucose.

7.7.2. **Yeast cultivation media and plates**

YPD medium: 20 g/l Bacto peptone, 10 g/l Bacto yeast extract, 20 g/l glucose.
YPD plates: 20 g/l Bacto peptone, 10 g/l Bacto yeast extract, 20 g/l glucose, 25 g/l agar.
SD medium: 1.45g/l YNB (yeast nitrogen base without aa and ammonium sulfate), 5 g/l ammonium sulfate, 20 g glucose.
SD plates: 1.45g/l YNB (yeast nitrogen base without aa and ammonium sulfate), 5 g/l ammonium sulfate, 20 g glucose, 25g/l agar.
5-FOA plates: 1.44 g/l YNB (yeast nitrogen base without aa and ammonium sulfate), 5 g/l ammonium sulfate, 20 g glucose, 25 g/l agar, 20 mM uracil, 1g/l 5-FOA.

7.8. Bacterial and yeast cultivation

7.8.1. **Bacterial cultivation**

Bacteria were grown in liquid media at 37 °C while shaking or on agar solid media at 37 °C in the incubator.

7.8.2. **Yeast cultivation**

Yeast strains were grown in liquid media at 30 °C while shaking or on agar solid media at 30 °C, 34 °C or 37 °C in the incubator.

7.8.3. **Strains storage**

Bacterial strains were stored for short terms on agar plates at 4 °C, for long terms at -80 °C in 40 % glycerol. Yeast strains were stored for short term on agar solid media at 4 °C, for long term at -80 °C in 20 % glycerol.

7.8.4. **Doubling time calculation**

Doubling time was calculated for specific strains in this study according to the formula: $[\ln(2)/\ln(OD_{END}/OD_{BEGIN})]$*time of growing (min).

7.9. DNA manipulation

7.9.1. Plasmid DNA isolation - QIAprep Spin Miniprep Kit (Qiagen)

The miniprep procedure is based on alkaline lysis of bacterial cells followed by adsorption of DNA onto the silica membrane in the presence of high salt. Bacteria are lysed under alkaline conditions, and the lysate is subsequently neutralized and adjusted to high-salt binding conditions. DNA is adsorbed onto silica membrane while cellular proteins and metabolites flow through and are discarded. DNA is eluted with water or EB buffer.

Kit contains: QIAprep Spin Columns, Buffer P1, Buffer P2, Buffer N3, Buffer PB, Buffer PE, RNase A.

Protocol:

- inoculate *E. coli* cells bearing plasmid of interest into 4-6 ml of LB/Amp/Kan media and grow them overnight
- pellet the cells by centrifugation at 13 000 rpm for 30 seconds
- resuspend the pellet in 250 µl Buffer P1 (containing RNAse A) and transfer to a microcentrifuge tube
- add 250 µl Buffer P2 (lysis buffer) and mix thoroughly by inverting the tube 4-6 times
- add 350 µl Buffer N3 (neutralization buffer) and mix immediately and thoroughly by inverting the tube 4-6 times
- centrifuge at 13 000 rpm for 10 minutes
- apply the supernatant to the spin column by decanting or pipetting
- centrifuge at 13 000 rpm for 30 seconds, discard the flow-through
- wash the spin column by adding 0.75 ml of Buffer PE and centrifuging at 13 000 rpm for 30 seconds
- discard the flow-through and spin for an additional 1 minute to remove residual wash buffer
- place the spin column in a clean microcentrifuge tube
- to elute DNA add 50 µl of water or EB buffer to the center of the spin column, let stand for 1 minute and centrifuge at 13 000 rpm for 1 minute. The usual approximate concentration of the isolated DNA is 400 ng/µl.

7.9.2. **DNA modifications**

DNA digestions were performed with restriction endonucleases according to manufacturer´s instructions (Roche or NEB) found on their websites.
For ligation reactions, the T4 DNA Ligase (Roche) was used together with the supplied reaction buffer. T4 DNA ligase catalyzes the formation of phosphodiester bonds between neighboring 3´-hydroxyl and 5´-phosphate ends in the dsDNA. It can join not only cohesive ends but also the blunt ones and can repair single-stranded nicks in dsDNA.

7.9.3. **Agarose gel electrophoresis**

Agarose gel electrophoresis is a method used to separate DNA, RNA or protein molecules by size. This is achieved by moving negatively charged nucleic acid or protein molecules through an agarose matrix that is placed in an electric field. For estimating size and concentration of DNA on the gel 1Kb Plus DNA Ladder (Invitrogen) was loaded.
Protocol:

- dissolve 1 % (or different concentration if needed) of agarose in 1x TBE by heating in a microwave oven
- after cooling down to approximately 60 °C add ethidium bromide to final concentration 0.5 μg/ml
- stir the solution to disperse the ethidium bromide, then pour it into the gel rack and insert the comb
- when the gel has cooled down and become solid, remove the comb and put the gel with the rack into a tank with 1xTBE
- load the samples mixed with Sample buffer for agarose gel electrophoresis
- apply current, voltage 5 V/cm for approximately 1 hour or different time/voltage depending on which bands you need to separate (longer run in lower voltage for better separation)

7.9.4. **Isolation of DNA from the gel - QIAEX®II Gel extraction Kit (Qiagen)**

Extraction and purification of DNA fragments are based on the solubilization of agarose and selective adsorption of DNA to the silica-gel particles in the presence of high salt. All impurities such as agarose, proteins, salts and ethidium bromide are removed during washing steps. The elution of the DNA is accomplished with a low-salt solution or water.

Kit contains: QIAEX II Suspension, Buffer QX1 and Buffer PE

Protocol:

- excise the DNA band from agarose gel with a clean scalpel
- weigh the gel slice in a microcentrifuge tube and add 3 volumes of Buffer QX1 to 1 volume of the gel
- add 15 µl QIAEX II Suspension to the sample and mix
- incubate at 50 °C for 10 minutes, mix every 2 minutes to keep QIAEX II in suspension
- centrifuge at 13 000 rpm for 30 s, remove supernatant
- wash the pellet with 500 µl of Buffer QX1
- wash the pellet twice with 500 µl of Buffer PE
- air-dry the pellet for 10 – 15 minutes until the pellet becomes white
- to elute DNA add 20 µl of water, resuspend the pellet by vortexing and incubate in 50°C for 10 minutes
- centrifuge at 13 000 rpm for 30 s and save the supernatant

7.9.5. **Polymerase chain reaction (PCR)**

The polymerase chain reaction was used to construct several recombinant plasmids in this study. The typical PCR amplification program is shown below. The annealing temperature was adjusted according to the melting temperature of primers used in the reaction. Elongation time was adjusted according to the length of a fragment being amplified (1 minute/1kb length).

Initial denaturation	95°C	5 minutes	
Denaturation	95°C	1 minute	
Annealing	55°C	1 minute	25x
Elongation	72°C	1 minute	
Final elongation	72°C	5 minutes	
	4°C	hold	

Composition of the PCR reactions: 1x ThermoPol Reaction Buffer (NEB), 800 µM dNTP mix (200 µM of each), ~20 ng template DNA, 2 µM primers, 1 Unit VentR® DNA Polymerase (NEB), ddH_2O to a final volume of 50 µl.

7.9.6. **Sequencing**

All sequencing analysis was conducted at SeqMe facility. The sequencing reaction was prepared according to the instructions on their website-for details please see: https://www.seqme.eu/documents/standardseq-instructions-cz.pdf.

Precisely, 500 ng of plasmid DNA, together with 25 pmol of specific primers was prepared in 10 µl of dH_2O . The sequencing data were analyzed with the Clone Manager program.

7.9.7. **Introducing DNA into target cells**

Transformation of *E. coli* by electroporation method

This method was used for introducing newly constructed vectors directly from the ligation reaction.

Protocol:

- thaw electrocompetent cells (EP-MAX™ 10B Competent Cells) on ice
- mix 20 µl of the cells and 1 µl of the ligation reaction in a clean microcentrifuge tube
- transfer the mixture into precooled electroporation cuvette
- apply the pulse in the Gene Pulser Xcell Electroporation System using the „*E. coli* 1mm“ setting (conditions: 1.8 kV; 25 µF; 200 Ω)
- immediately add 180 µl of SOC medium and transfer to a clean microcentrifuge tube
- incubate for 30 minutes at 37 °C with shaking

- spread on LB/Amp or LB/Kan plate

Transformation of *E. coli* by the heat-shock method

This method was used for introducing plasmid DNA isolated by QIAprep Spin Miniprep Kit.

Protocol:

- thaw competent cells (Subcloning Efficiency™ DH5α™ Competent Cells) on ice
- mix 100 µl of the cells with 1 µl of plasmid DNA (500 ng) and incubate on ice for 30 minutes
- heat shock the cells at 42 °C for 30 seconds
- add 200 µl of SOC medium and incubate for 30 minutes at 37 °C with shaking
- spread on LB/Amp or LB/Kan plate depending on plasmid resistance

Transformation of *S. cerevisiae* by LiAc transformation method

Protocol:

- grow the *S. cerevisiae* strain you want to transform in 50 ml of liquid media (SD or YPD) to OD_{600} of approximately 0.5
- centrifuge at 2500 rpm for 3 minutes and discard the supernatant
- wash the cells in 1 ml of (1xLiAc/TE)
- resuspend the cells in 200 µl (1xLiAc/TE)
- add 20 µl of Salmon sperm DNA (Invitrogen)
- mix 50 µl of the cells with 1 µl of plasmid DNA (500 ng) and 300 µl 1x transformation solution (PEG/LiAc/TE)
- incubate at 30°C for 30 minutes with shaking
- incubate at 42°C for 15 minutes without shaking
- add 1 ml dH2O and centrifuge at 2 500 rpm for 3 minutes, discard the supernatant
- add 200 µl dH2O and spread on an appropriate plate

7.10. Protein manipulation

7.10.1. SDS-PAGE

Protocol:

- mix samples for SDS-PAGE with 6x sample loading buffer and boil for 5 minutes at 95 °C
- put Criterion Precast Gel into the electrophoretic tank and pour in SDS-PAGE running buffer
- load samples on Criterion Precast Gel
- load Precision Plus Protein^{TM} Standards Dual Color (Bio-Rad)
- apply current, voltage 200 V for 1 hour

7.10.2. Western Blotting

Protocol:

- gel after SDS-PAGE wash with dH_2O
- assemble the blotting device (cathode, plastic net, sponge, filter paper, gel, nitrocellulose membrane, filter paper, 2 sponges, plastic net, anode)
- fill the blotting tank with cool blotting buffer
- apply current, voltage 25 V for 1.5 hour
- reassemble the blotting device
- incubate the membrane in blocking solution (5 % milk in TBS-T) for 1 hour
- cut the membrane apart if probing for different antibodies
- incubate every part of membrane with appropriate primary antibody diluted in blocking solution overnight at 4 °C
- wash the membrane strips with TBS-T twice for 10 minutes
- incubate the membrane strips with secondary antibody diluted in TBS-T for 1 hour
- wash the membrane strips with TBS-T twice for 10 minutes

Chemiluminescent detection

Protocol:

- assemble the membrane strips

- incubate with SuperSignal West Femto Maximum Sensitivity Luminol and SuperSignal West Femto Maximum Sensitivity Stable Peroxidase Buffer (1:1 solution) for 1 minute
- take pictures in G: BOX iChemi with various exposure times

Staining and drying of polyacrylamide gels

Protocol:

- after running SDS-PAGE, wash the gel for 5 minutes in water
- incubate 1 hour with Gel Code® Blue Stain Reagent
- destain 1 hour or overnight in water
- put on wet filter paper and dry on a gel dryer

7.10.3. Purification of GST fused proteins

Protocol:

- inoculate in 5ml of LB/Amp BL21 cells bearing desired pGEX plasmid and grow overnight at 37 °C
- inoculate 2 ml from the overnight culture into 200ml of LB/Amp, grow to OD_{600} of 0.7
- induce by 1mM IPTG and grow 2 hours in 37 °C or at 30 °C or 16 °C overnight depending on the expected protein yield
- harvest cells by centrifugation at 4 750 rpm for 14 minutes at 4 °C and wash 10 ml of ice-cold water
- resuspend in 10 ml of ice-cold 1xPBS
- break by FastPrep instrument, speed 6, 1 minute
- add 400µl of 20 % TritonX-100 and rotate 30 min at 4 °C
- get rid of cell debris by centrifugation at 13 000 rpm for 10 minutes in 4 °C
- add 400 µl of glutathion-Sepharose™ (50 % slurry) to the supernatant and rotate for at least 30 minutes in room temperature
- spin down at 1 000 rpm for 5 minutes at 4 °C
- wash 3 times with 5 ml of ice-cold 1xPBS
- resuspend in 100 µl 1xPBS
- make 50 µl aliquots and freeze them at -80 °C

- use one aliquot for estimation of protein amount by SDS-PAGE: 3-4 dilutions of BSA (2µg, 5 µg, 12 µg) and 3µl, 6 µl, 9 µl and 18 µl of the GST fusion protein (or adopt the protein/BSA amount with respect to the protein yield).

7.10.4. TnT® Quick Coupled Transcription/Translation System (Promega)

Protocol:

- upon removal from storage at -80 °C, rapidly thaw the TnT® Quick Master Mix by hand and place on ice
- assemble the reaction components in a 0.5 ml microcentrifuge tube and gently mix by pipetting

Components	Standard Reaction
TnT® Quick Master Mix	40 µl
[^{35}S]methionine (1000Ci/mmol at 10mCi/ml)	2µl
DNA template (0.5 µg)	2.4 – 5 µl
Nuclease-Free water to a final volume of	50 µl

- incubate reaction at 30 °C for 60 to 90 minutes

7.10.5. GST-pull down experiment

Protocol:

- before use add 1mM DTT and possibly 1 % fat-free powder milk to buffer B
- for one reaction: 250 µl buffer B + GST fusion protein (1–5 µg; it should be the same amount of every GST fusion protein used in one assay; always make control with GST only) + 10 µl of TnT® reaction
- vortex at low rpm
- incubate rotating for 2 hours in 4 °C
- spin down at 500 rpm for 2 minutes, remove supernatant
- wash 3 times with 1 ml of ice-cold 1xPBS

- run SDS-PAGE with the entire reaction, always load Input (usually 20 %, 2 µl of the TnT® reaction)
- subject the dried gel to autoradiography
- The quantifications were performed in Quantity One software and at least three independent experiments were analyzed. The percentages shown were obtained as a ratio of autoradiography signal between the wild type and mutant protein and were normalized to the corresponding inputs.

7.10.6. Sucrose density gradient preparation

Protocol:

- gradients should be prepared a day before the main experiment
- prepare gradient solutions bearing the required percentage of sucrose according to the table below- usually Grad 45% (1xGB buffer- contains 45% saccharose), Grad 30%, Grad 7.5%, Grad 5% according to the number of gradients you will use:

number of grads	Grad 30%			Grad 7.5%			Grad 5%		
	2	4	6	2	4	6	2	4	6
GA solution	5 ml	9 ml	13 ml	15 ml	25 ml	35 ml	16 ml	24 ml	32 ml
GB solution	10 ml	18 ml	26 ml	3 ml	5 ml	7 ml	2 ml	3 ml	4 ml
1M DTT	15 µl	27 µl	39 µl	18 µl	30 µl	42 µl	18 µl	27 µl	36 µl

- label Beckman Polyallomer tubes using special labeling toll
- put the tubes into a rack on the Gradient Master
- load Grad 5 % solution with a syringe up to the mark
- load Grad 45 % solution with a syringe under the Grad 5 % solution until the tube is full, make sure these two solutions do not mix
- put caps on the tubes
- Run the Gradient Master (setting: Grad; choose correct rotor, SW41 or SW32-Ti; 5-45% program or other percentages if preparing different gradient)
- gently remove caps and put tubes into the buckets
- weigh the buckets with gradients and balance the opposite ones with 1xGF buffer
- store at 4 °C overnight

7.10.7. Polysomal profile analysis

For polysome profile analysis, strains were grown in yeast extract-peptone-dextrose (YPD) media at 30◦C to OD_{600} of ∼1. Cycloheximide (50 µg/ml) was added 5 min before harvesting, and WCEs were prepared in the breaking buffer GF (composition listed in Section 7.3).

Cells were broken FastPrep Instrument (MPBiomedicals) at the intensity level of 5 in two 20 s cycles.

Fifteen A_{260} units of WCEs (100x diluted sample: A_{260}x100=number of units/ml) were loaded on a 5–45% sucrose gradient prepared as described in the previous Section and spun in the ultracentrifuge at 39 000 rpm for 2.5 h in an SW41 Ti rotor (Beckman Coulter). Resulting gradients were scanned at A_{260} using Teledyne ISCO UA-6 UV/VIS gradient detector in the cold room at 4˚C to visualize the ribosomal species.

7.10.8. Analysis of pre-terminating 80S resedimented species

For the heavy polysomal analysis, the following protocol was used:

Protocol:

- grow yeast cell culture in 250 ml of liquid media to OD_{600} of 1
- incubate with 50 µg/ml cycloheximide for 5 min while shaking
- cool the culture down by adding two times 50 ml of ice in a Falcon tube
- add 3.4 ml of formaldehyde 36.5 % (final concentration 0.5 %), incubate for 30 minutes on ice
- add 12.5 ml of glycine (2.5 M stock solution)
- spin down at 4 000 rpm, 25 min at 4 °C
- resuspend the cells in 10 ml of GF buffer
- centrifuge at 2 500 rpm for 3 minutes at 4 °C
- resuspend the cells in 1 ml per gram (wet weight) of cells in GF buffer
- add 4 mm diameter acid-washed glass beads equal to one half of the total volume of resuspended cells
- break by the FastPrep Instrument (MPBiomedicals) - speed 5, 40 s
- centrifuge at 13 000 rpm for 10 minutes at 4 °C to preclear the WCE
- transfer supernatant into pre-cooled microcentrifuge tube
- centrifuge at 13 000 rpm for another 10 minutes at 4 °C to clear the WCE

- carefully transfer WCE into the new pre-cooled microcentrifuge tube
- measure A_{260} (100x diluted sample: A_{260}x100=number of units/ml)
- For analysis of pre-terminating 80S pre-TCs, prepare 100 U of the WCE into final volume 1ml (dilute with 1xGF buffer) and carefully load on on the top of the 5-45% gradient prepared in SW32 Ti big tubes according to instructions in Section 7.10.6. Make sure that the opposite tubes are balanced.
- screw on the caps
- put in the ultracentrifuge and run at 16 800 rpm overnight for 13.5 hours at 4 °C in vacuum
- after the centrifugation process, fractionate the gradients in the cold room using Brandel BR-188 Density Gradient Fractionation System, collect 30 fractions (approx. 1200 µl each)
- take the last five fractions (from pentasome and more), pool them and dilute them slowly drop by drop in the cold room with ice-cold 1xGA buffer. The goal is to get sucrose concentration under 5 % (the samples will be loaded on the new 5-45 % gradient again). The dilution is followed by concentrating steps in Ultracel-100k Amicons to get the final volume of the pooled sample to around 200-300 µl.
- In the first step, dilute to approx. 15ml- (2x dilution)
- spin for 4 °C, 4 000 g in Ultracel-100k Amicons to the lower volume- approximately 25 mins
- dilute with 1xGF and repeat the procedure until the concentration of sucrose is lower than 5%
- transfer the sample to pre-cooled 1.5 ml ice-cold microcentrifuge tube
- add 6 ul of RNAseI and incubate 25 min at 25 °C temperature in the shaker (300 rpm)
- load thus obtained samples on a new 5-45 % sucrose gradient
- subject them to another round of sedimentation for 2.5 hrs at 4 °C at 39 000 rpm (SW41 rotor)
- Separate the gradient once more-collect 14 fractions, each containing 12 drops (approx.600 ul)
- Select 80S fractions (usually F9+F10 fractions) and precipitate with 1ml of ethyl alcohol (stored in the freezer)

- Store precipitated fractions in -20 °C freezer at least overnight
- Spin the tubes 30 min at 4 °C
- Discard liquid phase
- Wash once more with 1ml of ethanol
- Spin 5 min at 4 °C
- Discard the supernatant; remove even the last drop of liquid; let the pellet dry for at least 30 min
- Add 1x loading buffer, usually 50 µl per tube
- Vortex 15 s, let stand 10 min at room temperature to allow the pellet dissolve
- Vortex once more
- Heat up at 95°C for 5 min
- Spin down for 30 s and pool the corresponding fractions to one tube (F9+F10)
- Prepare the two-fold dilution series for Western blot, store the prepared fractions at -20 °C until ready to load the prepared dilutions on the gel and perform Western blot as in 7.10.2.

7.11. Dual-luciferase assay

The readthrough measurements were carried out using a bicistronic reporter plasmid bearing a *Renilla* luciferase gene followed by an in-frame firefly luciferase gene, in between separated with either a tetranucleotide termination signal (UGA-C) or, in control purposes, the CAA sense codon followed by cytosine (see (Beznosková et al., 2015)). In indicated cases, the termination signal and/or the following nucleotide context was modified.

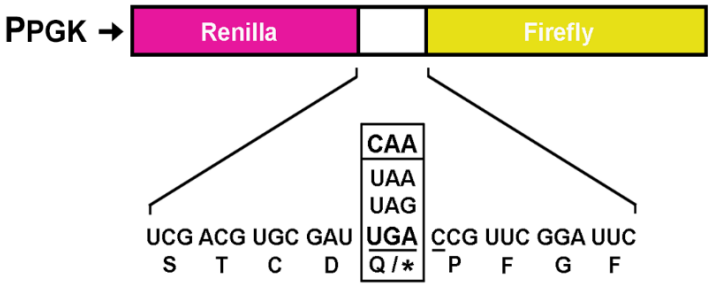

Figure 11 Schematics of the standard dual luciferase readthrough reporter constructs. Variable stop codons (or a CAA coding codon) under the P_{PGK} promoter are shown. Adapted from (Beznosková et al., 2015).

The assay was originally developed by the Atkins group (Grentzmann et al., 1998) and uses the commercial kit Dual-Glo Assay manufactured by Promega, UK.

The experiment was conducted as follows: individual transformants of strains transformed with the luciferase-based reporter constructs were inoculated into 150 µl of SD liquid medium into the wells of a 96 well plate and grown with shaking (550 rpm, 30 °C) overnight.

After overnight growth, 10 µl of these cultures were transferred into 150 µl of fresh SD media in a new 96 well microplate and grown for an additional 4 h.

Immediately before the luciferase measurements, 40 µl of passive lysis buffer (PLB, Promega, UK) was added per well. Culture+PLB mixture (40 µl) was then mixed with 40 µl of the Firefly luciferase substrate in the wells of an opaque 96 well plate, incubated for 20 min with shaking (550 rpm, 30 °C) and Firefly luciferase activity was measured in a BMG Fluostar microplate reader. Stop-and-Glo reagent (40 µl) was then added per well, and the *Renilla* luciferase activity was measured after another 20 min of incubation (550 rpm, 30 °C). Readthrough values were calculated as follows: *F/R* ratios were calculated by dividing Firefly and *Renilla* values from each well. The percentage of readthrough was then calculated by dividing the *F/R* ratio of a construct containing the relevant stop codon by the *F/R* ratio of control construct without any stop codon. Each experiment was repeated at least three times and the value represents mean ± SD from triplicates (n = 6).

8. Results

This Thesis contains published and unpublished data from 3 projects in which I participated during my PhD.studies in the laboratory. All projects deal with eukaryotic translation, either in yeast or in mammals, with eIF3 being the connecting factor between them.

8.1. Identification and selection of *rps3* and *a/tif32* mutants of *S. cerevisiae* with defects in translation

8.1.1. Preparation of constructs for analysis of mutant *rps3* and *a/tif32* alleles

The list of all plasmids is given in Section 7.5 in Material and methods.

For detection and analytical purposes, all *RPS3* containing plasmids were constructed with the FLAG-tag at the N-terminus of the *RPS3* coding region. Thus modified *RPS3* genes were inserted under the control of pRPS28B promoter which is commonly used for the expression of the small ribosomal proteins (Ferreira-Cerca et al., 2007). The KP22, KP23, KP34, KP35, KP36, ZP40, and KP41 plasmids were constructed by inserting the 4567 bp fragment digested with *AlwNI* and *NsiI* from pTH477, pTH460, PBB75, PBB76, PBB77, Yep-R/T-UAGC-L and Yep-R/T-UAAC-L, respectively, into the YEplac112 digested by *AlwNI* and *NsiI*.

The KP26, KP27, and KP28 plasmids were constructed by inserting the 4675-bp *ApaI-SacI* cleaved fragment obtained from cleavage of B196, PBB119 and PBB120, respectively, into the pRS314 digested by *ApaI* and *SacI*.

KP44 was obtained by inserting the *BamHI* and *BmgBI* digested GeneString fragment *RPS3* (sequence listed in Section 7.6 Oligonucleotides) obtained by gene synthesis in Invitrogen into the *BamHI-BmgBI* digested ME232.

The KP19, KP20 and KP21 plasmids were created by inserting the *BamHI-SalI* digested PCR product obtained with primers KP21_BamHI and KP22_SalI using ME232, ME234 and KP15 as templates, respectively, into pGEX5X-3 vector digested with *BamHI* and *SalI*.

The KP37 plasmid was created by fusion PCR as follows. The ME234 plasmid was used as a template for 2 PCR reactions, one with primers KP19_R and TK135, second with primers KP20_F and TK134. The resulting products were used for a fusion PCR with primers TK134 and TK135. The product was digested by *BamHI* and *PstI* and ligated into the ME231 plasmid backbone cut with *BamHI* and *PstI*.

The ME112 plasmid was created by inserting the 282 bp *EcoRI-BamHI* fragment from ME111 into the YCplac111 digested with EcoRI and BamHI.

The ME113 plasmid was created by PCR using ME102 as a template with primers TK134 and TK135 and the resulting product was cut by *BamHI* and *PstI* and ligated into the ME112 cut with *BamHI* and *PstI*.

The ME119 plasmid was created by fusion PCR as follows. The ME232 plasmid was used as a template for 2 PCR reactions, one with primers TK151 and TK134, second with primers TK150 and TK135. The resulting products were used for a fusion PCR with primers TK134 and TK135. The product was digested by *BamHI* and *PstI* and ligated into the YEplac111 vector cut with *BamHI* and *PstI*.

The ME231 plasmid was created by inserting the 282-bp *EcoRI-BamHI* fragment from ME111 into the YCplac111 digested with *EcoRI* and *BamHI*.

The ME232 plasmid was created by PCR using ME102 as a template with primers TK134 and TK135 and the resulting product was cut with *BamHI* and *PstI* and ligated into the ME231 cut with *BamHI* and *PstI*.

The ME233 plasmid was created by fusion PCR as follows. The ME232 plasmid was used as a template for 2 PCR reactions, one with primers TK149 and TK134, second with primers TK148 and TK135. The resulting products were used for a fusion PCR with primers TK134 and TK135. The resulting product was digested by *BamHI* and *PstI* and ligated into the ME231 *BamHI* and *PstI* cut vector.

The ME234 plasmid was created by fusion PCR as follows. The ME232 plasmid was used as a template for 2 PCR reactions, one with primers ME105 and TK134, second with primers ME104 and TK135. The resulting products were used for a fusion PCR with primers TK134 and TK135. The resulting product was digested with *BamHI* and *PstI* and ligated into the ME231 *BamHI* and *PstI* cut vector.

The KP15 plasmid was created by fusion PCR as follows. The ME232 plasmid was used as a template for 2 PCR reactions, one with primers KP20_F and TK134, second with primers KP19_R and TK135. The resulting products were used for a fusion PCR with

primers TK134 and TK135. The resulting product was digested by *BamHI* and *PstI* and ligated into the ME231 *BamHI* and *PstI* cut vector.

The ME235 plasmid was created by fusion PCR as follows. The ME232 plasmid was used as a template for 2 PCR reactions, one with primers ME107 and TK134, second with primers ME106 and TK135. The resulting products were used for a fusion PCR with primers TK134 and TK135. The resulting product was digested by *BamHI* and *PstI* and ligated into the ME231 *BamHI* and *PstI* cut vector.

Finally, the ME194, ME229 and KP14 plasmids were created by inserting the 1033-bp *BamHI-PstI* fragment from ME232, ME234, and KP15 respectively, into the pT7 plasmid digested by *BamHI* and *PstI*.

8.1.2. Preparation of yeast strains for analysis of mutant *rps3* and *a/tif32* alleles

Preparation of *Δrps3* strain

The *S. cerevisiae* strain bearing a deletion of *RPS3* gene (ME166) was prepared using H417 as parental strain (genetic background MATa Δleu2-3, -112, Δura 3-52, trp1Δ). The H417 strain was transformed with *rps3::KanMX* deletion cassette prepared by two successive PCR reactions (**Figure 12**). The 1st PCR was carried out with pFA6a-KanMX4 (B897) as template using TK132-RPS3uptag and TK133-RPS3downtag primers. The resulting 1617 bp product was subjected to the 2nd PCR with TK105-RPS3UP and TK106-RPS3DOWN primers. The amplified cassette was introduced into the H417 strain and the resulting transformants were selected on plates containing geneticin. The successful *rps3* deletion was further verified by PCR.

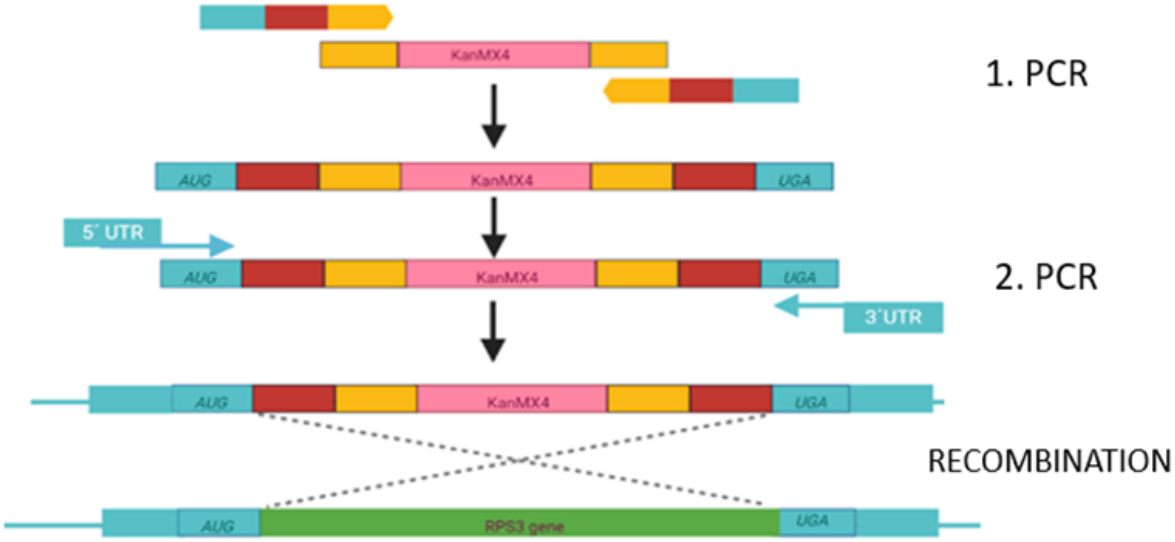

Figure 12 Schematics of preparation of *RPS3* deletion cassette. The deletion *rps3:: KanMX* cassette was prepared in two successive PCR reactions. In the first PCR, uptag and downtag primers were used with added specific 18 nts from the yeast ORF to be deleted. In the second PCR, primers (called UP and DOWN) with added sequences that are complementary to the 3´ UTR regions of the gene of interest were used. The complete cassette was integrated into the yeast chromosome by homologous recombination.

Preparation of *Δrps3Δtif32* strain

The *S. cerevisiae* strain bearing double deletion *Δrps3Δtif32* (KPH31) was generated by a genetic cross between single deletion strains *Δrps3* (ME538) and *Δtif32* (H424) and selection for a haploid spore growing on SD plates with geneticin and tryptophan was performed. At the same time, selection pressure was applied for keeping the resident URA3-based covering plasmid.

Additional yeast strains bearing different mutant *rps3* and *a/tif32* alleles were prepared from the corresponding parental strains by the so-called plasmid shuffling. During this process, the covering wt allele containing an URA plasmid is evicted by selection on solid media containing 5-fluoroorotic acid, and a plasmid carrying different auxotrophic selection marker and mutant or wt allele of interest is transformed at the same time. This way strains ME538 (bearing YCp111-pRPS28-N-FLAG-RPS3-WT), ME540 (bearing YCp111-pRPS28-N-FLAG-RPS3-K108E) and KPH28 (YCp-pRPS28-N-FLAG-RPS3-R116D) were prepared from the parental ME166 strain.

Preparation of strains with regained sensitivity to aminoglycoside antibiotics

In order to measure readthrough defects of *rps3* mutants in the presence of miscoding agent paromomycin, the usage of strains without the *KanMX4* resistance gene was required. Both agents, paromomycin and kanamycin, belong to the same group of antibiotics and therefore resistance to geneticin confers resistance to paromomycin as well, which had to be avoided (See further in Section 8.2.4).

For this reason, the *S. cerevisiae* strains with *RPS3* gene interrupted by *TRP1* containing cassette were prepared. In particular, the KPH126, KPH127 and KPH128 were prepared from the ME538, ME540, and KPH28 parental strains, respectively, by transforming with the *NotI* digested *kanMX::TRP1* deletion cassette (B471). Subsequent simultaneous selection for tryptophan prototrophy and sensitivity to geneticin was performed to obtain the desired strains.

8.1.3. Phenotypic analyses of yeast strains bearing mutant *rps3* and *a/tif32* alleles

List of analyzed *rps3* and *tif32* mutations

Table 2 lists all the *rps3* and *a/tif32* mutations that were tested in the Thesis. The specific localization of mutations in Rps3 on its protein structure is presented in **Figure 13.** The localization of modified residues of a/Tif32 in protein structure is not shown, because to this date the complete structure of this protein has not been solved. The structural data for segments containing amino acid residues 496-813 and 939-964 are still missing, with the latter segment corresponding to positions of the analyzed a/*tif32 box* mutations. The best available a/Tif32 structure is shown later in **Figure 34.**

Table 2 List of a/*tif32* and *rps3* mutants analysed in this Thesis.

rps3 mutants	
E28A E31A E32A	*[rps3-137]*
E28R E31R E32R	*[rps3-138]*
R40A T42A T44A K45A E47A	*[rps3-139]*
Y87A E89A R90A	*[rps3-141]*
Q56A D57A E61A N62A R64A R65A N67A E68A	*[rps3-145]*
K108A N111A R117A	*[rps3-149]*
R116A Y120A R124A Y125A E128A	*[rps3-151]*
Y120A R124A Y125A E128A	*[rps3-152]*
E28R	
E31R	
E32R	
F107A	
K108E	
R116D	
R116A	
R117D	
N111A	
K108E R116D	
rps3_1-190	[truncation from aa 190]
rps3_1-205	[truncation from aa 205, rps3-153]
tif32 mutants	
box32	[10 Ala stretch 951-960 aa]
box33	[10 Ala stretch 955-964 aa]

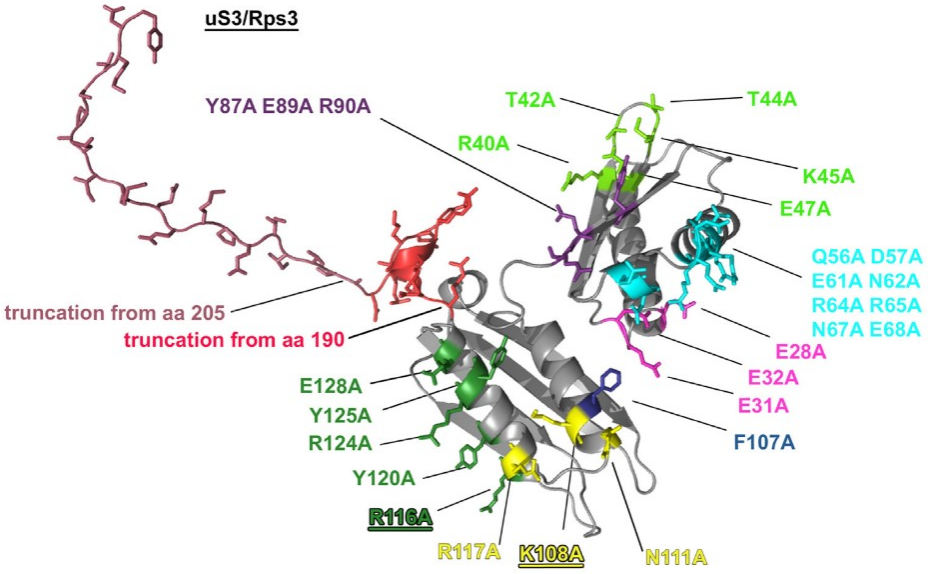

Figure 13 Yeast Rps3 protein and the schematic of its site-directed mutagenesis. Color coded mutations/deletions of Rps3 residues either in blocks or individually are shown in the structure. Figure prepared using structure (PDB ID 4V88).

Growth assays of *rps3* and *tif32* strains

As the first step in our study, we analyzed the impact of the aforementioned mutant rps3 alleles on S.cerevisiae colony growth in both, standard and increased temperature conditions, in a spot assay test on solid media. As can be seen in **Figure 14**, only two of the tested mutants (rps3-139 and rps3-153) possessed a significant slow growth phenotype (Slg^-) that was not further intensified during cultivation at 37 ˚C, indicating for a defect in the translation process. Those two were then selected for further analyses by polysome profiling shown in the next section. The mutant rps3Δ190, bearing a C- terminal truncation from aminoacid 190 was lethal. However, this was not surprising, because it had been already shown earlier that the amino acids 1-211 of Rps3 are essential for the viability of *S. cerevisiae* (Limoncelli et al., 2017).

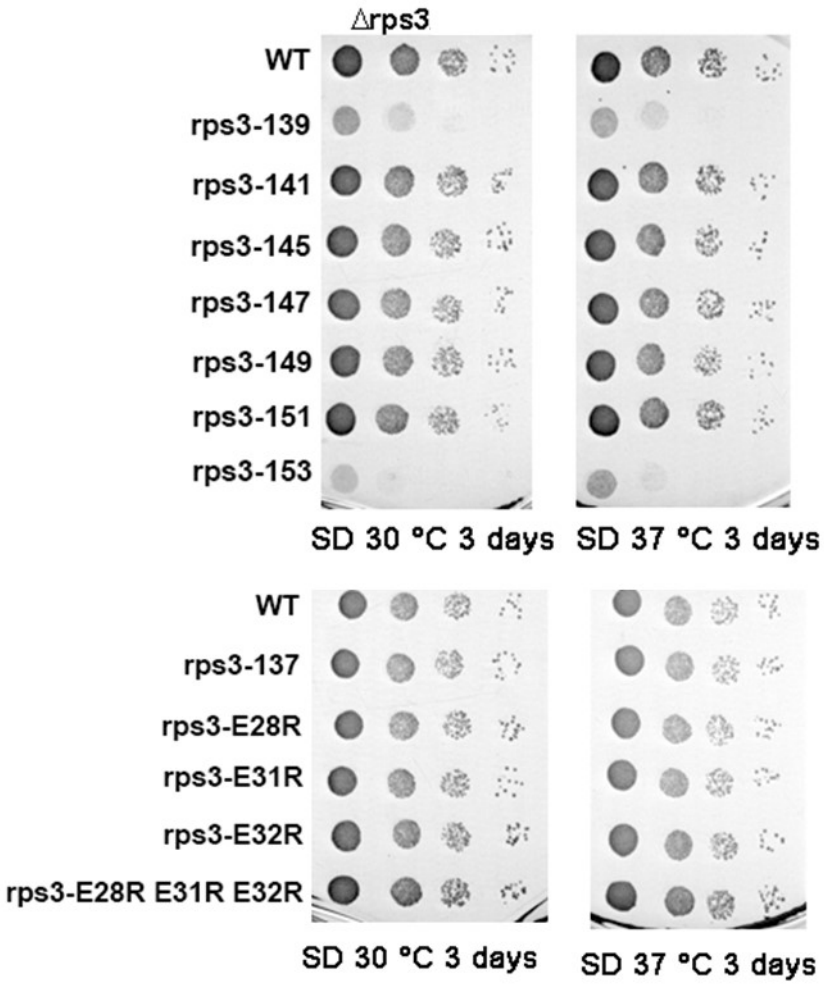

Figure 14 The *rps3-139* and *rps3-153* mutants display slow growth phenoype. Transformants of ME166 (*rps3Δ*) bearing the indicated wt or mutant alleles were spotted in four serial 10-fold dilutions on SD medium and incubated at 30◦C and 37◦C. Expermiment performed by Myrte Jansen.

Next, the spot assay test was also used for the analysis of eIF3 mutants in a/Tif32 as this subunit was previously shown to interact with Rps3 (Chiu et al., 2010). Specifically, *a/tif32-box32* and *a/tif32-box33* mutants were selected because of the observed defect in translation termination (see Section 8.2.5) The schematics of *a/tif32* box mutations is given in **Figure 15**B. Both of these mutations are located practically at the extreme C-terminus of a/Tif32 which encompasses amino acids from 792 to 964. In contrast to *a/tif32-box32* mutant, the a/*tif32-box33* mutant possessed a mild slow-growth phenotype, again indicating for a partial defect in translation (**Figure 15**A).

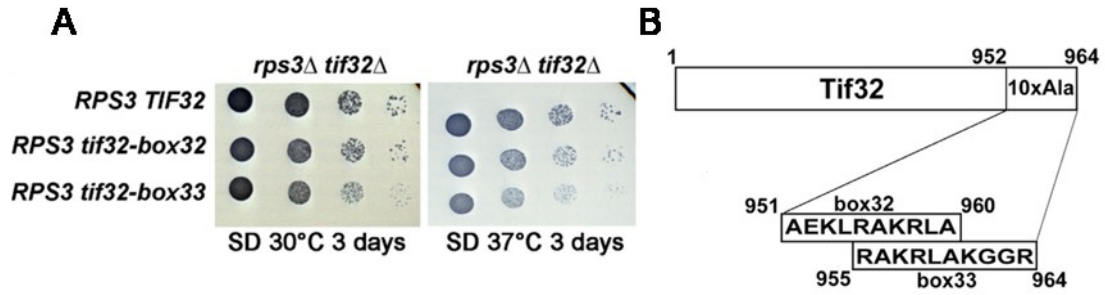

Figure 15 (A) The *a/tif32-box33* mutation causes a mild slow growth phenotype. Transformants of KPH31 (*rps3Δ tif32Δ*) bearing the indicated wt or mutant *TIF32* alleles were spotted in four serial 10-fold dilutions on SD medium and incubated at 30◦C and 37◦C**. (B) The schematic of the a/Tif32 protein with amino acids that were substituted with a stretch of alanines and named box32 and box33.**

Last set of spot assay tests concerned specifically selected *rps3* mutants, which did not show any prominent phenotype in previous spot assay analyses of multiple *rps3* mutants tested but were found to show an impact on the precision of stop codon recognition when tested in reporter assay monitoring stop codon readthrough (*rps3-K108E* and *rps3-R116D*) (See Section 8.2.1). Therefore it was interesting to find out whether the presence of defects in translation of these mutants could be uncovered by the simultaneous presence of *a/tif32* mutation by testing for the possible mutual genetic interaction between the two genes.

Interestingly, the mild slow growth phenotype of the *a/tif32-box33* mutant was further exacerbated when combined with the *rps3-R116D* mutation which itself did not significantly affect the yeast growth (**Figure 16**), indicating an additive interaction.

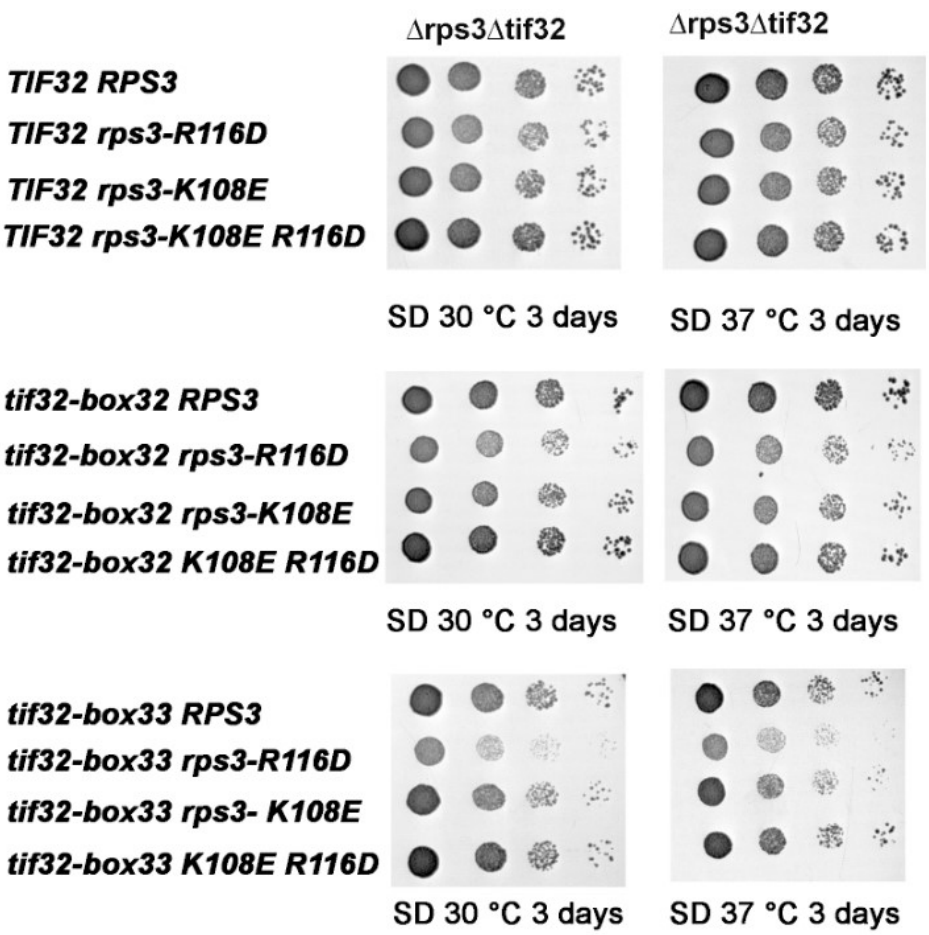

Figure 16 The *rps3-K108E, rps3-R116D and rps3-K108E R116D* mutations do not cause defects in growth. Only when the mutations of *rps3-R116D* and *a/tif32-box33* are combined, the slow growth phenotype of the former mutant is exacerbated. Transformants of KPH31/KPH46 (*rps3Δtif32Δ*) bearing the indicated wt or mutant *TIF32* and *RPS3* alleles were spotted in four serial 10-fold dilutions on SD medium and incubated at 30°C and 37°C.

Polysome profile analysis of *rps3* and *tif32* strains

The general translational activity of all *rps3* and *a/tif32* mutants that showed compromised translation, selected either according to the growth defects detected in spot assay (*rps3-139* and *rps3-153*) or according to the decreased fidelity of translation termination measured *via* the dual-luciferase reporter assay (*rps3-K108E* and *rps3-R116D*), was further investigated by polysome profiling technique.

Polysome profiling is used to separate the translated mRNAs on a sucrose gradient according to the number and type of translating ribosomes already from the 1960s (Britten and Roberts, 1960). First, cells are lysed and loaded on top of a 15–45 % sucrose gradient (details are described in Section 7.10.6) and ultracentrifuged at high speed. Next, the absorbance of the gradient fractions is monitored at A_{260} using a flow cell coupled to a spectrophotometer. A characteristic profile is recorded: untranslated mRNAs (top fractions)

are separated from mRNAs containing only 40S and 60S subunits, and also from 80S-associated and polysome-associated mRNAs (bottom fractions). Efficiently translated mRNAs are bound with multiple ribosomes (which are called the polysomes). From the resulting graph (**Figure 17**), the peaks corresponding to 40S (43S), 80S, di-, tri- and further polysomes can be derived. According to the recorded curve profile and to the so-called polysome to monosome (P/M) ratio (a ratio of actively translating ribosomes to those not engaged in active translation), one can easily observe if tested mutants have defects in ribosomal biogenesis or even in individual translational steps.

As can be deduced from the representative polysomal profiles of *rps3-139* and *rps3-153* mutants, both of them possess a defect in the 40S ribosomal biogenesis. Most ribosomes are dissociated into 40S and 60S subunits and due to the defect in the 40S biogenesis, only the peak representing the large 60S subunit is extremely increased. Besides, the global translation is shut down as indicated by the low polysomal peak area (**Figure 17**).

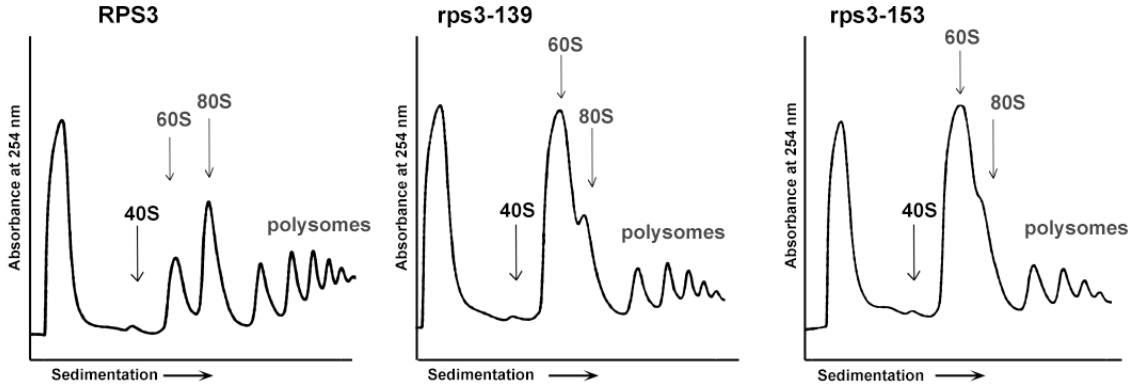

Figure 17 *Rps3-139* and *rps3-153* possess a defect in 40S ribosomal subunit biogenesis. Transformants of ME166 (*rps3Δ*) bearing the indicated wt or mutant *RPS3* alleles were grown in the YPD medium at 30°C to an OD600 ~1 and processed for polysomal gradient analysis as described in Material and methods. Positions of 40S, 60S, and 80S species are indicated by arrows.

In **Figure 18**, the polysomal profiles of the *rps3-K108E* and *rps3-R116D* mutants are recorded. In contrast to *rps3-149* nad *rps3-153* mutants, the *rps3-K108E* and *rps3-R116D* did not exhibit any significant defect in neither the 40S biogenesis nor in the rate of translation. Only for *rps3-R116D* mutant, a moderate reduction in the P/M ratio can be seen, suggesting a reduced rate of general translation initiation. This may probably explain the exacerbation of the Slg$^-$ phenotype observed in the double *tif32-box33 rps3-R116*D mutant **(Figure 16)**, while the sensitivity of the spot assay method was most likely not sensitive enough to detect such a mild defect in translation for the single *rps3-R116*D mutant **(Figure 16)**. However, because no obvious perturbations of the 60S to 40S subunits ratio were

evident (**Figure 18**), the translation defects of the *rps3-K108E* and *rps3-R116D* do not arise from any abnormalities in their 40S biogenesis or stability of their mature 40S subunits but could indicate altered small subunit function. Indeed, this was later confirmed by showing the defects of these mutants in controlling the accuracy of translation termination (see further **Figure 22**).

In addition, our initial hypothesis that the *rps3-K108E* and *rps3-R116D* mutations could alter small subunit function primarily in termination and not in initiation of translation was also confirmed in an enzymatic reporter assay using uORF-less *GCN4-lacZ* mRNA. We did not observe any significant changes in measured ß-galactosidase activities between wt and mutant strains, which points out to preservation of translation initiation efficiencies (note that compared to termination, initiation of translation is the main regulatory checkpoint, therefore, any perturbations in the efficiency of initiation should significantly decrease levels of the *GCN4-lacZ* expression) (**Figure 19**).

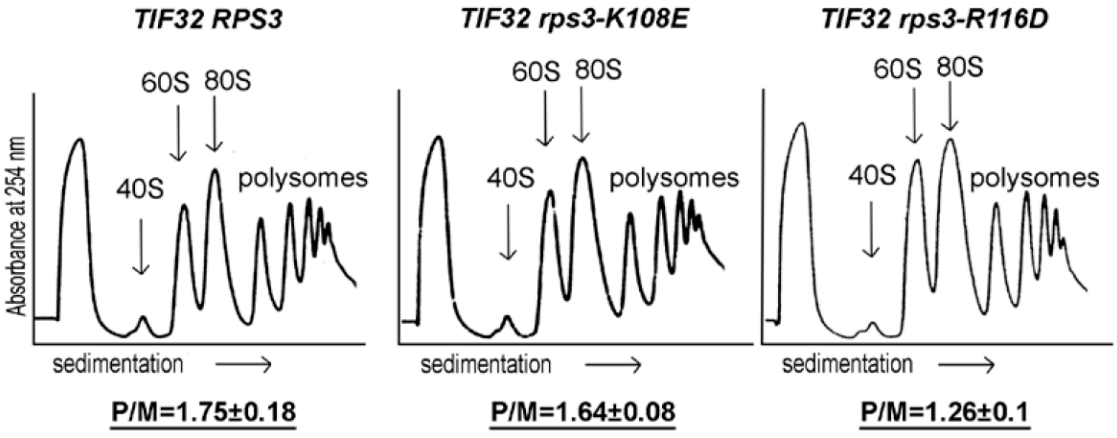

Figure 18 Mutants *rps3-K108E* and *rps3-R116D* do not have any 40S biogenesis defect. Transformants of KPH46 (*rps3Δ tif32Δ*) bearing the indicated wt or mutant *RPS3* alleles were grown in the YPD medium at 30°C to an OD_{600} ~1 and processed for polysomal gradient analysis as described in Material and methods. Positions of 40S, 60S and 80S species are indicated by arrows. Graphs represent the results from three independent experiments ± SD. P/M, polysome to monosome ratio.

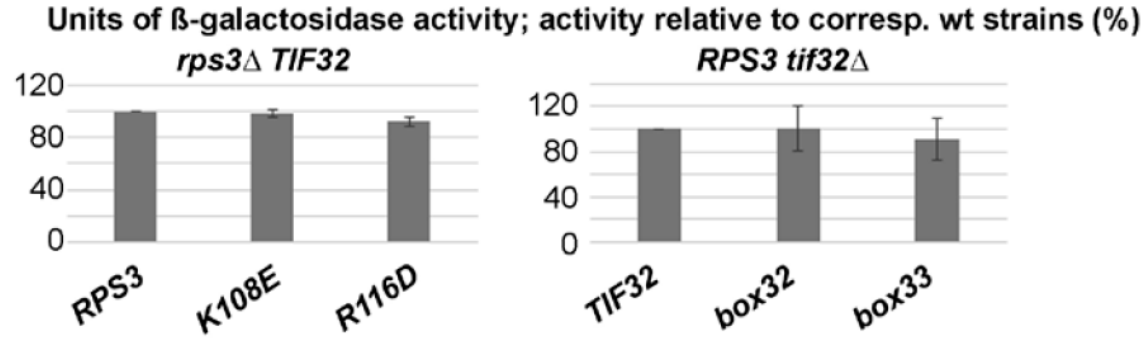

Figure 19 Neither *rps3-K108E/R116D nor tif32-box32/33* mutants significantly impair expression from the control *GCN4-lacZ* reporter plasmid. Strains ME538, ME540, KPH28, KPH41, KPH42, and KPH43 were transformed with p227 bearing the uORF-less mRNA leader of *GCN4* fused to *lacZ*. The mean values and standard deviations obtained from at least 3 independent measurements with three independent transformants are shown as percentages of wt set to 100. Experiments performed by Dr. Stanislava Gunišová.

Neither *rps3* nor *a*/*tif32*mutations alter protein expression levels

To make sure that the above-observed phenotypes result from the specific changes introduced into *RPS3* and *a/TIF32* alleles and not from changes in their expression levels, whole-cell extracts prepared from *S.cerevisiae* cells bearing *rps3-K108E*, *rps3-R116*D, *tif32-box32* and *tif32-box33* mutation were subjected to Western blot analysis. The expression levels of wt and mutant Rps3 and a/Tif32 proteins, as well as other control factors (different ribosomal protein and translation initiation factors), were analyzed. As can be seen in **Figure 20**, the protein levels of both Rps3 and a/Tif32 are not altered in mutant strains, confirming that the observed phenotypes are reflecting changes in translation caused solely by the introduced mutations.

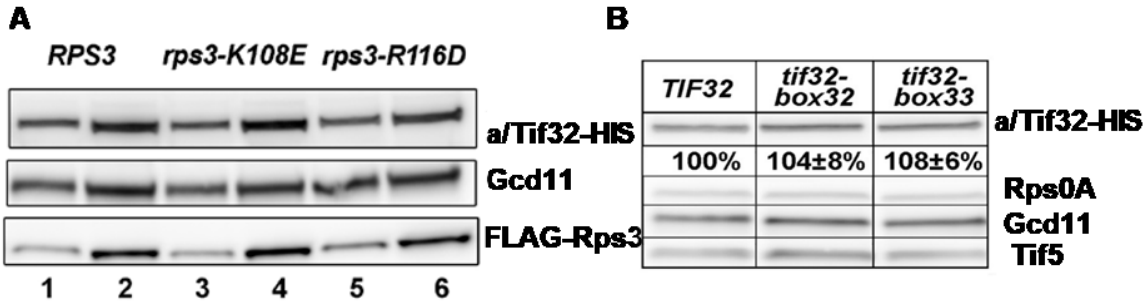

Figure 20 (A and B) The *rps3* and *a/tif32* mutations do not influence protein levels of expressed proteins. Transformants of KPH31 (*rps3Δ tif32Δ*) bearing the indicated wt or mutant alleles were grown in the YPD medium at 30◦C to an OD_{600} ~1. Whole-cell extracts were prepared and subjected to Western blot analysis with antibodies indicated on the right side of the panel. In panel **(B)** the levels of a/Tif32 were quantified and normalized to Rps0A serving as a loading control, three biological replicates were quantified.

8.2. Investigation of aspects of stop codon recognition controlled by Rps3 and a/Tif32 of eIF3

One of the best and routinely used options on how to investigate different aspects of the accuracy of stop codon recognition or the potential of a given stop codon to get readthrough is by using a suitable reporter assay, such as the dual-luciferase assay.

Here we used a bicistronic reporter plasmid bearing a *Renilla* luciferase gene followed by an in-frame firefly luciferase gene, in between separated with either a tetranucleotide termination signal (e.g UGA-C) or, for control and normalization purposes, the CAA-C tetranucleotide signal (for details see Section 7.11).

In simple words, any factor that would decrease or increase the fidelity of termination codon recognition would have the opposite effect on its RT efficiency and will be manifested by an increase or decrease of the second (firefly) reporter translation, respectively. Any difference in the measured firefly to *Renilla* (F/R) ratio will, therefore, indicate for a defect in stop codon recognition which, however, in some instances could be even intentionally programmed *via* a so-called programmed stop codon RT mechanism (see Section 3.2).

The mutants listed in **Table 2** were subjected to stop codon readthrough assay as described in Section 7.11 Dual-luciferase assay.

8.2.1. The basic K108 and R116 residues of Rps3 confer opposite effects on termination efficiency

From all of the *rps3* mutants (**Table 2)** tested using the above mentioned dual-luciferase assay, we identified just two with significant influence on termination efficiency, both carrying multiple aminoacid changes: the *rps3–149* (*rps3-K108A N111A R117A*) and *rps3–151* (*rps3-R116A Y120A R124A Y125A E128A*) mutants. Interestingly, these two mutants displayed opposite phenotypes: the *rps3–149* decreased RT levels by ∼20 % while the *rps3–151* increased them by robust ∼40% (**Figure 21**).

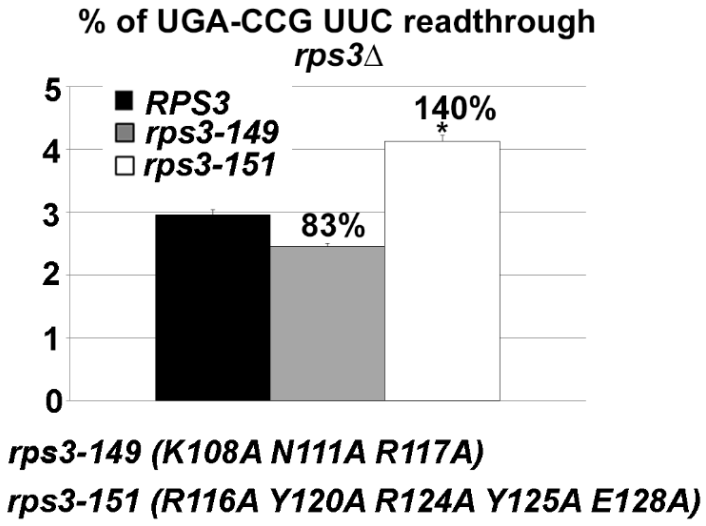

Figure 21 The *rps3-K108A N111A R117A* and *rps3-R116A Y120A R124A Y125A E128A* mutants display opposite effects on termination efficiency. The *S. cerevisiae rps3Δ* strain (ME166) bearing the indicated *rps3* mutant alleles on a single-copy plasmid was introduced with the pTH477 dual-luciferase construct. The strains were grown in SD media and processed for stop codon readthrough measurements as described in Material and methods. Statistical significance was determined by the Student's t-test and is indicated by * ($P < 0.05$).

In order to determine which of the mutated residues account for the observed effects, each of the 8 residues in question was individually replaced either with alanine or with a residue of an opposite charge. The constructs bearing resulting mutant *rps3* alleles were again subjected to dual-luciferase assay. Ultimately, the conserved residues forming the 40S RNA entry channel were found to be responsible: the *Rps3-K108* (originally part of *rps3–149* mutant*)* and *Rps3-R116* (originally part of *rps3–151* mutant*)* **(Figure 22).**

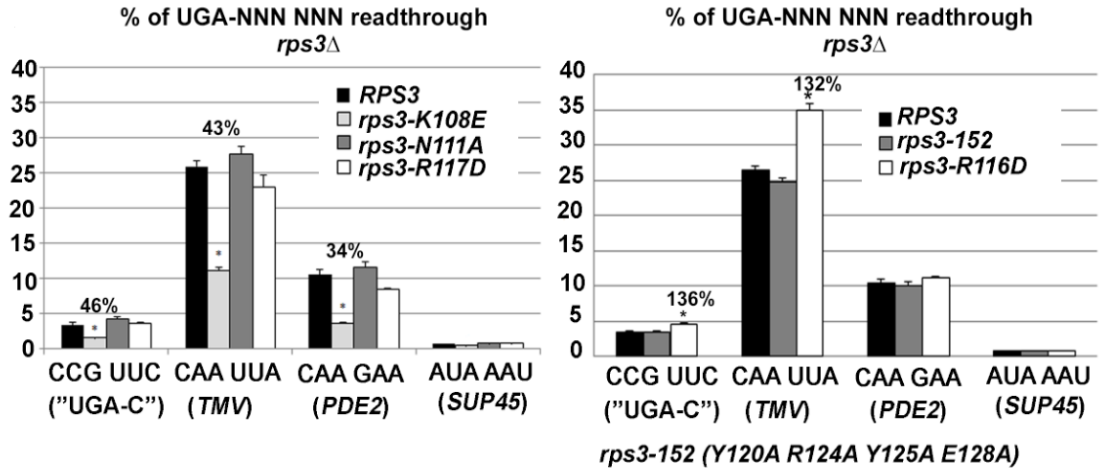

Figure 22 Single residue *RPS3* mutations *rps3-K108E* and *rps3-R116D* are responsible for the opposite effects on termination efficiency. The *rps3Δ* strain (ME166) bearing the indicated *rps3* mutant alleles on a single-copy plasmid was introduced with the indicated dual-luciferase readthrough reporter constructs (pTH477 as 'UGA-C'; PBB82 for *TMV* (tobacco mosaic virus)-6 nts context; PBB84 for *PDE2* (phosphodiesterase 2) context; and PBB85 for *SUP45* stop codon context), grown in SD media and processed for stop codon readthrough measurements as described in Material and methods. Statistical significance was determined by the Student's t-test and is indicated by * ($P < 0.05$).

These residues are located in the neighboring helices of the Rps3 protein structure and face opposite planes, as is apparent from the structure close-up (**Figure 23**). To confirm the specificity of the imposed effects, various stop codon contexts were used for measurements of termination efficiencies: the UGA stop codon immediately followed by a C nucleotide at the 4th position in the UGA-CCG-UUC hexanucleotide (which allows relatively high levels of RT, in detail discussed in Section 3.2.1) and the UGA-hexanucleotides from two genes known to undergo programmed stop codon readthrough. These included the UGA-CAA UUA of the tobacco mosaic virus (TMV), which allows the highest possible levels of RT and the genuine RT-permissive context of *S. cerevisiae PDE2* gene (encoding a phosphodiesterase enzyme which modulates cellular cAMP levels according to the RT efficiency on its mRNA) (Namy et al., 2002). The UGA-AUA AAU context derived from the *S. cerevisiae SUP45* gene known for highly efficient accuracy of termination served as a negative control where no significant difference was observed (Beznosková et al., 2015) (**Figure 22**).

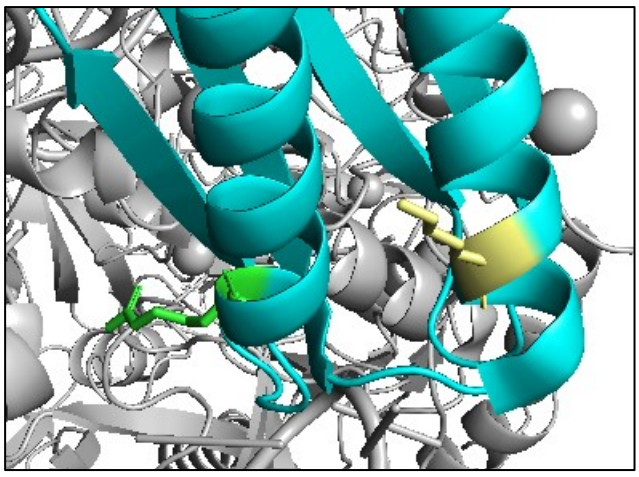

Figure 23 A close-up of Rps3 residues that were identified as important for translation termination. The R116 residue is shown in green and K108 residue in yellow. The neighboring helices of Rps3 are shown in cyan (α4 and α5), the rest of the ribosome structure is grey. The figure was prepared using the PDB structure ID 3JAP**.**

Interestingly, the single alanine substitution in *rps3-R116A* showed no impact on readthrough frequency (**Figure 24**) and the *rps3-K108A* substitution had also only a smaller effect **(Figure 21 and 22**, compare the ~20% decrease of the RT efficiency of the triple alanine *rps3-149* mutant with the ~40% decrease of the RT efficiency of the *rps3-K108E* single mutant). This underscores additional importance of the given charges of those residues, arginine 116 and lysine 108.

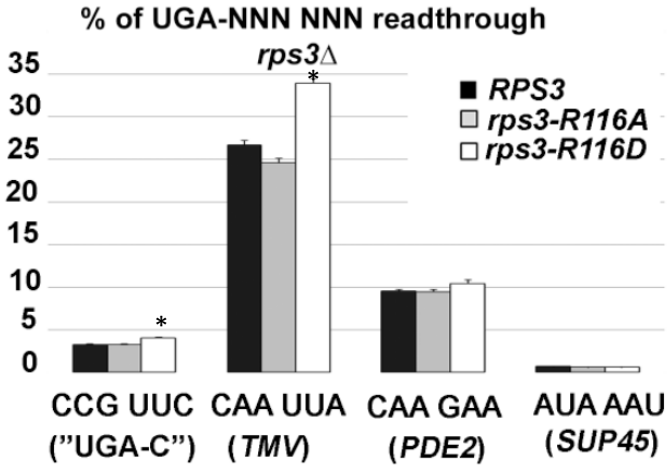

Figure 24 The basic arginine residue of Rps3-R116 gives additional importance to its role in regulating the efficiency of translation. The *rps3Δ* strain (ME166) bearing the indicated *rps3* mutant alleles on a single-copy plasmid was transformed with the indicated dual-luciferase readthrough reporter constructs (pTH477 as 'UGA-C'; PBB82 for *TMV*-6 nt context; PBB84 for *PDE2*; and PBB85 for S*UP45* contexts), grown in SD media and processed for stop codon readthrough measurements as described in Material and methods. Statistical significance was determined by the Student's t-test and is indicated by * ($P < 0.05$).

8.2.2. **The combined mutant *rps3-K108E R116D* compensates for termination defects**

As described in **Figure 23**, the K108 and R116 residues of Rps3 lie in each other´s vicinity, yet their side chains face different directions thus creating a potential for those residues to influence different aspects of translation termination. To confirm their antagonistic roles in the process of termination (already seen in **Figures 21** and **22**) a combined *rps3-K108E R116D* mutant was created. Indeed, the absence of both basic residues led to the nullification of the opposite effects that had been observed for individual single mutants displaying a compensatory genetic interaction (**Figure 25** A).

Further in-depth analysis of both residue's closest surroundings revealed a possible explanation. The R116 residue directly contacts the translated mRNA, whereas the K108 residue probably contacts the helix 34 of 18S rRNA **(Figure 25**, panel B|). In support, the role of helix 34 in controlling translation termination efficiency has already been previously described in *E.coli*, where base substitutions of the rRNA residues in the h34 (C1054 and C1200) were described to alter the UGA nonsense suppression (Gregory and Dahlberg, 1995).

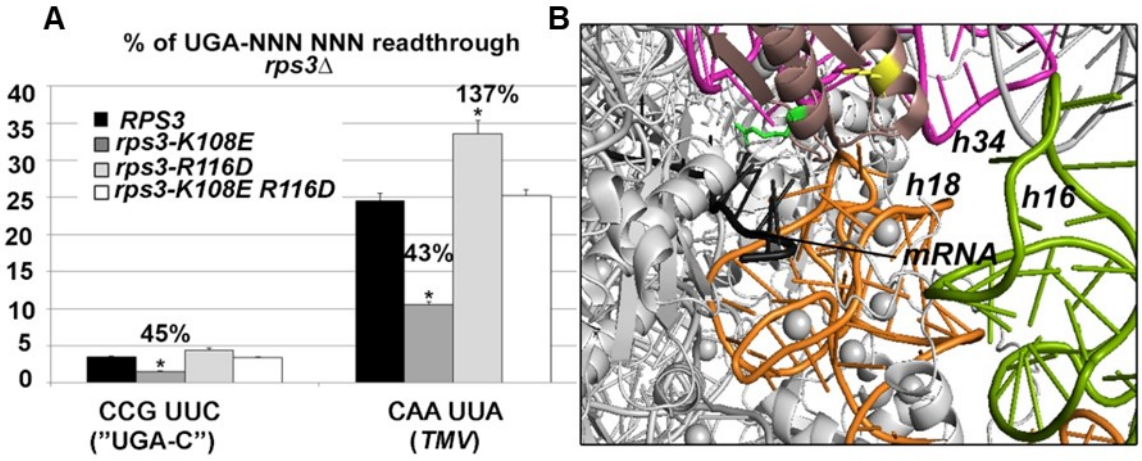

Figure 25 (A) The combined mutant *rps3-K108E R116D* compensates the opposite readthrough phenotypes of *rps3-K108E* and *rps3-R116D* single mutants. The *rps3Δ* strain (ME166) bearing the indicated *rps3* mutant alleles on a single-copy plasmid was introduced with the indicated dual-luciferase readthrough reporter constructs (pTH477 as 'UGA-C'; PBB82 for *TMV*-6 nt context), grown in SD and processed for stop codon readthrough measurements as described in Material and methods. Statistical significance was determined by the Student's t-test and is indicated by * (P< 0.05) **(B) close look to the yeast´s 40S mRNA entry channel pore.** The residues K108 and R116 of Rps3 have different contacts in the 40S mRNA entry pore, which might explain their antagonistic roles in translation. Rps3 is shown in bronze with R116 in green and K108 in yellow, mRNA is shown in black and helices 16, 18 and 34 of 18S rRNA in green, orange and violet, respectively. Prepared using PDB ID 3J81.

8.2.3. **The interplay of Rps3 and near-cognate tRNAs on the accuracy of stop codon recognition**

Previous extensive research in our laboratory led to the characterization of decoding rules describing the impact of +4 base immediately following stop codon on the identity of amino acids incorporated during the readthrough (Beznosková et al., 2016).

Near-cognate tRNAs with high specificity for selective tetranucleotides were identified and named rti-tRNA (readthrough inducing). For the UGA stop codon, we described that tryptophan tRNA ($tRNA^{Trp}$) is preferentially incorporated on UGA-C and UGA-A stop codon contexts while cysteine tRNA ($tRNA^{Cys}$) at UGA-C and UGA-G contexts. Near-cognate tyrosine tRNA ($tRNA^{Tyr}$) is preferentially incorporated at the UAA stop codons and incorporation is induced by all 4 contexts (UAA-N). Glutamine tRNA ($tRNA^{Gln}$) incorporation was also induced by all four UAG-N contexts, although a slight preference for UAG-G could be spotted (Beznosková et al., 2015; Beznosková et al., 2016; Beznosková et al., 2019). Furthermore, we described that eIF3 interferes with the decoding of the third (the so-called wobble) base pair during the programmed stop codon readthrough (see also Section 3.2.1) (Beznosková et al., 2015) and that Rps3 interacts with eIF3 (Chiu et al., 2010).

Only the conserved K108 residue in Rps3 affects the efficiency of termination at the UGA stop codon in the +4 base-specific manner

In order to test whether Rps3 is also involved in the stimulation of incorporation of rti-tRNA in a tetranucleotide specific manner and thus contributes to the setup of the decoding rules, we subjected the *rps3* mutants to a dual-luciferase readthrough assay in the presence of overexpressed rti-tRNAs (Cys, Trp, Gln, and Tyr) and tested them in UGA-N, UAA-C and UAG-C contexts. As a control, empty vector transformants were used.

As can be seen in **Figure 26**, A and B, the bars annotated ´EV´, the *rps3-K108E* mutant interfered with the decoding on the UGA-C and UGA-G contexts, but decoding was not affected on the UGA-A and UGA-U contexts (**Figure 26**, C and D panels, see 93 % and 106 %; same can be observed in **Figure 27,** too). The decoding on the other two stop codons (UAG-C and UAA-C) was also slightly impaired (**Figure 26**, E and F panels, ´EV´ graphs).

Surprisingly, the *rps3-R116D* mutant increased levels of readthrough regardless of the identity of the stop codon and the +4 base following it, and thus did not interfere with

the decoding in the codon- and context-specific manner (**Figure 26**, A-F ´EV´ graphs). This is quite surprising, as the Rps3-R116 residue was previously proposed to contact directly the mRNA´s bases (Dong et al., 2017). The fact that the *rps3-R116D* mutant effect on RT was not limited only to a 'programmed context', suggests that its effect on RT could be more general.

The incorporation of the rti-tRNAs is affected mostly only by *rps3-K108E* mutation.

Regarding the involvement of Rps3 in stimulating of incorporation of specific rti-tRNAs in a tetranucleotide specific manner, the most pronounced effect was observed in *rps3-K108E* mutant for $tRNA^{Cys}$ in contexts UGA-C, UGA-G (contexts preferred by $tRNA^{Cys}$) and also UGA-U (See **Figure 26**, panels A, B, D). If you compare panels ´EV´ and hc tC(GCA)P1 (representing $tRNA^{Cys}$), you can observe a difference of approx. 1.7-fold between them. Tyrosine tRNA incorporation was increased only very modestly, ~ 1.3-fold at tested UAA-C stop codon context (**Figure 26**, panel F) and the incorporation of the last tRNAs tested, rti- $tRNA^{Glu}$ at UAG-C and rti-$tRNA^{Trp}$ at UGA-N was not affected (**Figure 26**, panel E and **Figure 27** respectively).

Taken together, these data suggest that the Rps3-K108 residue can sense the identity of termination contexts and promotes the specific incorporation of rti-$tRNA^{Cys}$ (and to a smaller extent also of rti-$tRNA^{Tyr}$), perhaps allosterically *via* its interaction with h34 and, most likely in co-operation with eIF3 on the programmed contexts.

On the contrary, *rps3-R116D* mutant did not much interfere with the incorporation of rti-tRNAs at the examined tetranucleotides (**Figure 26**).

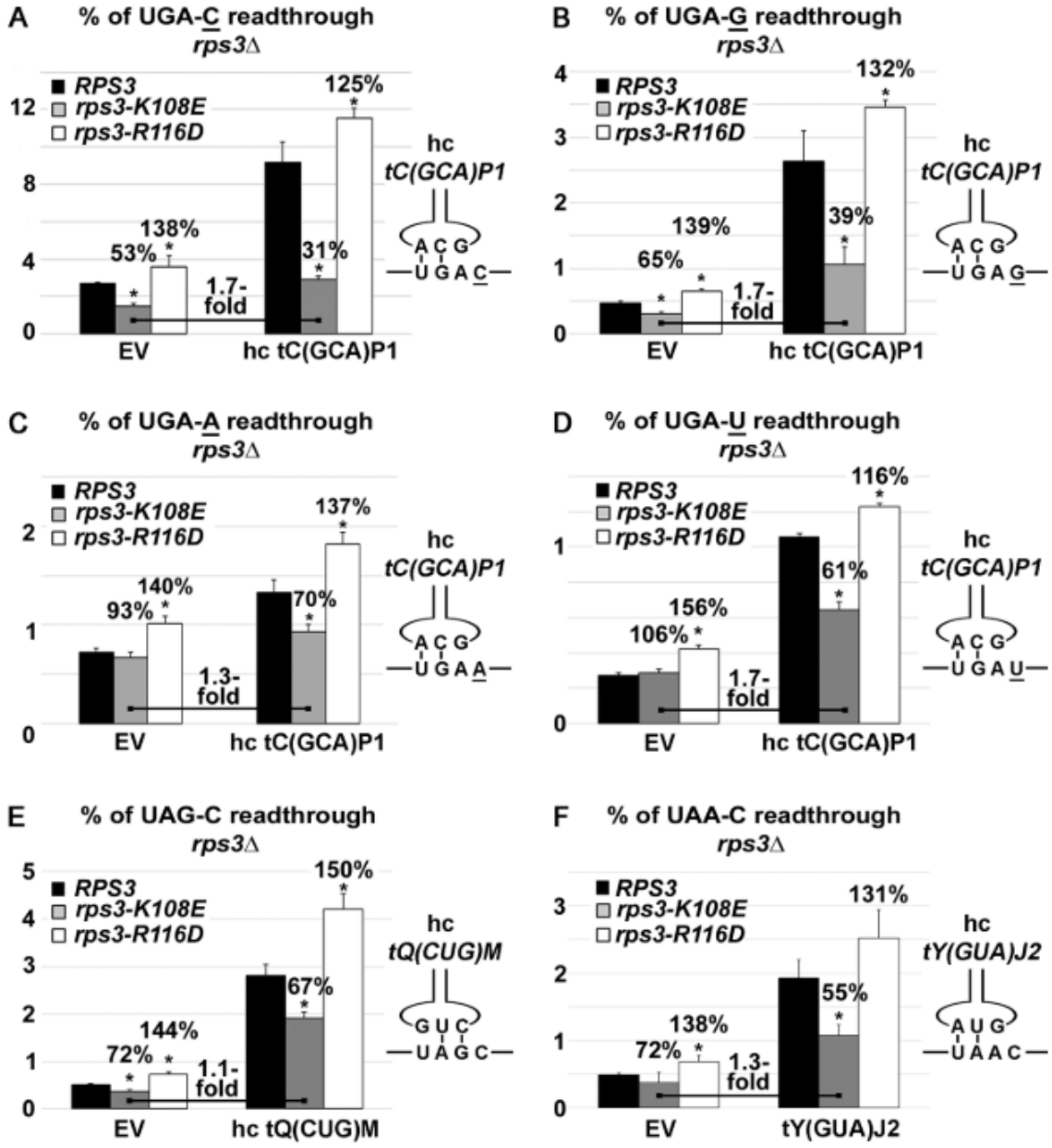

Figure 26 Cysteine tRNA incorporation is impaired in *rps3-K108E* mutant at the UGA stop in the +4 base-specific manner. (A–F) The *rps3Δ* strains ME166 bearing the indicated *rps3* mutant alleles on a single-copy plasmid were introduced with the indicated dual-luciferase readthrough reporter constructs (KP22 for UGA-C, KP35 for UGA-G, KP34 for UGA-A, KP36 for UGA-U, ZP40 for UAG-C and KP41 for UAA-C) in combination with either empty vector (EV) or indicated rti-tRNA on high copy plasmid, grown in SD media and processed for stop codon RT measurements as described in Material and methods. Schematics of individual rti-tRNAs base-pairing with the indicated stop codon tetranucleotides are given to the right of the plots; only the nucleotides of the anticodon loop are shown. Statistical significance was determined by the Student's t-test and is indicated by * ($P < 0.05$).

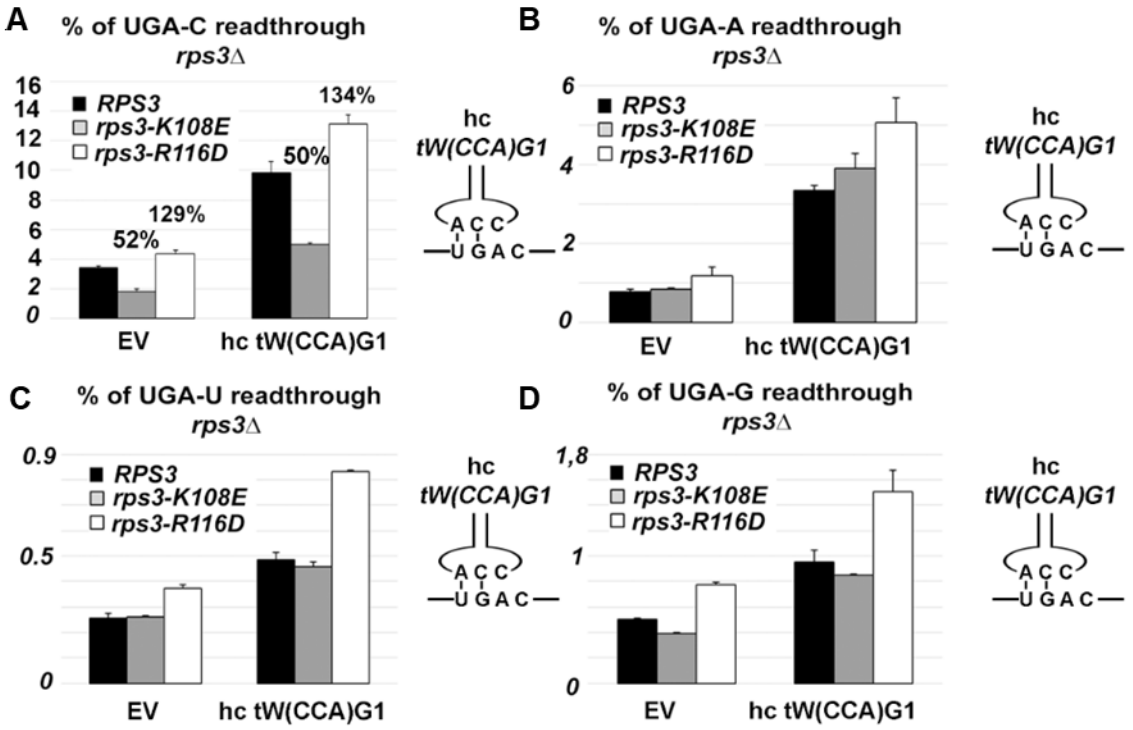

Figure 27 Tryptophan tRNA incorporation is not impaired in rps3-K108E mutant at the UGA-stop in the +4 base-specific manner. (A–D) The rps3Δ strains ME166 bearing the indicated rps3 mutant alleles on a single-copy plasmid were introduced with the indicated dual-luciferase readthrough reporter constructs (KP22 for UGA-C, KP35 for UGA-G, KP34 for UGA-A, KP36 for UGA-U, ZP40 for UAG-C and KP41 for UAA-C) in combination with either empty vector (EV) or indicated rti-tRNA on high copy plasmid, grown in SD media and processed for stop codon RT measurements as described in Material and methods. Schematics of tryptophan rti-tRNAs base-pairing with the indicated stop codon tetranucleotides are given to the right of the plots; only the nucleotides of the anticodon loop are shown.

To further support the specificity of our findings, we subjected the *rps3-N111A* mutant to a similar examination. As mentioned earlier, the *rps3-N111A* mutation did not influence the stop codon readthrough (**Figure 22**), and indeed, it did not show any effect on the discrimination against termination context in the presence of rti-tRNAs, too (**Figure 28**).

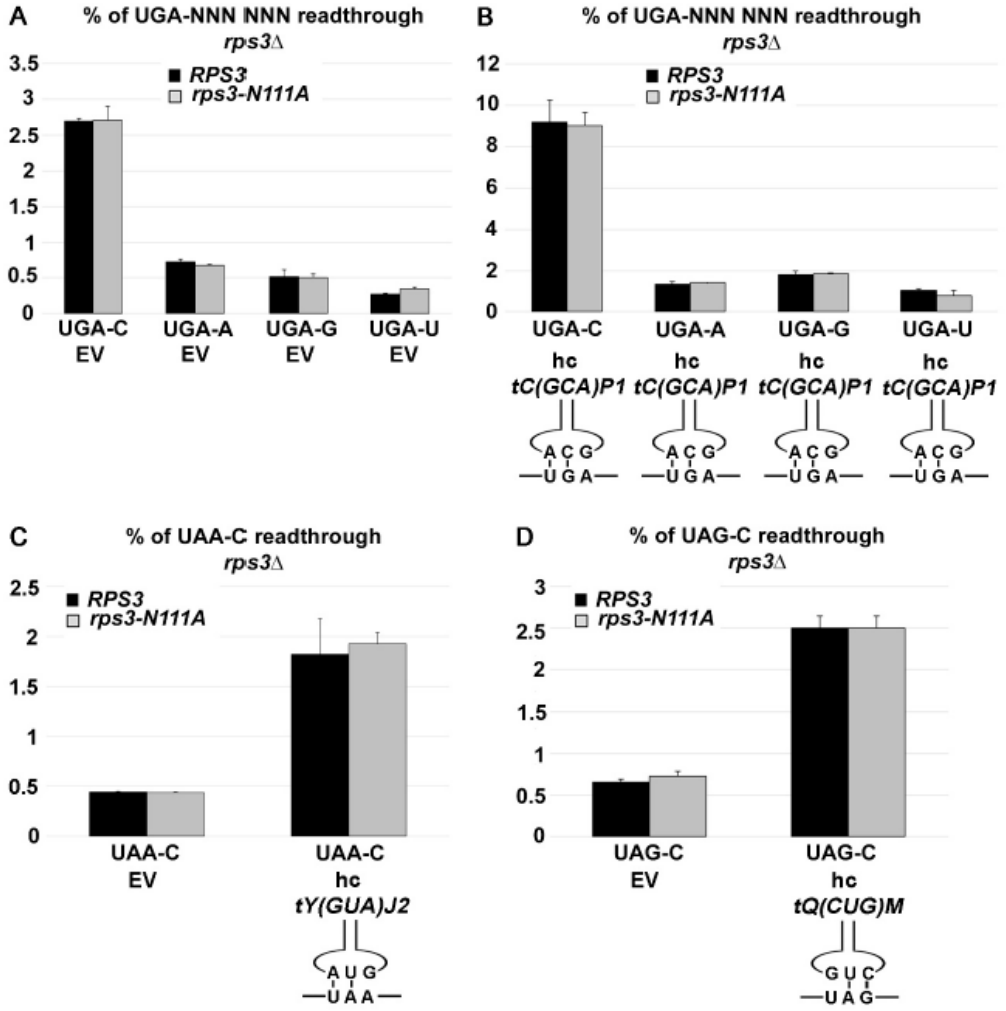

Figure 28 The N111 residue of Rps3 does not have any effect on readthrough on any of the reporters tested, nor does it interfere with the incorporation of Cys or Trp rti-tRNAs.
(A - D) The *rps3Δ* strains derived from ME166 (rps3Δ) bearing the indicated *rps3* mutant alleles on a single-copy plasmid were introduced with the indicated dual-luciferase readthrough reporter constructs (KP22 for UGA-C, KP35 for UGA-G, KP34 for UGA-A, KP36 for UGA-U; KP41 for UAA-C and ZP40 for UAG-C) in combination with either empty vector (EV) or indicated rti-tRNA on high copy plasmid, grown in SD media and processed for stop codon RT measurements as described in Material and methods. Schematics of individual rti-tRNAs base-pairing with the indicated stop codon tetranucleotides are given to the down of the plots; only the nucleotides of the anticodon loop are shown.

8.2.4. **The efficiency of stop codon readthrough in the presence of a miscoding agent**

Aminoglycosides represent a group of compounds that is well established to have a profound effect on the accuracy of the translation. They had been firstly described in great detail in bacteria, where they bind to the decoding center of the ribosome and promote miscoding, and later were found to promote miscoding in the eukaryotic ribosome, too (Davies et al., 1964; Singh et al., 1979). In our study, we used paromomycin, an

aminoglycoside antibiotic, which mechanism of action relies on the displacement of the phosphate groups of conserved bases A_{1492} and A_{1493} of the 18S rRNA in the ribosomal A-site caused by the compound binding (Fourmy et al., 1996; Prokhorova et al., 2017). This results in the ribosome sensing incorrectly the Watson-Crick geometry of the codon-anticodon interaction between the tRNA and mRNA and thus ultimately leads to a higher frequency of miscoding (Bidou et al., 2012).

Interestingly, we have previously described that readthrough decreasing eIF3 mutants lost their phenotypes in the presence of paromomycin, suggesting that eIF3 requires proper, unaltered conformation of the A-site to promote readthrough (Beznosková et al., 2015). To address whether here investigated Rps3 also requires a proper A-site conformation for controlling the efficiency of termination, the frequency of RT on UGA-C context in *RPS3* wt *versus* mutant strains in the presence of 400 μg/ml of paromomycin was investigated.

As can be seen in **Figure 29**, the presence of the miscoding agent increased the overall frequency of RT in wt as well as *rps3-K108E* and *rps3-R116D,* however, the *rps3* mutations showed different phenotypes. In the presence of paromomycin, the effect of the *K108E* mutation on readthrough was nearly nullified (see 44 % *versus* 86 % in the presence of paromomycin), however, the effect of the *R116D* mutation was preserved (see 138 % in both cases). This indicates once again that the mechanisms they impose on the efficiency of termination qualitatively differ, even though both residues lie relatively close to each other. We propose that the readthrough stimulatory effect of the Rps3-K108 residue requires proper conformation of the decoding center, the same as observed with eIF3 and that the R116 residue does not require an intact A-site to prevent readthrough.

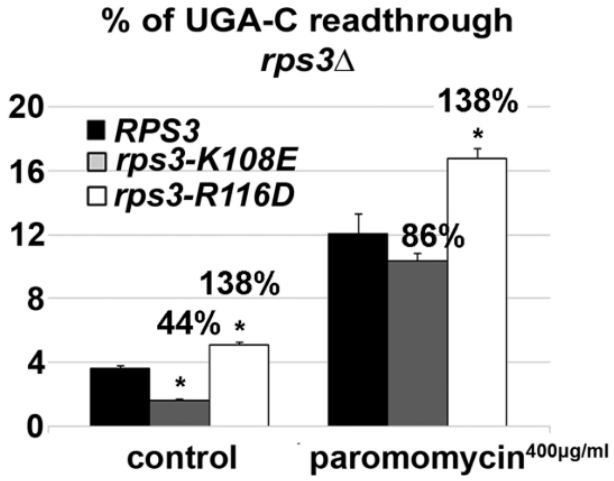

Figure 29 The readthrough stimulatory effect of the K108 residue requires proper conformation of the decoding center. The *rps3Δ* strains KPH126, 127 and 128 bearing the indicated *rps3* mutant alleles on a single-copy plasmid were grown in SD media without or with 400 µg/ml paromomycin for six hours and processed for stop codon readthrough measurements as described in Material and methods. Statistical significance determined by the Student's t-test is indicated by * ($P < 0.05$).

8.2.5. The interplay between Rps3 and a/Tif32 subunit of eIF3 on the accuracy of stop codon recognition

The extreme C-terminus of a/Tif32 controls the readthrough efficiency

In the previous work of our laboratory, we described the surprising role of initiation factor eIF3 in translation termination (see also Section 3.2.1). Mutants of several eIF3 subunits showed compromised levels of stop codon recognition. Among others, the N-terminal part of a/Tif32 (specifically the *box17* represented by aminoacid residues 161-170) was found to be involved in promoting RT (Beznosková et al., 2013). Here, we revealed that the extreme C-terminal part of a/Tif32 plays a role in promoting stop codon readthrough as well. Both C-terminal boxes mutants, *a/tif32-box32* and *a/tif32-box33* (the corresponding residues are depicted in **Figure 15)**, decreased the measured RT efficiencies, however, the effect of *box33* mutation was more prominent (**Figure 30**). Because the segments of these two boxes partly overlap, it is most probably the region of amino acid residues 955-964 (*box33*) that is critically involved.

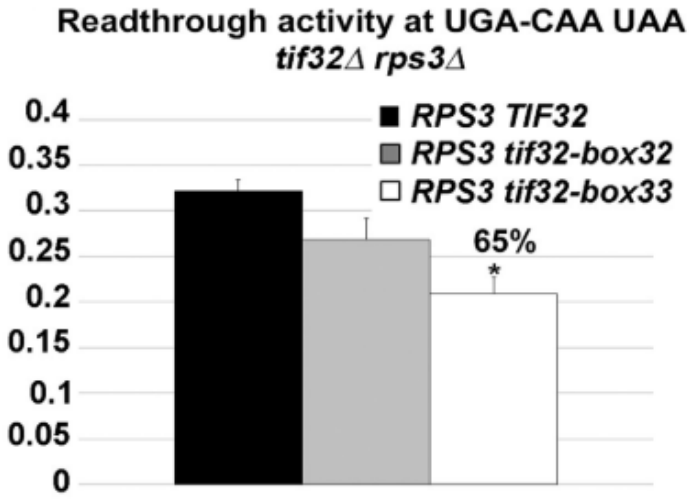

Figure 30 The extreme C-terminus of a/Tif32 subunit of eIF3 promotes programmed stop codon readthrough. Transformants of KPH31 (*rps3Δ tif32Δ*) bearing the indicated wt or mutant *TIF32* alleles were introduced with ′UGA-C′ (pTH477) dual-luciferase readthrough reporter construct and processed for stop codon readthrough measurements as described in Material and methods. Statistical significance determined by the student's t-test is indicated by * ($P < 0.05$).

The eIF3 co-operates with Rps3 in programmed stop codon RT

Several lines of evidence suggest that Rps3 and a/Tif32 might co-operate in controlling the efficiency of stop codon readthrough. These include:

i) The interaction between the C-terminal domain of a/Tif32 and Rps3 (Chiu et al., 2010).

ii) The a/Tif32-CTD has now been described to promote stop codon readthrough (**Figure 30**). Because it is not known to make contacts with any other eIF3 subunits and it is dispensable for the eIF3 complex integrity *in vivo* (Valášek et al., 2002; Llácer et al., 2018; Zeman et al., 2019), the interaction with Rps3 could thus be directly involved in modulating the termination efficiency.

iii) In addition, both the Rps3 and a/Tif32-CTD, have been described to be involved in open-to-close latch 'acrobatics' mechanism occurring during translation initiation. Precisely, the a/Tif32-CTD was also found to interact with h16 and h18 of 18S rRNA near the entry channel (Valášek et al., 2003) and its mutations were described to have phenotypes indicating destabilization of the open (scanning-conducive) latch state, as well as phenotypes suggesting the opposite effect of destabilizing the closed (scanning-arrested) latch conformation (Cuchalová et al., 2010; Chiu et al., 2010).

iv) The mutations of Rps3 residues that interact with mRNA and rRNA residues of the entry channel were also shown to decrease the stability of the closed-latch state during initiation (Dong et al., 2017).

In light of these findings, it was tempting to examine whether similar re-arrangements do also occur during termination, involving the same players and serving the same purpose - to clamp the mRNA into the mRNA entry channel to stabilize the termination complex, as it prepares for the peptide release.

To investigate the delicate interplay between Rps3 and a/Tif32 during termination, their combined mutants were tested for mutual genetic interactions (suppression, additivity, epistasis, etc.) in readthrough assay. Interestingly, combining *a/tif32-box33* with *rps3-R116D* mutation had a compensatory effect resulting in a nearly complete nullification of their phenotypes (**Figure 31**, panel A) which indicates their antagonistic roles. A similar effect, although without statistical significance, was also observed in the *a/tif32-box32 rps3-R116D* double mutant.

On the other hand, testing of combined *tif32-box33 rps3-K108E* mutant revealed an additive effect: further exacerbation of the reduced readthrough effect observed in both single mutants (**Figure 31,** panel B, see a drop by 64 %). Again, a similar effect, but to a lesser extent, was also observed with the *a/tif32-box32 rps3-K108E* double mutant **(Figure 31**, panel B).

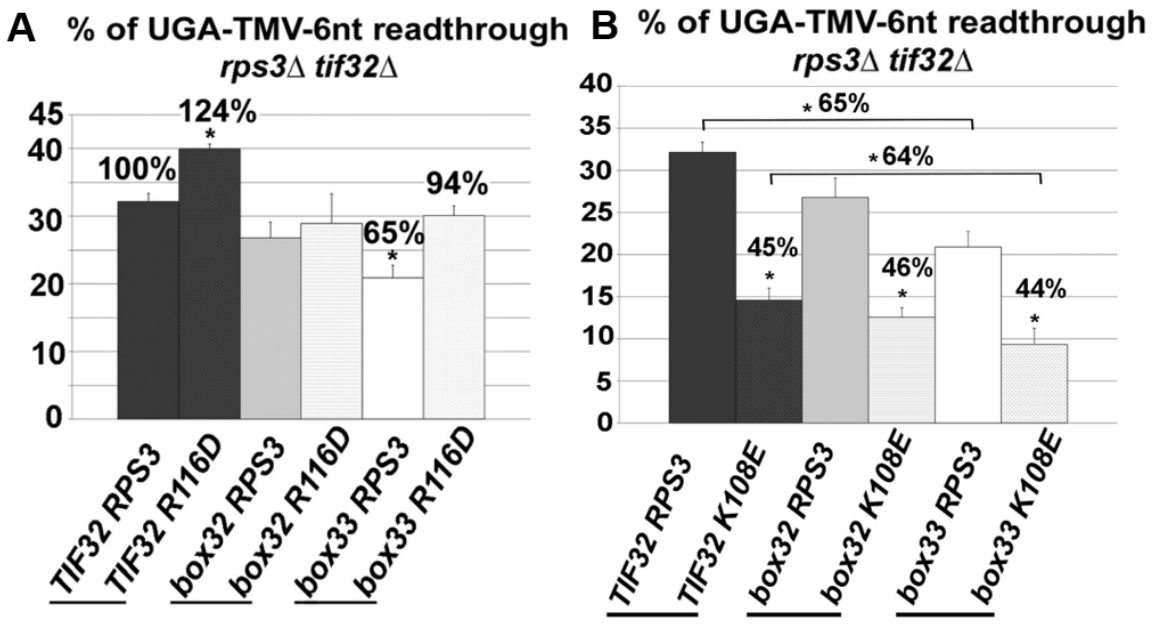

Figure 31 Analysis of the genetic interaction between the a/tif32 C-terminal mutants and *rps3* mutants. (A) Combining *a/tif32-box33* with *rps3-R116D* results in complete suppression of individual readthrough phenotypes**. (B) On the contrary, combining *a/tif32-box* mutations with *rps3-K108E* further exacerbates the negative stop codon readthrough phenotype of the individual mutants**. Transformants of KPH31 or KPH46 (*rps3Δ tif32Δ*) bearing the indicated wt or mutant *TIF32* and *RPS3* alleles were introduced with the TMV- 6 nt context (PBB82) dual-luciferase readthrough reporter construct and processed for stop codon readthrough measurements as described in Material and methods. Statistical significance determined by the student's t-test is indicated by *(P< 0.05).

Noteworthy, the combined *rps3-R116D tif32-box33* mutant conferred an exacerbated Slg$^-$ defect of the *tif32-box33* mutant while *rps3-R116D* single mutant possessed no obvious growth defect (**Figure 16)**. Here, however, the *rps3-R116D* in *rps3-R116D tif32-box33* was found to compensate for the *tif32-box33* increased termination efficiency impact. This speaks for a more complex genetic interaction between the a/Tif32-CTD and Rps3-R116 residue. Interestingly, the combined *rps3-K108E R116D tif32-box33* triple mutant rescued the mild Slg$^-$ defect of *tif32-box33* mutant (See **Figure 16**) and also, the *rps3-K108E R116D* double mutant compensated the readthrough phenotype of the single *rps3-R116D* mutant. This further underscores the antagonistic roles of the R116 and K108 residues of Rps3.

Interestingly, the exacerbated readthrough phenotype of *rps3-K108E tif32-box33* did not manifest itself into the growth defect (**Figure 16**).

8.2.6. **Effect of increased eIF1 levels on Rps3 mediated control of stop codon recognition**

The *rps3-R116D* mutant was earlier shown to reduce the steady-state expression of eIF1 (Dong et al., 2017). We have been able to confirm the same observation and simultaneously to show that *rps3-K108E* did not have this effect on eIF1 levels (**Figure 32**, panel A, eIF1 panel). To verify that perspective changes in eIF1 expression in the *rps3-R116D* do not affect the stop codon readthrough, we overexpressed eIF1 in *rps3* mutant strains. As anticipated, because eIF1 protein has never been implicated in termination, the readthrough phenotypes neither of *rps3-R116D* nor *rps3-K108E* were affected (**Figure 33**).

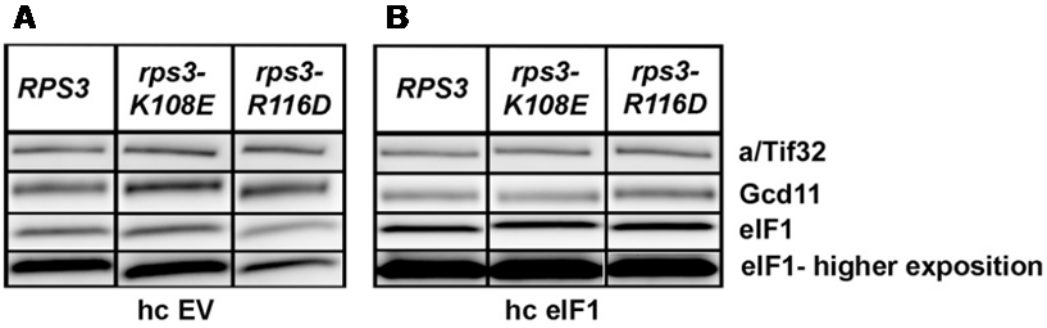

Figure 32 (A and B) Verification of overexpression of eIF1 in *rps3-K108E* and ***rps3-R116D*** **strains. The *rps3-R116D* exhibits lower levels of eIF1 (A)**, but it does not influence its RT phenotype. (**B**) The eIF1 levels are indeed elevated in the strain overexpressing eIF1. Transformants of ME166 (*rps3Δ*) bearing the indicated wt or mutant *RPS3* alleles plus either EV control (YEplac112) or high copy eIF1 plasmid (B596) were grown in the YPD medium at 30°C to an OD_{600} ~1, Whole-cell extracts were prepared and subjected to Western blot analysis with antibodies indicated on the right side of the panel. eIF1 antibody is shown at two expositions.

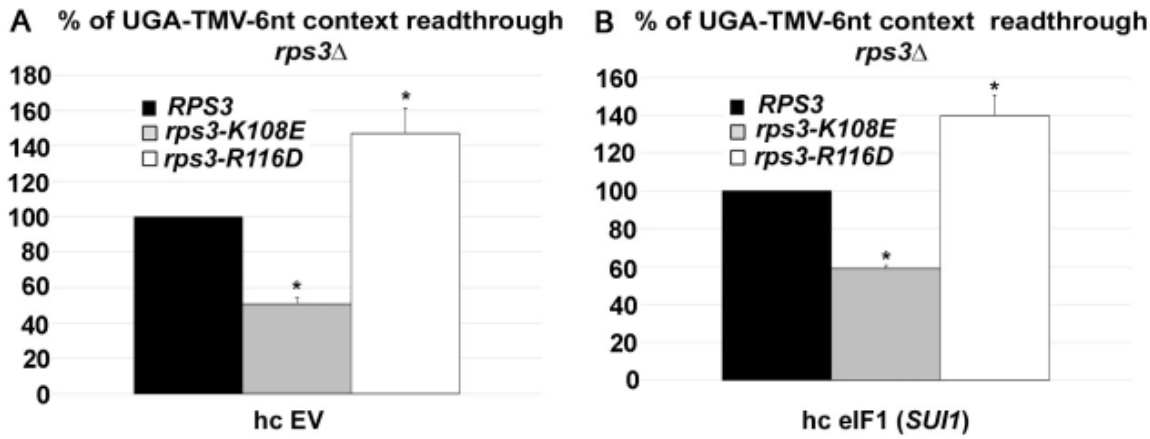

Figure 33 (A-B) Overexpression of eIF1 does not have any effect on the RT phenotypes observed with *rps3-K108E* and *rps3-R116D* mutations. Transformants of ME166 (*rps3Δ*) bearing the indicated wt or mutant *RPS3* alleles and either EV control (YEplac112); panel **(A)** or hc eIF1 plasmid (B596); panel **(B)** were introduced with the TMV- 6 nt context (PBB82) dual-luciferase readthrough reporter construct and processed for stop codon readthrough measurements as described in Material and methods.

8.3. Discovering the delicate interplay of contacts between a/Tif32 and Rps3 *in vitro*

Earlier reports have already indicated that a/Tif32-CTD interacts with Rps3 (Chiu et al., 2010). **Figure 34** shows positions of both proteins on the ribosome, however, as already mentioned earlier, the whole structure of a/Tif32 has still not been completely solved therefore only assigned parts are shown. To examine the Rps3-a/Tif32 interaction in greater detail and to uncover whether the quantitative changes in this interaction could be responsible for the defects in translation observed in Rps3 and a/Tif32 mutants (described in previous sections), a series of terminally GST-tagged, both wt and mutant *RPS3* and *a/TIF32* alleles, were created and various arrangements of GST-pull down experiments of recombinantly produced proteins were performed.

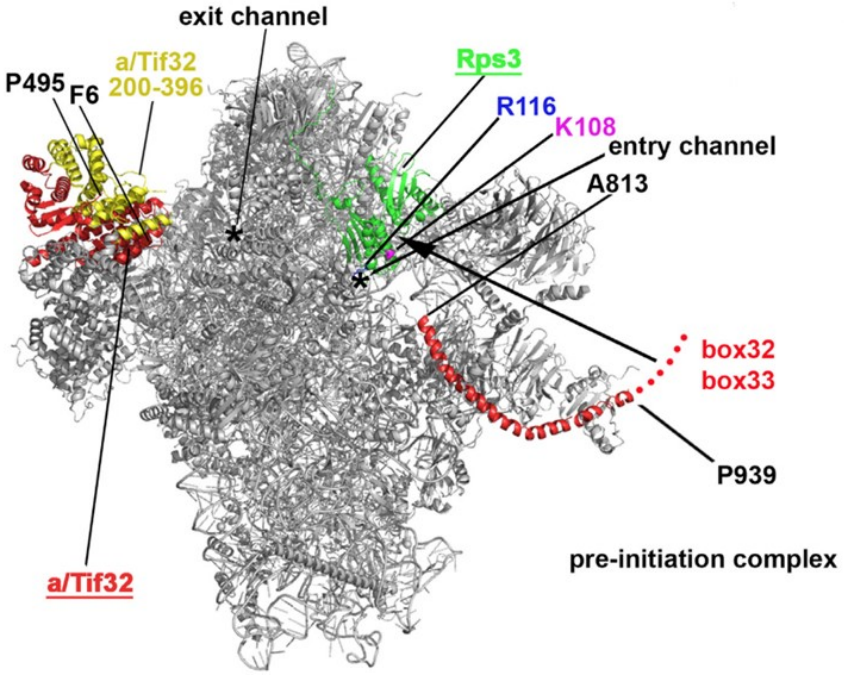

Figure 34 Positions of Rps3 and the structure-solved/modeled parts of the a/Tif32-NTD and -CTD (defined by the amino acid coordinates) in the context of the small ribosomal subunit. Rps3 is shown in green with positions of R116 and K108 highlighted; a/Tif32 in red with the residues 200–396 highlighted in yellow and the putative placement of the extreme C-terminal boxes 32 and 33 indicated. Entry and exit channels are indicated by an asterisk. The interaction between the latter boxes and Rps3 identified in this study is illustrated by an arrow. Prepared using PDB ID 6FYY.

8.3.1. **Purification of GST-proteins**

For all GST-pull down experiments (GST- glutathione S-transferase), the bait proteins or protein fragments were prepared in *E. coli* as C-terminally tagged GST-a/Tif32-CTD and N-terminally tagged GST-Rps3 or mutant variants thereof. Representative protein preparations are illustrated in **Figure 35** and **Figure 36**. The stability and amount of all protein preparations was analyzed using SDS-PAGE. Different amounts of commercially prepared BSA (bovine serum albumin) protein of known concentration were used as a loading control. Besides, the BSA loading also helped to better assess the amounts and ratios of individual GST-tagged proteins for their further usage in the GST-pull down experiments. The prey proteins or protein fragments of Rps3 and a/Tif32 or their mutant variants were prepared as [^{35}S]-labeled polypeptides using rabbit reticulocyte lysates.

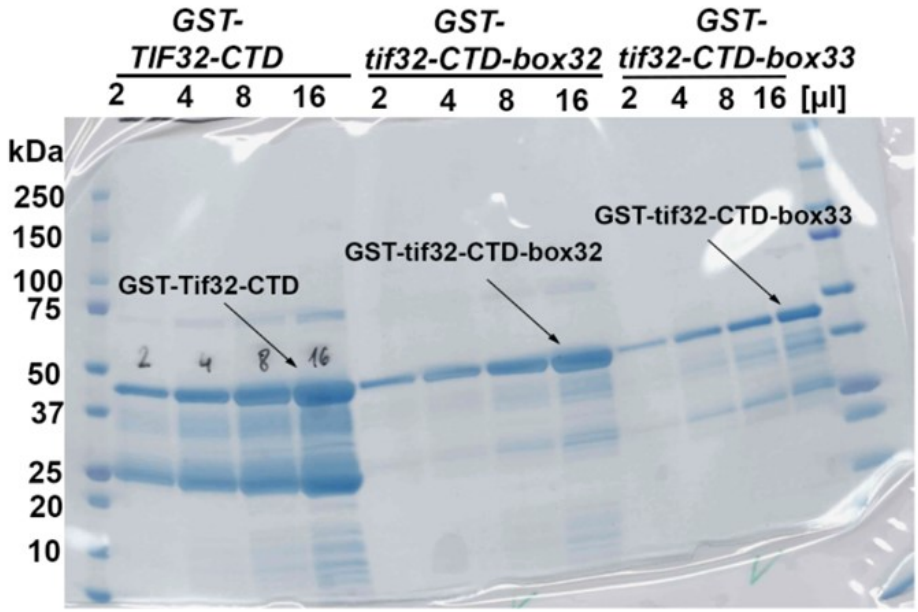

Figure 35 The Coomassie-stained gel showing GST-a/Tif32-CTD, GST-a/Tif32-CTD-box32 and GST-a/Tif32-CTD-box33 proteins. Loading amounts of preparations of individual proteins are shown in [µl]. CTD, C-terminal domain.

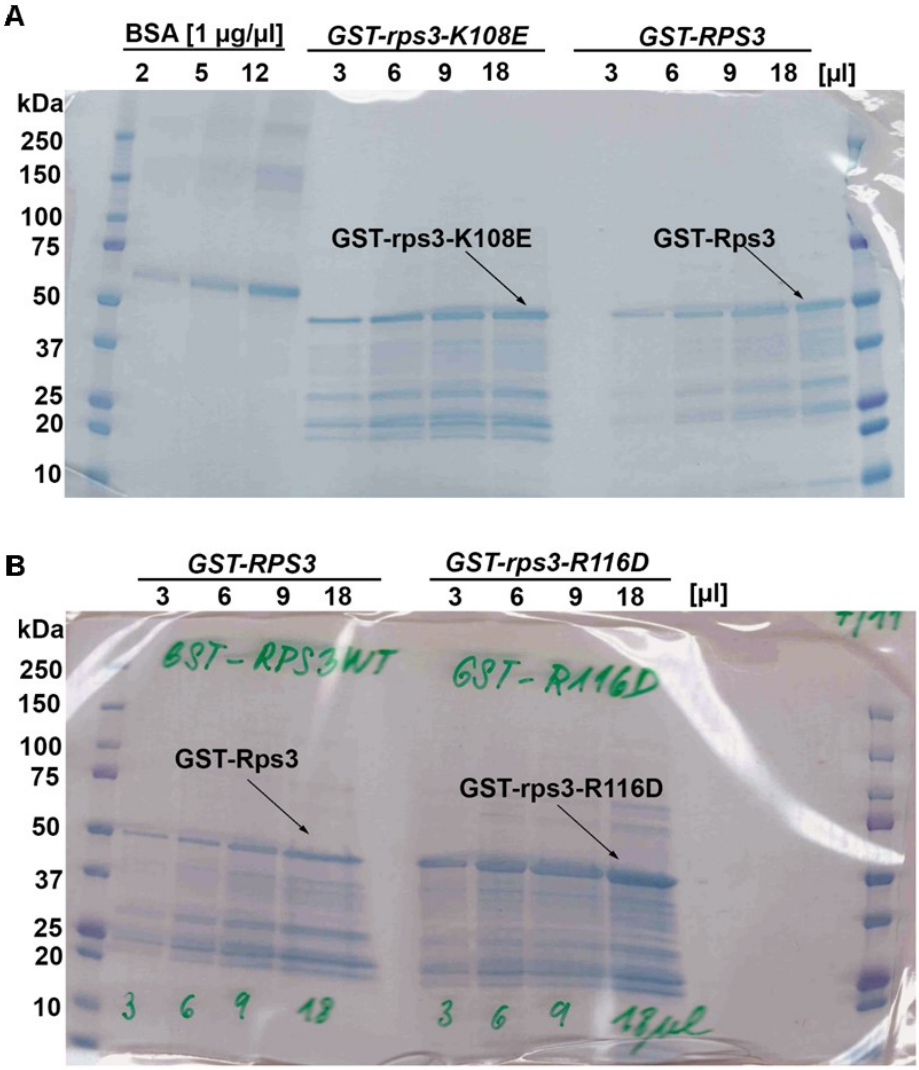

Figure 36 (A) and (B). The Coomassie-stained gels showing GST-Rps3, GST-rps3-K108E (A), and GST-rps3-R116D and BSA proteins (B). Loading amounts of preparations of individual proteins are shown in [µl]. BSA was used as a loading control for the estimation of corresponding amounts of purified proteins.

8.3.2. **Both, the NTD and extreme CTD of a/Tif32 interact with Rps3**

In the initial experiment, three segments of [^{35}S]-labelled a/Tif32 representing two parts of NTD (a/Tif32 1-200 and a/Tif32 200-396) and a middle part of the protein (a/Tif32 490-790) were tested for binding against GST-fused Rps3. As can be seen in **Figure 37A,** the binding of a/Tif32 to Rps3 is selective: only the a/Tif32-NTD segment encompassing amino-acid residues 200-396 shows strong interaction with the Rps3 protein. The previously reported binding of the a/Tif32-CTD domain towards Rps3 protein was shown in the opposite arrangement (e.g. [^{35}S]-labelled Rps3 towards GST-a/Tif32-CTD) (Chiu et al., 2010). Therefore, as next, this experimental setup was performed. Indeed, the

[^{35}S]-labelled Rps3 against GST-tagged extreme CTD of a/Tif32 (amino acid residues 792-964 that included the regions of boxes 32 and 33) demonstrated a strong interaction (**Figure 37** B). These findings indicate the existence of two independent Rps3 binding sites in Tif32: one in the NTD and another one in the extreme CTD.

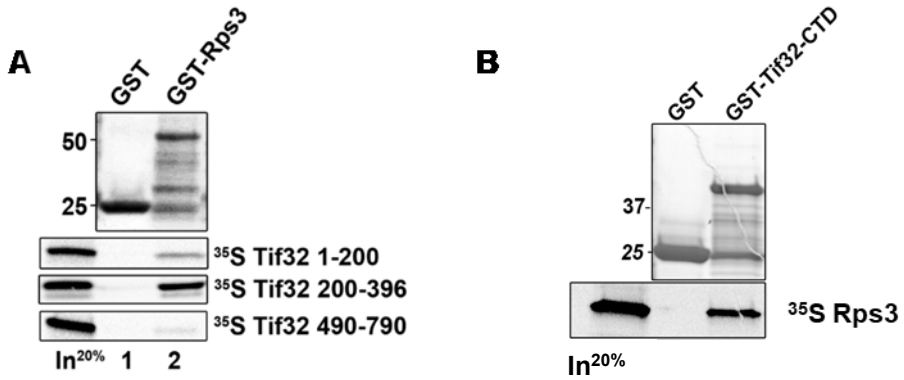

Figure 37 (A) The a/Tif32-NTD segment (aa 200–396) and (B) a/Tif32-CTD segment (aa 792-964) show strong interaction with Rps3. (A) The indicated wt Rps3 protein was fused to the GST moiety and together with the GST alone control tested for binding to the indicated [^{35}S]-labeled fragments of a/Tif32. **(B)** The indicated wt a/Tif32-CTD protein was fused to the GST moiety and together with the GST alone control tested for binding to the indicated [^{35}S]-labeled fragment of Rps3. (In) indicates input amounts of proteins added to each reaction.

8.3.3. **The a/Tif32-CTD mediates two independent contacts with Rps3 *via* Rps3-R116 and the extreme CTD of a/Tif32**

Next, we were curious about how the above-identified contacts are influenced by *rps3* mutations that conferred the readthrough phenotypes (see Section 8.2.1). First, we examined the physical interaction between the a/Tif32-CTD and readthrough inducing mutant *rps3-R116D*. Interestingly, the [^{35}S]-labelled rps3-R116D protein imposed dramatic reduction (by ~90 %) in binding to the last 173 residues of wt a/Tif32-CTD (aa residues 791-964) fused to the GST moiety (**Figure 38**, panel A and B). Similarly, both box32 and box33 mutations in a/Tif32-CTD reduced binding to wt Rps3 by robust ~80% (**Figure 38,** see a drop to 23 % and 21 %). However, since practically the identical reductions were also observed with the binding of box32 and 33 to the mutant rps3-R116D protein (**Figure 38**, panels A-C, see 26 % and 17 %), it is clear that at least two independent contact points exist between the CTD of a/Tif32 and Rps3: one mediated by the arginine 116 of Rps3 protein and part of a/Tif32-CTD outside the boxes regions, and another one mediated by the box regions of the a/Tif 32-CTD and so far unknown segment of Rps3.

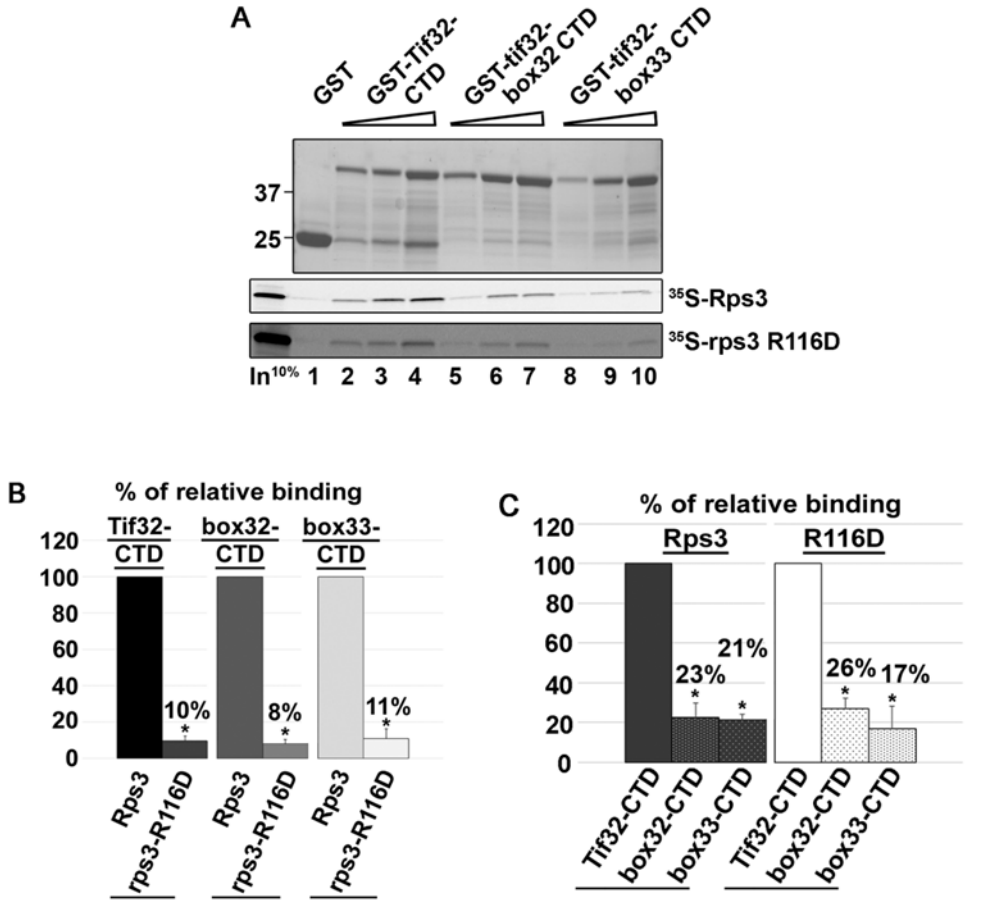

Figure 38 (A–C) Both *a/tif32-box32* and *a/tif32-box33* mutations, as well as *rps3- R116D* impair the a/Tif32-Rps3 interaction independently of each other. The indicated wt or mutant proteins (or their segments) were fused to the GST moiety and together with the GST alone control tested for binding to the indicated [^{35}S]-labeled proteins or their mutant derivatives. (In) indicates input amounts of proteins added to each reaction. The plots represent average values obtained from the analysis of at least 3 GST-pull down experiments; standard deviations are given. Statistical significance determined by the student's t-test is indicated by * ($P < 0.05$).

8.3.4. **The NTD of a/Tif32 does not contact the Rps3 residues K108 and R116**

In agreement with previous results, the examination of binding between GST-Rps3-R116D and the full length [^{35}S]-labelled a/Tif32 showed also a reduction in binding, down to 68 % when compared to the wt GST-Rps3 protein (**Figure 39** A, lanes 1 and 2 and panel B), regardless the presence of the *box32* mutation (the [^{35}S]-labelled a/Tif32-box33 is not shown as the construct did not stably express) (**Figure 39** A and B). Interestingly, as the difference in binding between a/Tif32-box32 *versus* wt GST-Rps3 or rps3-R116D is reduced less dramatically, by ~50 % (**Figure 39**, panels A and C) compared to ~80 % decrease in case of only the short C-terminal domain of a/Tif32-box33 **(Figure 38** A and C), the existence of another contact outside of the a/Tif32-CTD was confirmed. As also shown in

Figure 37, this extra-CTD contact has already been identified as the 200-369 NTD segment of a/Tif32. Moreover, we further show that this region interacts with Rps3 in a K108- and R116-independent manner (**Figure 40**). The existence of this contact also explains the difference in binding affinity between rps3-R116D towards the a/Tif32-CTD (~90 % reduction) and rps3-R116D towards the full length a/Tif32 protein (~35 % reduction) (**Figure 38** and **Figure 39**, panels A and B).

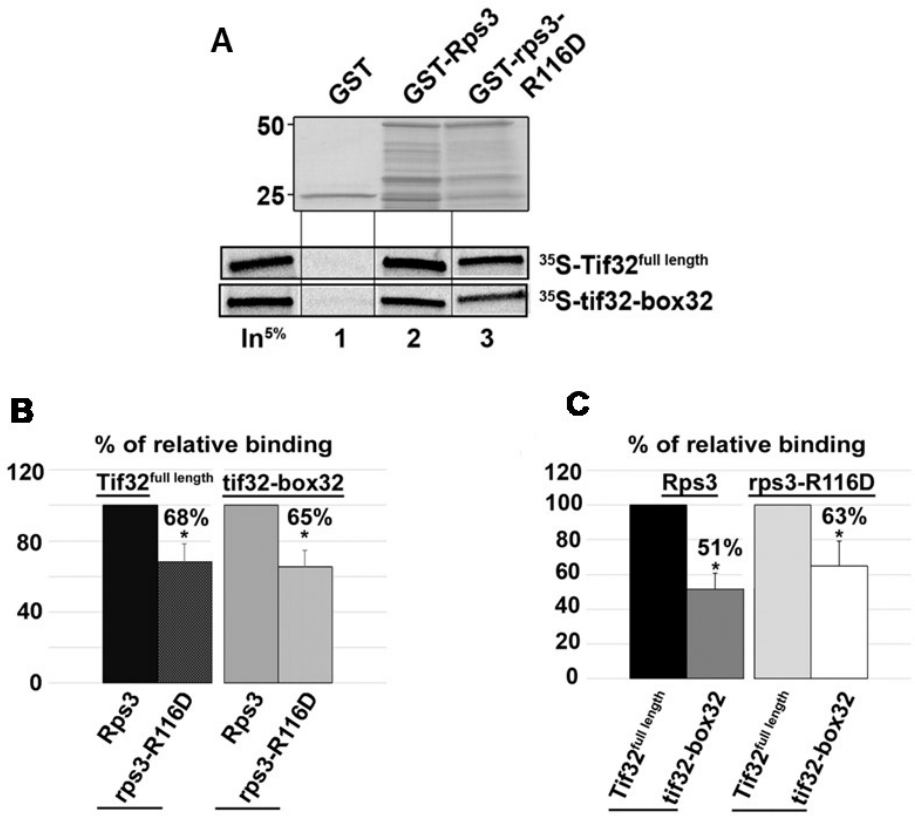

Figure 39 (A–C) Both *tif32-box* mutations, as well as *rps3-R116D* impair the a/Tif32-Rps3 interaction independently of each other. The indicated wt or mutant proteins (or their segments) were fused to the GST moiety and together with the GST alone control tested for binding to the indicated [^{35}S]-labeled proteins or their mutant derivatives. (In) indicates input amounts of proteins added to each reaction. The plots represent average values obtained from the analysis of at least 3 GST-pull down experiments; standard deviations are given. Statistical significance determined by the student's t-test is indicated by * ($P < 0.05$).

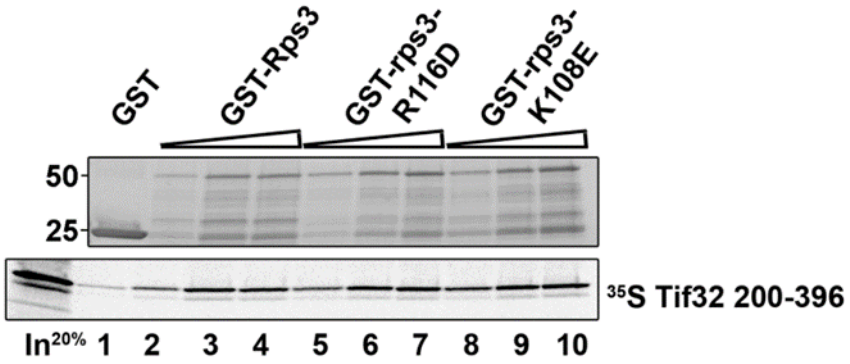

Figure 40 The a/Tif32-NTD segment encompassing amino-acids residues 200-396 interacts with Rps3 in the R116- and K108-independent manner. The indicated wt or mutant Rps3 proteins were fused to the GST moiety and together with the GST alone control tested for binding to the indicated [^{35}S]-labelled fragment of a/Tif32. (In) indicates the input amount of protein added to each reaction.

8.3.5. **The Rps-K108 represents an additional contact to a/Tif32-CTD**

Last, we analyzed *in vitro* binding of the Rps3-K108E protein towards a/Tif32. First, we started again with testing of binding of Rps3-K108E *versus* GST-a/Tif32-CTD. Interestingly, the reduction of binding towards the amino residues 792-964 of the a/Tif32-CTD region was less profound (reduction by ~50 %, **Figure 41** A and B) than, in the case of Rps3-R116D, almost complete loss of binding, **Figure 38**A and B). Moreover, this reduction was only seen with the C-terminal truncation but not with the full-length a/Tif32 protein (**Figure 41** D and E). Because the phenotypes of mutations in both of the Rps3 residues are quite different, it is likely that they contact slightly different amino acids in the a/Tif32-CTD region. Taking together, this might indicate that in the a/Tif32-CTD, first the contact between Rps3-R116 has to be established to promote the second, Rps3-K108 mediated interaction and that for the overall a/Tif32-Rps3 interaction the Rps3-K108 is not critical. The co-operation between K108 of Rps3 and the a/Tif32 to fine-tune the fidelity of termination could probably have more functional than a physical character.

In summary, our results suggest for existence for at least four independent contacts between a/Tif32 and Rps3: one in a/Tif32-NTD not dependent on the RT modulating Rps3 residues K108 and R116 and additional three present in a/Tif32-CTD, one in the box32-33 region not contacting R116 and K108 and other two outside the box32-33 region one of which interacts with R116 (stronger interaction) and the second one with K108. These findings indicate for existence of a delicate network of contacts between those two binding partners, which could stimulate and/or be a part of critical conformational changes and the

latch ‘acrobatics’ movement that the ribosome undergoes during initiation and probably termination (for further description see Section 9.2.2).

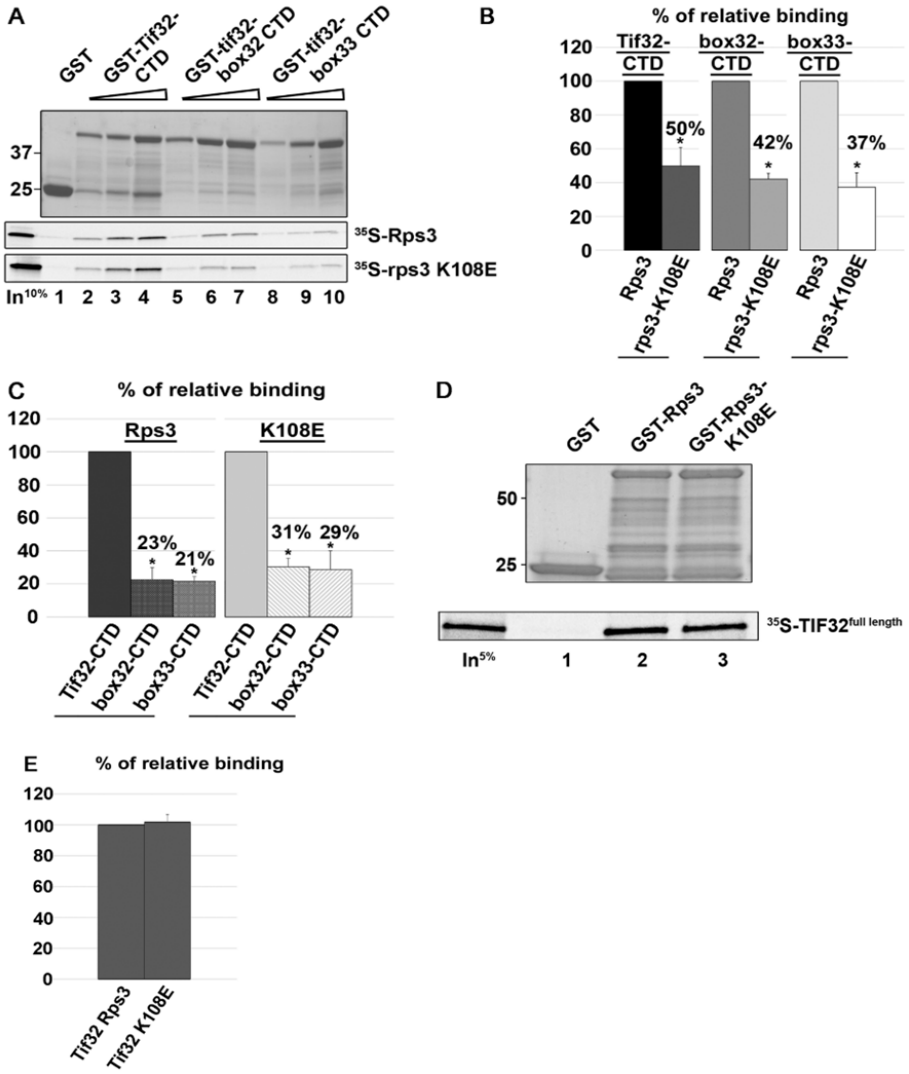

Figure 41 Analysis of the physical interaction between mutations in a/Tif32 C-terminal regions and *rps3-K108E*. (A–E) Both *tif32-box* mutations, as well as *rps3-K108E* impair the a/Tif32-Rps3 interaction independently of each other; the latter one only in when interacting with the a/Tif32-CTD (compare panels **A–C** versus **D–E**). The indicated wt or mutant proteins (or their segments) were fused to the GST moiety and together with the GST alone control tested for binding to the indicated [^{35}S]-labeled proteins or their mutant derivatives. (In) indicates input amounts of proteins added to each reaction. The plots represent average values obtained from the analysis of at least three independent GST-pull down experiments; standard deviations are given. Statistical significance determined by the student’s t-test is indicated by * ($P < 0.05$).

8.4. Analysis of the composition of the pre-termination 80S ribosomal complexes in *rps3* mutants with defects in stop codon recognition

Our past research on yeast eIF3 revealed that, in addition to its expected association with 40S, it also associated with 80S species isolated from the so-called heavy polysomal fractions of the gradient such as pentasomes and higher (heavy polysomes represent mRNA highly occupied with ribosomes therefore sedimenting and collected in 'heavier' fractions of higher sucrose concentration). Because its association was also dependent on the simultaneous presence of the release factors Sup45 (eRF1) and Sup35 (eRF3), it implied that those eIF3 bound 80S ribosomes represent a fraction of pre-terminating 80S complexes (pre-TCs) (Beznosková et al., 2013).

To investigate whether the above-described *rps3* and *a/tif32-box33* mutations causing defects in efficiencies of translation termination (please see Section 8.2.1), also influence the composition of pre-termination complexes *in vivo*, we analyzed the amounts of eIF3 (represented by essential subunit a/Tif32) as well as other initiation (eIF1), elongation (eEF1A) and termination factors (Sup35 and Sup45) bound to the 80S couples isolated from heavy polysomes. The re-sedimentation protocol was described previously in Beznosková et al. (2013) and Beznosková et al. (2015). The general overview of the technique is given in **Figure 42.**

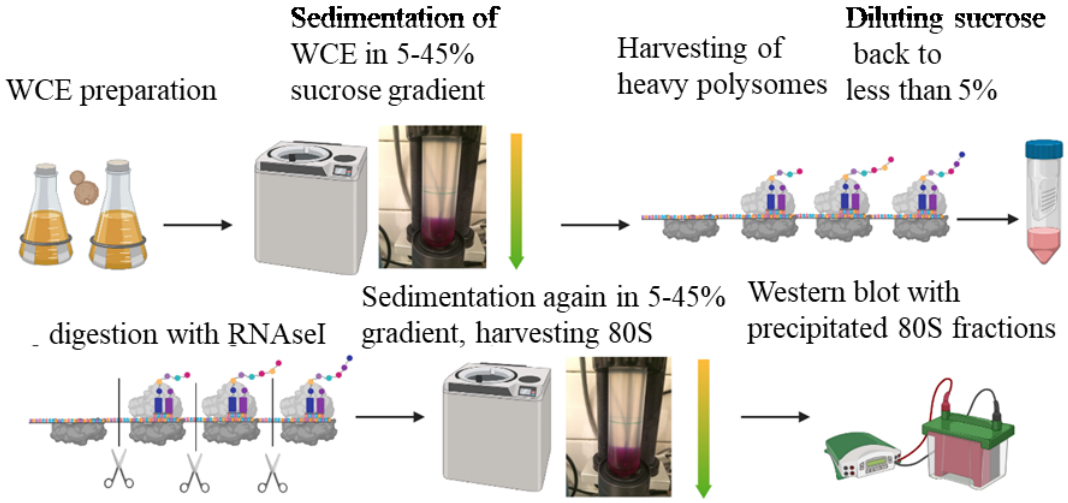

Figure 42 Schematics of the analysis of pre-termination complexes using re-sedimentation of 80S ribosomal species. For details see text or Material and methods section. Prepared using Biorender. WCE, whole-cell extract. Prepared using Biorender.

Briefly, the whole-cell extracts derived from formaldehyde cross-linked wt or mutant *S. cerevisiae* cells prepared as described in Section 7.10.8, were resolved on 5-45 % sucrose gradients after high-velocity centrifugation. The higher polysomal fractions (pentasome and higher) were collected and treated with RNAse I and the resulting 43S-48S pre-initiation complexes and 80S species were separated in the second round of centrifugation on the new 5-45% sucrose gradient (the so-called re-sedimentation).

The isolated 80S couples were then loaded in five serial two-fold dilutions onto SDS-PAGE gel and the amounts of the small ribosomal protein Rps0A and 80S-associated factors were analyzed by quantitative Western blotting and repeated at least five times (**Figure 43**, **Figure 44**, **Figure 45**). All figures show three representative and consecutive dilutions for each factor.

8.4.1. The *rps3-K108E* and *rps3-R116D* mutations have opposite effects on the composition of pre-termination 80S complexes *in vivo*

In the initial experiment, we checked the composition of the pre-termination 80S complexes of the readthrough-increasing *rps3-R116D* mutant along with the *tif32-box33* mutant. As can be observed in **Figure 43**, this mutant displayed statistically significant enrichment of a/Tif32 (representing the eIF3) and also release factors Sup45 and Sup35 in resedimented heavy polysomes compared to the wt strain. On the contrary, the levels of the other two translation factors, eIF1 and eEF1A, that we used as specificity controls were not

significantly altered. This further confirmed that eIF1 and eEF1A are not involved in the termination process as has already been shown previously by the absence of any defect in translation termination when eIF1 and eEF1A were down-regulated (Beznosková et al., 2015).

It was surprising to observe, however, that eIF1 associated with 80S pre-TCs, as the separation of 40S subunits during the re-sedimentation procedure should get rid of all of the initiation factors that are supposed to leave the small subunit before the subunit joining step. Therefore these 80Ses could most probably reflect the existence of an eIF1-containing eIF3-'translasome' complex that was proposed to associate with 80S ribosomes and contain several eIFs, all eEFs, subunits of the proteasome, etc. (Sha et al., 2009). The increased abundance of release factors in the *rps3-R116D* mutant cells suggests that this mutation leads to the enrichment of terminating ribosomes. This indicates that the rate of the termination reaction is slower, which may indeed manifest itself in the increased frequency of stop codon readthrough (**Figure 22**).

On the contrary, the *tif32-box33* mutant displayed decreased occupancy of a/Tif32 and terminating ribosomes (with Sup45 and Sup35 bound) in the heavy polysomes (**Figure 43**). This could mean that the rate of the termination reaction is faster, maybe due to the less eIF3 present in the complexes (eIF3 was earlier described to interfere with the eRF1 role in termination (Beznosková et al., 2015), which would reduce the readthrough frequency as already observed (please see **Figure 43**).

Interestingly, the combined mutant *rps3-R116D tif32-box33*, which compensated the readthrough phenotype of both single mutants to the wt levels (**Figure 31A**), seems to partially compensate the changes in the composition of the pre-termination complexes too (**Figure 43**, factors a/Tif32, Sup35 and Sup45). However, the *rps3-R116D tif32-box33* mutant did not correct the slow growth defect of *tif32-box33* single mutant, but, what is more, it further exacerbated it (**Figure 16**). This indicates that impaired termination is not the major defect of this double mutant.

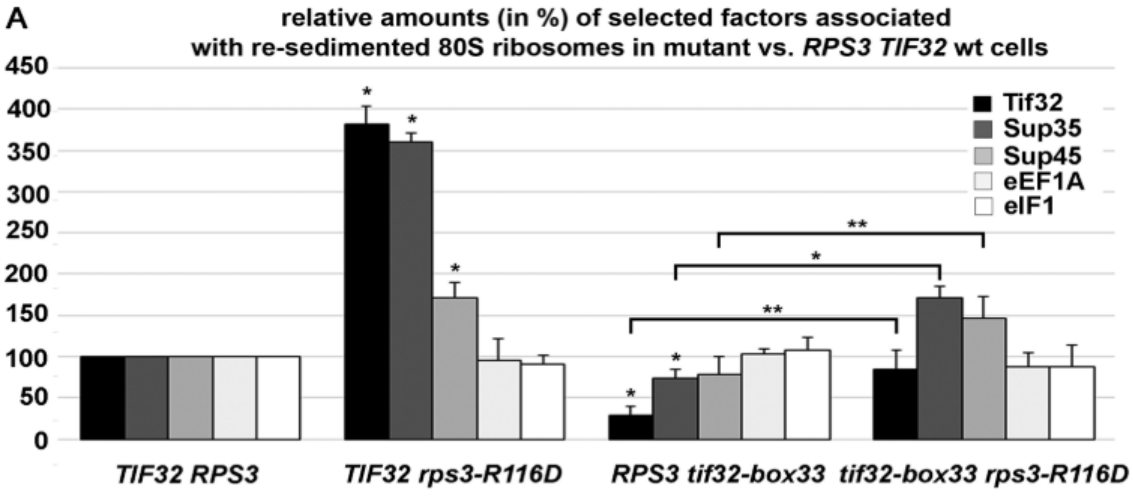

	Rps0A	Tif32	Sup35	Sup45	eEF1A	eIF1
TIF32 rps3-R116D	100±15	382±22*	360±11*	156±18*	90±11	96±26
RPS3 tif32-box33	86±5	28±11*	74±12*	79±21	107±16	103±6
tif32-box33 rps3-R116D	109±12	85±22	172±28	147±26	88±17	87±26

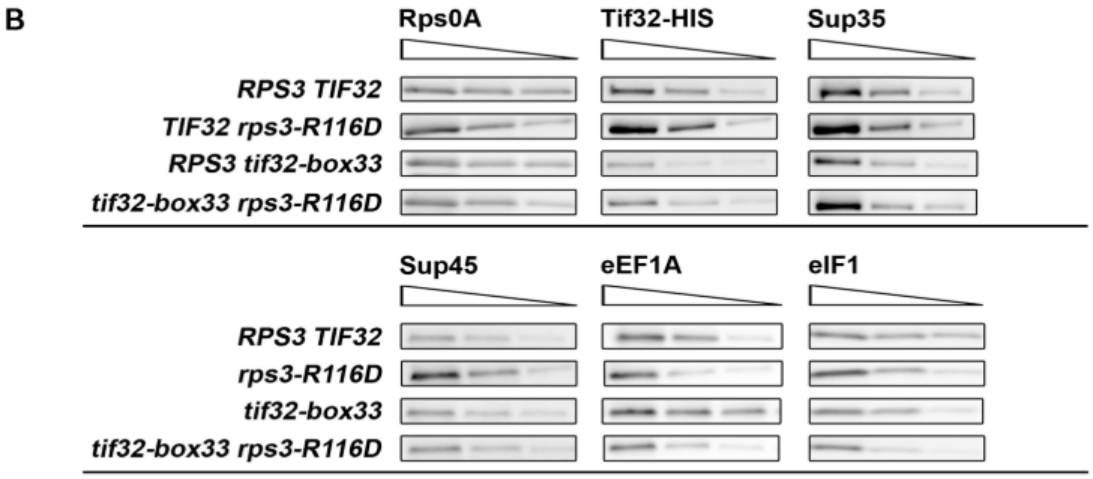

Figure 43 Readthrough-increasing *rps3-R116D* displays statistically significant enrichment of eIF3, Sup35 and Sup45 factors in heavy polysomes, whereas *tif32-box33* reduces their amounts. (A and B). Transformants of KPH31 (*rps3Δtif32Δ*) bearing the indicated wt or mutant *TIF32* and *RPS3* alleles were subjected to the re-sedimentation protocol (described in Material and methods) and processed for Western blot analysis with antibodies raised against factors shown above the strips. Three representative dilutions for each factor are shown **(B). (A) The quantification of selected factors was performed as follows.** WB signals from each of the five 2-fold dilutions obtained with individual antibodies were quantified by Quantity One and plotted against their corresponding loadings. Individual slopes (representing relative amount of each factor in mutant cells) calculated from the linear regression of resulting plots were normalized to the slope obtained with the *TIF32 RPS3* wt strain, which was set to 100%. Statistical significance determined by the student's *t*-test is indicated (**P*< 0.05; ***P*< 0.1).

Next, the composition of pre-termination complexes was analyzed in the *rps3-K108E* mutant, again along with the *tif32-box33* mutant. The *rps3-K108E* mutation decreases readthrough levels (**Figure 22**) and it also led to the reduction of a/Tif32 levels in the pre-TC (**Figure 44)**. This further supports the idea that eIF3 presence is needed for efficient stop codon readthrough. The *rps3-K108E* mutant also conferred a statistically significant increase in the level of Sup35 (eRF3) termination factor, but without an associated increase in the Sup45 (eRF1) termination factor (**Figure 44**). However, it is not known whether the abundance of the termination factors is proportional to their activities (Janzen and Geballe, 2004).

The combined *rps3-K108E tif32-box33* mutant exhibited further reduced a/Tif32 occurrence on pre-TCs which could explain the observed exacerbated readthrough phenotype of this mutant (**Figure 31**) and also supports the notion that eIF3 is needed to promote stop codon readthrough. Besides, it also partially compensated for the increase of the eRF3 levels shown in the *rps3-K108E* single mutant **(Figure 44).**

As a control, the *rps3-N111A* mutant that did not affect the efficiency of termination (**Figure 22**) was subjected to the 80S re-sedimentation assay. In agreement with the readthrough assay, virtually no difference was observed in the composition of *rps3-N111A* pre-TCs (**Figure 45**). This gives further significance to the revealed role of Rps3-K108 and Rps3-R116 in translation termination.

In accordance with the experiments described in previous chapters showing different phenotypes of *rps-R116D* and *rps3-K108E,* the analysis of the composition of *rps-R116D* and *rps3-K108E* pre-termination complexes further underscores the different roles of the structurally neighboring Rps3 residues R116 and K108 on ribosome function.

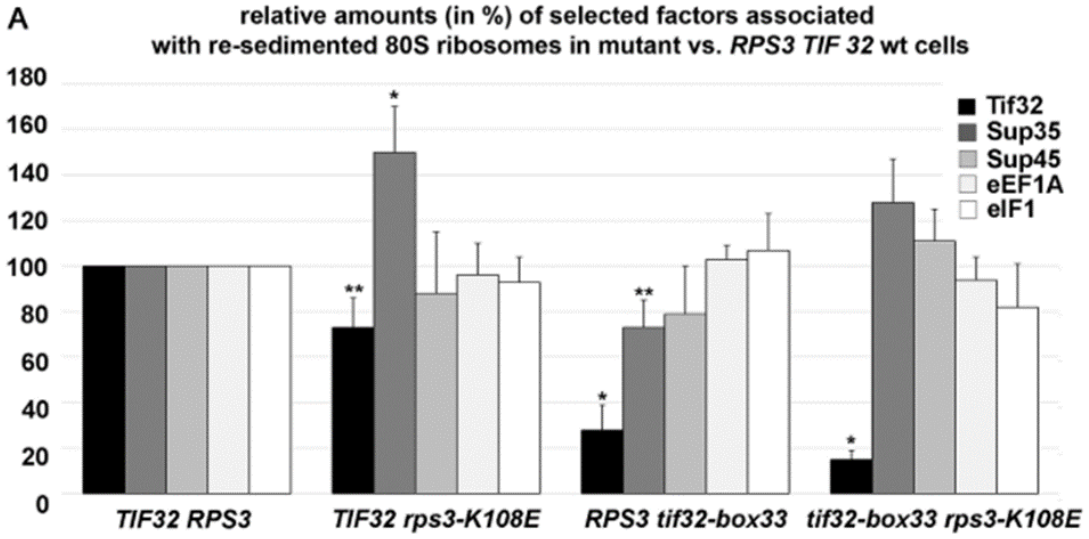

	Rps0A	Tif32	Sup35	Sup45	eEF1A	eIF1
TIF32 rps3-K108E	90±12	73±13 **	150±20 *	88±27	93±11	96±14
RPS3 tif32-box33	86±5	28±11 *	74±12 **	79±21	107±16	103±6
tif32-box33 rps3-K108E	109±20	15±4 *	128±19	111±14	82±19	94±10

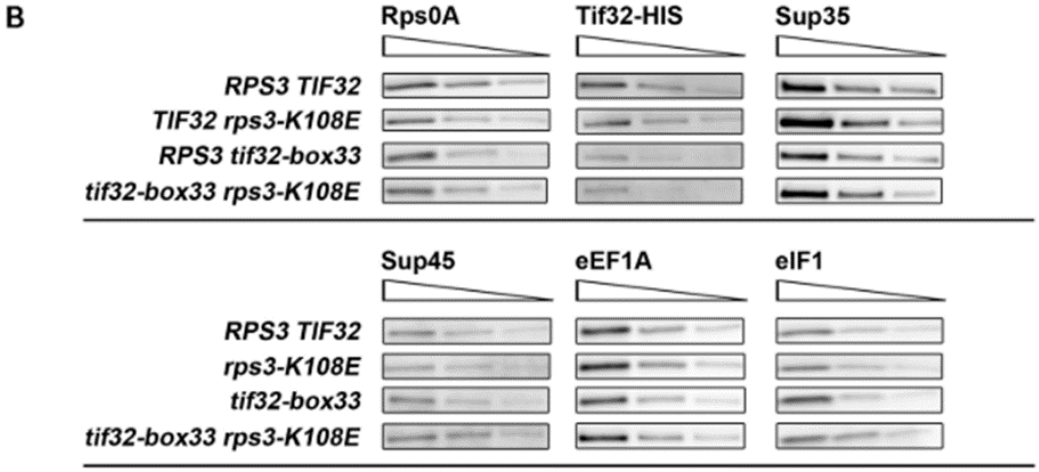

Figure 44 Readthrough-decreasing *rps3-K108E* mutant exhibits a statistically significant increase in the level of eRF3 (Sup35) in heavy polysomes and, at the same time modestly reduces levels of eIF3. All details are the same as in **Figure 43**, except that *rps3-K108E* was analyzed.

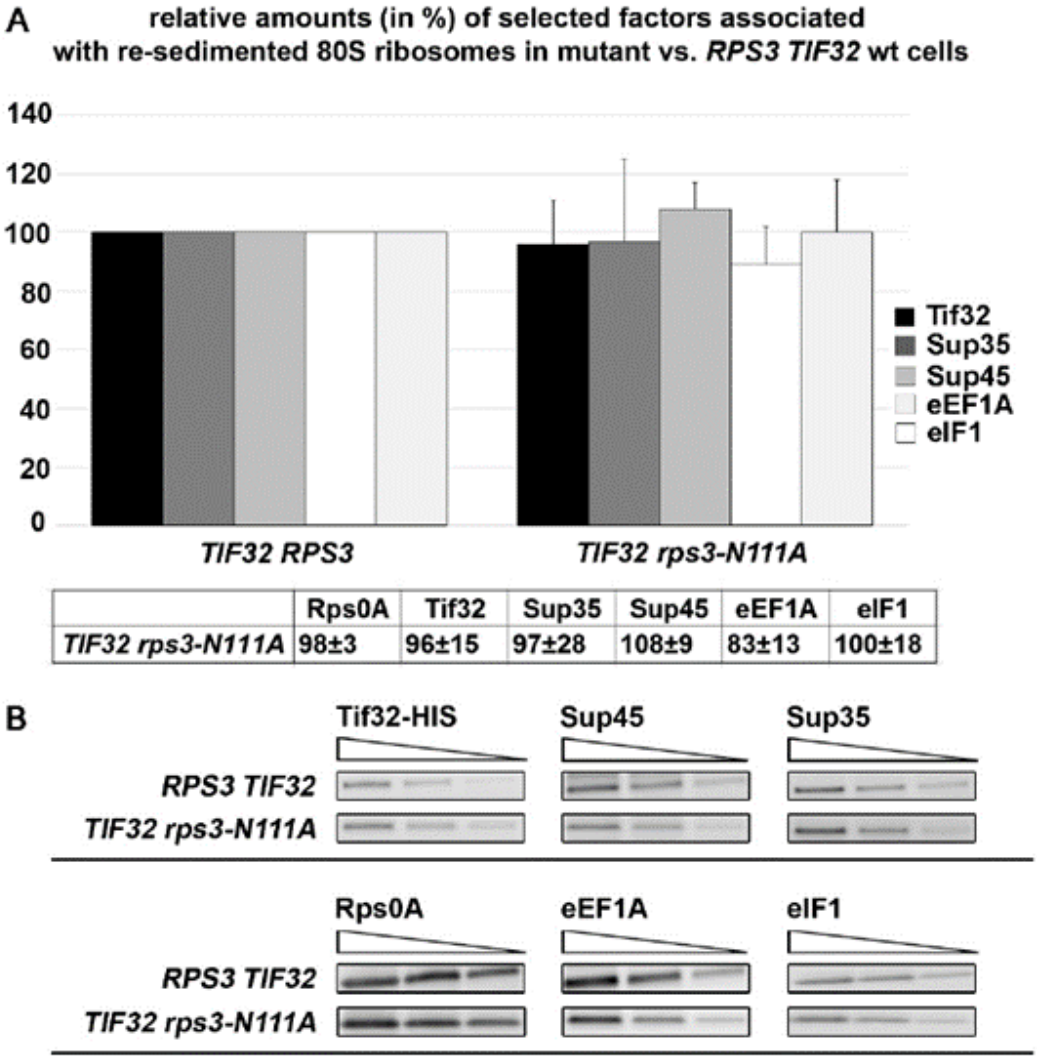

	Rps0A	Tif32	Sup35	Sup45	eEF1A	eIF1
TIF32 rps3-N111A	98±3	96±15	97±28	108±9	83±13	100±18

Figure 45 The *rps3-N111A* mutation does not have any effect on the composition of the pre-termination complexes. (A-B) All details are the same as in **Figure 43**, except that *rps3-N111A* was analyzed**.**

8.5. Investigation of *in vitro* interactions between mammalian eIF3a and Yeast-like–core subunits eIF3i and eIF3g

The YLC subunits in the mammalian eIF3 represent a very compact part of the complex, with b, g, i and C-terminus of eIF3a located in very close proximity **(Figure 10B).** This mutual proximity of those proteins prompted us to revisit current models, where eIF3g was reported only to interact with eIF3b, while eIF3i was reported to contact both, eIF3a (spectrin domain) and eIF3b subunits (Dong et al., 2013).

8.5.1. **Purification of recombinant GST-tagged subunits of eIF3**

The GST-tagged mammalian eIF3g, eIF3i and fragments corresponding to N- and C-halves of eIF3a were prepared and the quality and quantity of their preparation were checked using the same procedure as for yeast GST–tagged proteins described in Section 8.3.1. Representative preparations are illustrated in **Figure 46.** The [^{35}S]-labeled eIF3a, eIF3g and eIF3i were prepared using rabbit reticulocyte lysates.

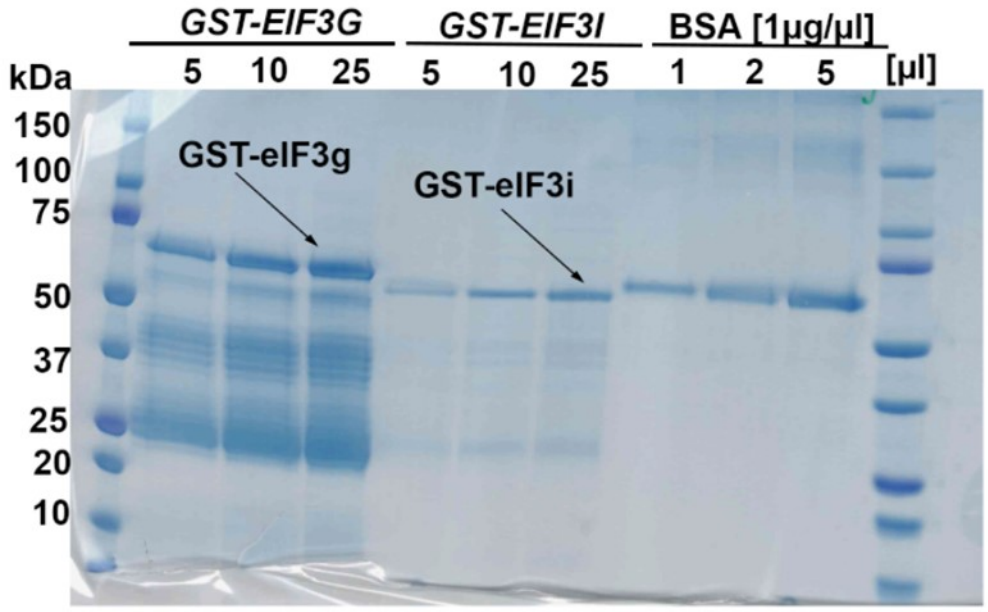

Figure 46 The Coomassie-stained gel showing GST-eIF3g, GST-eIF3i and BSA proteins. Loading amounts of preparations of individual proteins are shown in [µl]. BSA was used as loading control for estimation of corresponding amounts (in [ug]) of purified proteins.

8.5.2. **The eIF3a binds both, eIF3i and g subunits, of the YLC *in vitro*.**

For the examination of mutual interactions between eIF3a and eIF3g as well as eIF3a and eIF3i, both possible settings of the experiments were tested. In the first one, [^{35}S]-labeled full-length eIF3a was tested against GST-fused eIF3g and eIF3i. As can be seen in **Figure 47A,** both subunits were capable of interaction with eIF3a, however, the interaction of GST-eIF3i was very weak. Therefore in the subsequent experiment opposite scenario was investigated – the [^{35}S]-labeled eIF3g and eIF3i were tested against GST-fused N-terminal (aa 1–498) and C-terminal (aa 499–1382) fragments of eIF3a. In this setting, both proteins demonstrated specific interaction with C-terminal half of eIF3a which was even stronger for eIF3i (**Figure 47B**). It is therefore important to emphasize that the here provided inspection of interactions has more qualitative than quantitative character and the differences seen in

different settings of the experiment might arise from different abilities of *in vitro* purified polypeptides to adopt properly folded conformation in case it is needed for efficient interaction.

In conclusion, here presented experiment together with others presented in Hermannova et al. (2019) reveal a web of mutual stabilizing interactions among the human YLC subunits b, g, i and a that qualitatively more resemble a similar web of mutual interactions among the yeast eIF3a-b-c trimeric complex (Herrmannova et al., 2011)

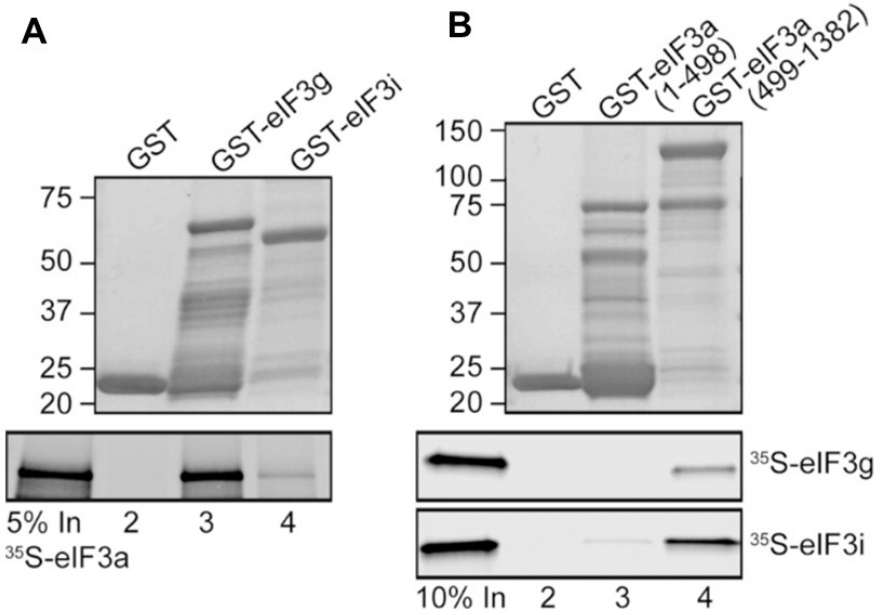

Figure 47 The eIF3a binds both eIF3i and g subunits of the YLC *in vitro*.
(A) The eIF3g (lane 3) and eIF3i (lane 4) subunits fused to GST moiety, and GST alone (lane 2) were tested for binding to [^{35}S]-labeled eIF3a. Lane 1 (In) contains 5 % of input amounts of radiolabeled eIF3a added to reaction mixture. **(B)** The eIF3a N-terminal fragment (aa 1–498) (lane 3) and the eIF3a C-terminal fragment (aa 499–1382) (lane 4) fused to GST moiety, and GST alone (lane 2) were tested for binding to [^{35}S]-labeled eIF3g and eIF3i. Lane 1 (In) contains 10 % of input amounts of radiolabeled eIF3g or eIF3i added to each reaction mixture. Adapted from Herrmannová et al., (2019).

9. Discussion

The main focus of this Thesis was centered on the selection and functional analysis of residues of ribosomal protein Rps3 critically involved in the control of termination codon recognition as well as characterization of their interaction with a/Tif32 subunit of translational initiation factor eIF3 that plays a crucial part in mediating the Rps3 role in termination. In the following chapters, our results will be discussed in a broader translation termination context and possible molecular mechanism of how Rps3 and a/Tif32 collectively operate in the termination process will be proposed.

9.1. Suitability of the use of dual-luciferase assay for measurements of biological phenomena occurring with low frequency

Reporter assays are biological assays routinely used for measurement of the expression levels of genes of interest that can normally be difficult to quantitatively evaluate. Hence, they can be of essential use especially when physiological (or for experimental purposes artificially induced) phenomena under study are occurring at very low frequencies. Defects in the accuracy of stop codon recognition that manifest into an increase (or decrease) of the so-called stop codon readthrough are precisely one such case, as more pronounced changes in RT frequencies would have lethal effects.

For the purpose of this work, all the stop codon readthrough measurements were done using a dual-luciferase assay with the construct shown in **Figure 11**. The constructs encode both *Renilla* and firefly luciferase enzymes separated by a stop codon (*Renilla*-stop-firefly). Therefore, when the stop codon readthrough occurs, all the firefly luciferase activity is obtained from the fused protein product *Renilla*-firefly, whereas *Renilla* activity is measured as a combination of activities from both, the recoded *Renilla*-firefly fusion product (cases of RT events) as well as from product of standard translation without recoding (only *Renilla*, cases of standard termination events). |Because, as already mentioned above, the cases of RT represent rather rare events, the activity measured from sole *Renilla* protein is far more abundant. This was reported to bring bias into the assay because the normalization step of the firefly activity towards *Renilla* activity is needed. However, the *Renilla* activities derived from fused *Renilla*-firefly proteins and *Renilla* proteins alone are not necessarily similar and

also, the sense codon containing control construct derives its activity only from the fused *Renilla*-firefly protein (Loughran et al., 2017). It is, therefore, possible that some especially very weak effects might still be overlooked, as this assay setting is just not sensitive enough to reveal them. The new trend is thus to use reporters with *Renilla* and firefly coding sequences divided by so-called StopGo signals. These are special sequences that allow ribosomes to stop translation at a particular codon ('Stop') and then reinitiate translation again at the subsequent codon ('Go') thus ultimately leading to production of two separate protein products from one mRNA (Donnelly et al., 2001; Atkins et al., 2007). This way the luciferase activities will be always measured from two individual luciferase enzymes irrespective of the RT event. The constructs bearing StopGo sequences were reported to faithfully reflect firefly and *Renilla* activities and avoid artificialities that can confound interpretation of bi-cistronic reporters for studying stop codon readthrough (Loughran et al., 2017).

However, as the here used dual-luciferase system based on the production of fused dual-luciferase protein led to the observations of readthrough phenotypes (both increased and decreased) of the *rps3* and *a/tif32* mutants that were also accompanied by the demonstration of inter-related defects in other assays (such as spot assay, GST-pull downs, 80S re-sedimentation of heavy polysomes, etc.), it is reasonable to say that the role of here investigated Rps3 residues, K108 and R116, as well as of the extreme CTD of a/Tif32 in the regulation of stop codon recognition is well-founded.

9.2. Ribosome function is dependent on the intricate interplay of molecular interactions among rRNA, ribosomal proteins and associated factors

9.2.1. Rps3 and a/Tif32 - mates in translational regulation

The Rps3 and a/Tif32 interactions were examined *in vitro* using GST-pull down experiments. Here, we revealed and described the existence of 4 critical points of contact between these two proteins (please see **Figure 37**, **Figure 38** and **Figure 39**), however, it is likely that the contact area is even wider and other, probably weaker, interactions could be also contributing *in vivo*. In summary, these four contacts include one situated in the N-terminal domain of a/Tif32 and three in its C-terminal domain: one mediated by a/Tif32

extreme C-terminus, one by Rps3-R116 and one by Rps3-K108. For schematic depiction, please see **Figure 48.**

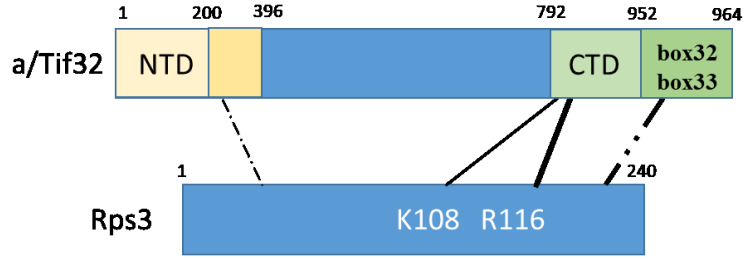

Figure 48 Schematics of binding sites between a/Tif32 and Rps3 proteins revealed by the GST-pull down experiments. The full line indicates mutual interaction of the proteins. The dashed line indicates the fact that the exact location of the contact in the Rps3 protein is unknown. Wider line indicates stronger interaction.

The eIF3 a/Tif32-CTD domain is extremely flexible and so far all attempts for resolving its structure failed. This CTD probably creates a long flexible arm that is frequently moving around the 40S subunit to modulate various translational events. For example, during initiation, the a/Tif32-CTD is able to transpose the b/Prt1-i/Tif34-g/Tif35 module from the solvent-exposed site to the decoding site and back (Valášek et al., 2017; Llácer et al., 2018). It is, therefore, conceivable to imagine that during the termination of translation, when the decoding site is occupied by the release factor complex, the flexible mechanical arm of a/Tif32-CTD moves upwards and makes three independent contacts with Rps3 that together modulate the efficiency of termination.

The fourth binding site between the two partners was revealed to appear in the a/Tif32-NTD (aa residues 200-396). Interestingly, this a/Tif32-NTD segment was also reported to contact *in vitro* the protein Rps0/uS2 that is situated in the close vicinity of Rps3 in the 40S structure (Kouba et al., 2012). The whole a/Tif32-NTD domain (aa residues 1-396) showed strong yeast two-hybrid interactions also with beak protein Rps10/eS10, which in turn contacts Rps3 (Valášek et al., 2003; Graifer et al., 2014). We can only speculate about the functional significance of the contact between the a/Tif32-NTD and the region surrounding Rps3 on the ribosome (see **Figure 4** for the 40S subunit structure with RPs highlighted**).** One interesting idea is that this contact might have a similar role as was already described in initiation during pre-initiation complex assembly. Dong and colleagues showed that Rps3-R116 and R117 residues that contact mRNA bases at the entry channel are important for the stabilization of eIF3 binding (mediated by a/Tif32-NTD) at the mRNA exit channel, too. When the mRNA exit channel was left mRNA unoccupied, the recruitment of the PIC and eIF3 was largely compromised (Dong et al., 2017). We might hypothesize that

similar, probably indirect, stabilization of the contacts between a/Tif32-NTD and Rps3 at the exit mRNA channel is required to allow proper stabilization of the termination complex, too.

9.2.2. **A detailed outline of a possible mechanism of action of Rps3 in stop codon recognition**

Rps3 residues K108 and R116 - so close yet so different

It was intriguing to discover that two Rps3 basic residues, K108 and R116, located in two α-helices running in parallel next to each other, might exhibit such different behaviors. The fact that their charged side chains face different planes and probably contact different functional groups could stand behind the differences that were observed in their mutants: in the composition of the pre-termination complexes *in vivo*, in *in vitro* studies of binding to a/Tif32 as well as in their opposite effects on the efficiency of stop codon recognition. The *rps3-K108E* mutation reduced frequency of readthrough on various stop codons with programmed contexts, showed increased levels of Sup35 (eRF3) and decreased levels of eIF3 in the pre-TCs. However, the levels of the Sup45 factor (eRF1), the one recognizing the stop codon, were not significantly changed. This suggests that the unique increase in the Sup35 protein (relatively mild itself) does not necessarily have to relate to the *rps3-K108E* defects in termination. It might be likewise associated with other functions of the Sup35 protein that have been described (Lyke et al., 2019).

Interestingly, the effect of the *K108E* mutation on the binding of a/Tif32 *in vitro* was negligible. We, therefore, concluded that rather than mere stabilization of binding to eIF3, K108 actively ensures a smooth progression of the termination process (discussed in detail later).

On the contrary, the *rps3-R116D* mutation increased the frequency of stop codon readthrough and analysis of the pre-TCs of this mutant revealed a statistically significant increase of eIF3 and Sup35 and Sup45 release factors compared to the wt yeast cells. Interestingly, *in vitro,* this mutant showed a reduction of the binding affinity towards a/Tif32 subunit. This was surprising at first, but it is important to notice that the ribosome is a very complex structure and loss of the R116 contact with a/Tif32 could lead to the stabilization of some other eIF3-40S contacts and compensate for it. The increased abundance of both release factors in the heavy polysomes suggests, in our opinion, that the rate of the

termination reaction is slower and this then ultimately results in increased stop codon readthrough efficiency.

Finally, when analyzing the effects of *tif32-box33* mutation, we saw a decreased representation of release-factors bound ribosomes and also eIF3 was very underrepresented in this mutant (**Figure 43**). In addition, the binding to Rps3 *in vitro* was very compromised (**Figure 38**). It is very likely that the extreme a/Tif32 C-terminus is responsible for tight anchoring of the eIF3 complex to the Rps3 in pre-TCs. When there is less eIF3 present, it can less efficiently interfere with the Sup45 protein decoding of the stop codon and the termination process is more efficient, faster. This results in decreased stop codon readthrough which was previously also observed in other eIF3 mutants (Beznosková et al., 2013; Beznosková et al., 2015).

Taking into account all the above-mentioned results, it seems possible that contacts mediated by a/Tif32-box32 and box33 regions and Rps3 residues K108 and R116 affect the termination reaction by different means. While the extreme CTD of a/Tif32 most probably mediates its attachment to 80S pre-TCs, the contacts mediated by the R116 and K108 residues of Rps3 are quite probably modulating the termination efficiency (though in different directions) by their involvement in the structural rearrangements of the ribosome that occur during termination (see below).

Could an intrinsic helicase activity of ribosomal protein Rps3 play a role in efficient stop codon recognition?

One of the possible ways of how to explain the observed defects in the efficiency of translation termination of the *rps3* mutants is to suppose that Rps3 has essential additional functions in translation and does not serve as just a structural scaffold for ribosome particles. Such essential function has been already described previously as helicase activity for the 70S bacterial ribosomes. Interestingly, this helicase activity was found to be affected by the conserved basic residues of the entry tunnel-forming proteins uS3 (corresponding to yeast Rps3) and uS4 (corresponding to yeast Rps9), as mutations of these residues markedly slowed down the elongation rate (Takyar et al., 2005). It was therefore proposed that these amino acid residues form a ring around the mRNA in the entry channel and act as a processivity clamp for the ribosomal helicase function, similar to the sliding clamp function during DNA replication. The identified bacterial residues correspond to R116 residue in yeast Rps3 (importantly, this amino acid is conserved throughout the evolution of Rps3),

and additionally, residue corresponding to the yeast Rps3 K108 was also described to influence the helicase activity in bacteria (Graifer et al., 2014).

Even though the intrinsic helicase activity in the 80S eukaryotic ribosome has never been examined so far, it might be possible that the defects either in the unwinding activity of the ribosome or in the ribosome clamping function *per se* are conserved and could stand behind the observed readthrough phenotypes. Because the speed of elongation is profoundly impacted by the secondary structure of the mRNA, encountering such obstacles results naturally in slowing down of the elongation rate. But this is not the case of termination, where its rate is mostly dependent on the rate of assembly and action of the termination complexes on the stalled ribosomes on stop codon. Therefore, termination efficiency should not be influenced by the helicase activity of the ribosome. On the other hand, it is tempting to speculate that the defects in the clamping function (for which functional helicase activity is not needed) might render the ribosomes termination non-productive, which increases the probability of the rti-tRNAs incorporation.

The ribosome latch 'acrobatics'

In the process of initiation, the 40S subunit is known to undergo several structural changes during scanning and subsequent start codon recognition. It was proposed that the binding of initiation factors eIF1 and eIF1A to the 40S subunit triggers conformational changes in the 40S head region and opens the entry channel latch formed by the helices h18 in the body and h34 and the Rps3 in the head region of 40S. The opening of the latch enables the binding of mRNA and consecutive inspection of its codons. During arrest accompanying AUG start codon recognition, the latch is closed again to clamp the 40S subunit on the mRNA to stop scanning (Hinnebusch, 2017). This arresting mechanism is further empowered by a similar constriction mechanism happening at the mRNA exit channel in which ribosomal protein Rps26/eS26 is involved (Marler, 2019). Besides, Rps3 was also found to interact with +6 nucleotide of so-called TISU mRNAs (mRNAs bearing very short UTRs, **T**ranslation **I**nitiator of **S**hort 5' **U**TR) in the 48S complex. Upon transition to elongation-competent 80S complex, this Rps3 (constricting) interaction was switched to another 40S protein, eS10/Rps10, most likely mediating a non-constricting interaction to promote elongation (Haimov et al., 2017). Furthermore, Rps3 was shown to interact with both, the initiation and termination associated factors: in initiation, it contacts eIF1A (Sehrawat et al., 2018) and during termination the N-terminal domain of eRF1 (Sup45 in

yeast) (Taylor et al., 2012). This further suggests that the role of Rps3 in the two processes could be very similar.

From the above-mentioned evidence, it is tempting to speculate that Rps3 is involved in analogous structural re-arrangements at the entry channel also during translational termination and that these rearrangements serve a similar purpose: to clamp the 40S subunit on the mRNA more tightly before peptide release. Indeed, it was already described that the elongation arrest occurring upon stop codon recognition also leads to a latch formation. This time, however, between h16 of the 40S head and Rps3 protein and is accompanied by the mRNA channel constriction (**Figure 49**) (Taylor et al., 2012). In support, this h16-Rps3 bridge also appeared in the ribosomes that were stalled on the mRNA during elongation and bound with the no-go mRNA decay complex factors Dom34 and Hbs1 (Becker et al., 2011).

In the light of obtained results and previously mentioned findings, we propose the following mechanisms for the Rps3 involvement in the fine tunning of termination, which will be described individually for K108 and R116 residues.

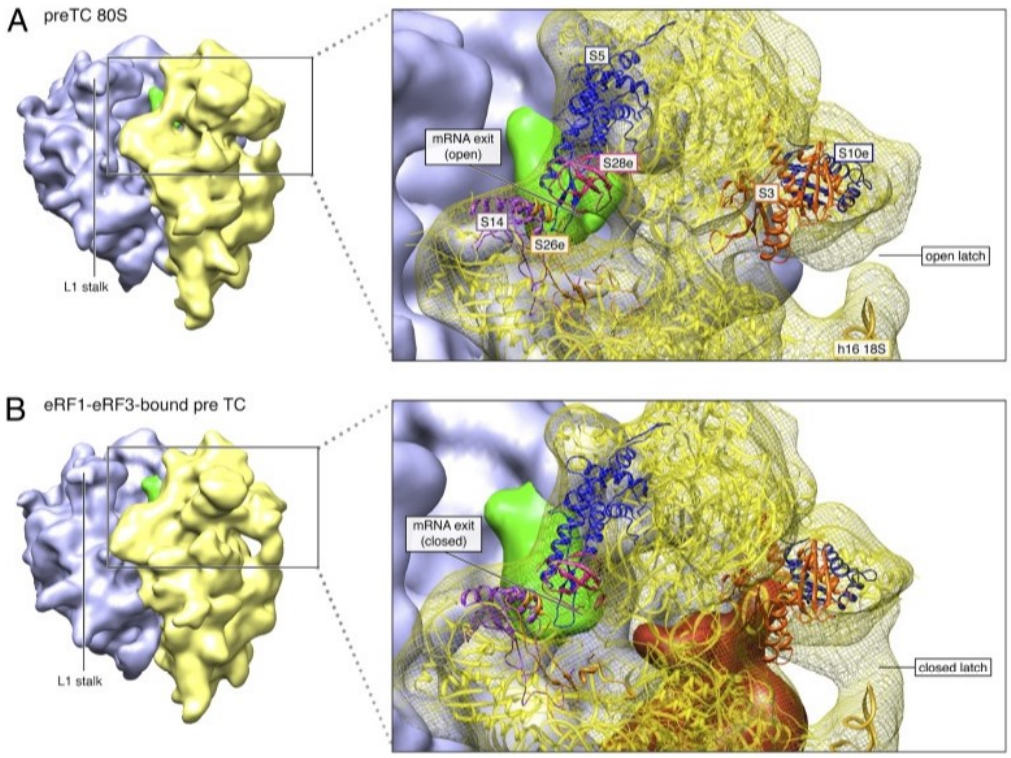

Figure 49 Structural rearrangements within the 80S pre-TC induced upon eRF1–eRF3–GMPPNP binding. Boxed portion of the 40S subunit is shown with yellow mesh for the density and yellow ribbon for the fitted structure. Green map is for P-tRNA and red for eRF1–eRF3**. (A) Cryo-EM map and the MDFF (molecular dynamics flexible fitting) structure of the pre-TC**. **(B) Cryo-EM map and the MDFF structure of 80S–eRF1–eRF3–GMPPNP complex.** The comparison between the two structures reveals significant structural rearrangements in the 80S pre-TC, upon binding of eRF1–eRF3– GMPPNP. Most notable differences occur in the 40S subunit and include the closing of an h16–rpS3 latch at the mRNA entrance and a constriction at the mRNA exit channel, each upon eRF1–eRF3–GMPPNP binding. Adapted from Taylor et al. (2012).

The role of Rps3-K108

The Rps3-K108 residue is probably involved in the timely closing of the termination latch - to boost the termination efficiency when the Sup45 release factor recognizes the stop codon in the A-site. However, on the programmed stop codon contexts, the factor eIF3 interferes with this role and can delay latch closure to promote stop codon readthrough. Upon mutation of K108 to opposite charge E108, functional impairment of the a/Tif32-Rps3 contact occurs and the influence of eIF3 over the latch closure delay is compromised. This means that the latch closes ‘prematurely‘ and readthrough is decreased which was indeed observed **(Figure 22**). In agreement, when the *tif32-box33* and *rps3-K108E* mutations were combined, the readthrough-decreasing phenotype of both single mutants was further exacerbated. Also, the levels of mutated eIF3 on the pre-TCs were further reduced when

compared to individual mutants. The a/Tif32 thus could not delay the latch closure and as a result, the termination was more efficient and the readthrough further dropped.

Strikingly, Wang and colleagues have recently shown that *rps3-K108E* mutation allows ribosomal frameshifting when translating through inhibitory CGA-CGA codons (Wang et al., 2018). In our opinion, the previously mentioned influence of K108 residue over the latch mechanism could also explain this phenomenon – simply, the lysine residue would prevent frameshifting by keeping the ribosome in proper, elongation specific conformation.

Next, we found that the Rps3-K108, but not Rps3-R116 residue interferes with the incorporation of Cys-tRNA and also that it affects the readthrough efficiency in the tetranucleotide specific manner. This was very surprising with respect to two facts: (i.) the R116 residue and not the K108 residue was described to be in close contact with the mRNA bases (Dong et al., 2017) and (ii.) the R116 residue was shown to impact the accuracy of initiation on near cognate start codons (Dong et al., 2017). Nonetheless, we observed similar tetranucleotide-specific effects on termination with few eIF3 mutants too (Beznosková et al., 2013, 2015). We proposed that the eIF3 is involved in altering allosterically the position of the A_{1493} phosphate group in poor-context stop codons. It is, therefore, possible that the sensing of the context for the K108 residue is exerted in co-operation between these two proteins, perhaps *via* h34 of 18S rRNA.This hypothesis was further supported when the frequency of stop codon readthrough was measured in the presence of miscoding agent paromomycin. This antibiotic destabilizes the geometry od the A-site, and the eIF3 stimulatory effect on readthrough was no longer observable upon the treatment (Beznosková et al., 2015). The same effect was observed for the *rps3-K108E*, but not for the *rps3-R116D* mutation.

These results suggest that both, eIF3 and Rps3-K108, can promote readthrough only if the geometry of the decoding center is not perturbed. The Rps3-R116, on the other hand, probably operates in a different manner not dependent on the proper A-site conformation (see further).

The role of Rps3-R116

The *rps3-R116D* mutation was found to increase the frequency of stop codon readthrough (**Figure 26**). In our opinion, the role of the Rps3-R116 residue over the termination mechanism is the following. This residue was earlier shown to contact directly

the mRNA bases downstream of the stop codon (Dong et al., 2017), however, upon mutation to the opposite charge, the electrostatic interaction between negatively charged phosphate backbone of the mRNA and positively charged arginine of Rps3 is lost. This way, the constriction of the mRNA entry channel that we believe accompanies the latch closure (mediated by the K108 residue), can not properly occur. In this situation, the ribosome is locked in a non-productive state, being unable to fully transform through the above proposed structural rearrangements associated with the stop codon recognition. As a result, the efficiency of the termination is lowered, the rti-tRNAs are incorporated at the stop codon, and the readthrough is increased.

Another supporting argument for this hypothesis arises from the study by Dong and colleagues (Dong et al., 2017). They show that *rps3-R116D* mutation destabilizes the closed (entry channel constricted) conformation of the 48S PIC in scanning arrest. As a result, the mutated ribosomes exhibited reduced initiation at suboptimal start codons (e.g. UUG or AUG in poor Kozak context). Overall, this suggests an important role of the Rps3-R116 residue in enhancing initiation accuracy, and our results here uncover its role in maintaining termination accuracy as well. However, it might be also possible that the effects on termination observed in the *rps3-R116D* mutant are rather caused by the increased eIF3 levels on the pre-TCs (**Figure 43**). As noted previously, the eIF3 complex has a stimulatory effect on stop codon readthrough and thus the increase in RT levels might be also attributed to the increased association of this factor with the ribosomes of the mutant. However, the observation that the effect of the Rps3-R116 was not limited only to the stop codons with programmed RT context argues more for the direct involvement of R116 residue in the termination-associated rearrangements of mRNA entry channel.

When the *rps3-R116D* mutation was combined with the *tif32-box33* mutation, the mutation in a/Tif32 relieved the RT stimulatory role of wt eIF3 and nullified the increased readthrough phenotype of *rps3-R116D*. This means that the latch was closed prematurely (a/Tif32-box33 mutant could not interfere with the latch closure mechanism), but the constriction of the mRNA channel could not materialize due to the *rps3-R116D* mutation. The combined mutant also partially corrected the eRFs accumulation phenomenon (**Figure 43**).

Interestingly, a recent study on Rps3 revealed the role of R116 residue also in the so-called no-go decay which deals with the degradation of mRNAs bearing stalled ribosomes. When the charge of the R116 residue was lost, a significant reduction of the accumulated cleavage fragments was observed. The authors suggested two possible reasons strikingly

analogous to ours: either the recruitment of the endonuclease is compromised in the mutant, or, the loss of electrostatic interaction at the mRNA entry channel holds responsible - the mRNA might be more flexible and thus less easily accessible for the cleavage reaction (Simms et al., 2018).

It is therefore clear that this residue possesses a huge impact over the ribosome function - from initiation, elongation (helicase activity so far described only in bacteria) to termination and also ribosome-associated quality-control pathways, which is in agreement with its evolutionary conservation.

10. Final remarks and conclusions

Ribosomes have been viewed for a long time as protein factories involved solely in the automatic production of proteins, without any direct involvement in the translational control. However, this is now beginning to change as new studies describing the precise roles of ribosomal RNAs and proteins in controlling gene expression have begun to emerge. The main goal of my postgraduate studies was to contribute to this effort and bring more insight into: (1) how ribosomal proteins control translation and (2) their interplay with other initiation factors such as eIF3 in the budding yeast *Saccharomyces cerevisiae*. Out of several tested ribosomal proteins, Rps3 was selected because its mutations unambiguously showed the highest impact on translation in assays monitoring translational termination and stop codon readthrough. Those findings are part of my first-author publication. In addition, I was also involved in projects aiming to characterize the roles of eIF3 in translational reinitiation and preinitiation complex assembly. These activities resulted in two co-author publications. However, it needs to be emphasized that the submitted thesis almost exclusively focused on ribosomal protein Rps3 and its involvement, together with eIF3, in translational termination and stop codon readthrough.

Specifically, I identified two Rps3 residues, K108 and R116, that lie in neighboring helices in the protein structure and upon mutation to the opposite charge:

i) exhibit an antagonistic effect on the efficiency of stop codon recognition.

ii) reduce the binding of Rps3 protein to the a/Tif32-CTD defined by amino-acid residues 792-964 *in vitro* indicating that the a/Tif32-CTD is a critically important region for their functional interaction.

iii) display different effects on the composition of the pre-termination complexes *in vivo* further highlighting the different mechanism of action of these two residues in the termination reaction.

iv) exhibited a genetic interaction with the mutation in the extreme C-terminal part of the a/Tif32 protein (the box33 region) that manifested as either exacerbation (*rps3-K108E tif32-box33*) or compensation (*rps3-R116D tif32-box33*) of defects in the stop codon recognition as well as in the composition of pre-termination complexes of single mutants. This indicates for functional co-operation between a/Tif32-CTD and Rps3-K108 in one hand and

antagonistic relationship between a/Tif32-CTD and Rps3-R116 on the other hand.

v) only the Rps3-K108E mutant exerted a tetranucleotide-specific impact on stop codon readthrough and also interfered with the ability of some rti-tRNAs to efficiently incorporate into the A-site during the RT process indicating that this residue significantly contributes to the setup of the stop codon decoding rules.

vi) led to the identification of 4 binding sites, in total, between a/Tif32 and Rps3: 3 located in the extreme C-terminus of the a/Tif32 and one in the a/Tif32-NTD.

In the projects dealing with mammalian eIF3 complex we reached these additional conclusions:

vii) both, the eIF3g and eIF3i subunits, individually interact with the C-terminal region of eIF3a indicating the existence of a web of mutually stabilizing interactions among the subunits creating the Yeast–Like-Core of mammalian eIF3.

viii) the uORF1 upstream region of *ATF4* mRNA contains structurally similar REI determinants to those found in yeast *GCN4* mRNA, however, the REI permissiveness of *ATF4* uORF1 depends on eIF3h and not eIF3a subunit of eIF3. This indicates evolutionary conservation of *cis*- and *trans*- REI determinants with divergence in eIF3 subunit-associated REI function connected to the more complex nature of mammalian eIF3.

11. Literature

Adam Ben-Shem, Lasse Jenner, Gulnara Yusupova Marat Yusupov (2010) Crystal Structure of the Eukaryotic Ribosome. *Science* **30:** 1203–1209

Albuquerque Claudio P, Smolka Marcu B, Payne Samuel H, Bafna Vineet, Eng Jimmy, and Zhou Huilin (2008) A multidimensional chromatography technology for in-depth phosphoproteome analysis. *Mol. Cell. Proteomics* **7:** 1389–1396

Alksne Lefa E, Anthony Richard A, Liebman Susan W, and Warner Jonathan R (1993) An accuracy center in the ribosome conserved over 2 billion years. *Proc. Natl. Acad. Sci. U. S. A.* **90:** 9538–9541

Amrani Nadia, Ganesan Robin, Kervestin Stephanie, Mangus David A, Ghosh Shubhendu, and Jacobson Allan (2004) A faux 3′-UTR promotes aberrant termination and triggers nonsense-mediated mRNA decay. *Nature* **432:** 112–118

Arisue Nobuko, Maki Yasushi, Yoshida Hideji, Wada Akira, Sánchez Lidya B, Müller Miklós, and Hashimoto Tetsuo (2004) Comparative analysis of the ribosomal components of the hydrogenosome-containing protist, Trichomonas vaginalis. *J. Mol. Evol.* **59:** 59–71

Armache Jean P, Jarasch Alexander, Anger Andreas M, Villa Elizabeth, Becker Thomas, Bhushan Shashi, Jossinet Fabrice, Habeck Michael, Dindar Gülcin, Franckenberg Sibylle, Marquez Viter, Mielke Thorsten, Thomm Michael, Berninghausen Otto, Beatrix Birgitta, Söding Johannes, Westhof Eric, Wilson Daniel N, and Beckmann Roland (2010) Cryo-EM structure and rRNA model of a translating eukaryotic 80S ribosome at 5.5-Å resolution. *Proc. Natl. Acad. Sci. U. S. A.* **107:** 19748–19753

Asano Katsura, Clayton Jason, Shalev Anath, and Hinnebusch Alan G (2000) A multifactor complex of eukaryotic initiation factors, eIF1, eIF2, eIF3, eIF5, and initiator tRNA(Met) is an important translation initiation intermediate in vivo. *Genes Dev.* **14:** 2534–2546

Atkins John F, Wills Norma M, Loughran Gary, Wu Chih Yu, Parsawar Krishna, Ryan Martin D, Wang Chung Hsiung, and Nelson Chad C (2007) A case for 'StopGo': Reprogramming translation to augment codon meaning of GGN by promoting unconventional termination (Stop) after addition of glycine and then allowing continued translation (Go). *RNA* **13:** 803–810

Ban Nenad, Beckmann Roland, Cate Jamie HD, Dinman Jonathan D, Dragon François, Ellis Steven R, Lafontaine Denis LJ, Lindahl Lasse, Liljas Anders, Lipton Jeffrey M, McAlear Michael A, Moore Peter B, Noller Harry F, Ortega Joaquin, Panse Vikram Govind, Ramakrishnan V, Spahn Christian MT, Steitz Thomas A, Tchorzewski Marek, Tollervey David, Warren Alan J, Williamson James R, Wilson Daniel, Yonath Ada, and Yusupov Marat (2014) A new system for naming ribosomal proteins. *Curr. Opin. Struct. Biol.* **24:** 165–9

Becker Thomas, Armache Jean P, Jarasch Alexander, Anger Andreas M, Villa Elizabeth, Sieber Heidemarie, Motaal Basma Abdel, Mielke Thorsten, Berninghausen Otto, and Beckmann Roland (2011) Structure of the no-go mRNA decay complex Dom34-Hbs1 bound to a stalled 80S ribosome. *Nat. Struct. Mol. Biol.* **18:** 715–720

Beier Hildburg (2001) Misreading of termination codons in eukaryotes by natural nonsense suppressor tRNAs. *Nucleic Acids Res.* **29:** 4767–4782

Bellotti Anita Sofia, Andreoli Luca, Ronchi Dario, Bresolin Nereo, Comi Giacomo P, and Corti Stefania (2019) Molecular Approaches for the Treatment of Pompe Disease. *Mol. Neurobiol.* ***57*:**1259-1280

Beznosková Petra, Cuchalová Lucie, Wagner Susan, Shoemaker Christopher J, Gunišová Stanislava, von der Haar Tobias, and Valášek Leoš S (2013b) Translation Initiation Factors eIF3 and HCR1 Control Translation Termination and Stop Codon Read-Through in Yeast Cells. *PLoS Genet.* **9:** e1003962

Beznosková Petra, Gunišová Stanislava, and Valášek Leoš S (2016) Rules of UGA-N decoding by near-cognate tRNAs and analysis of readthrough on short uORFs in yeast. *RNA* **22:** 456–66

Beznosková Petra, Pavlíková Zuzana, Zeman Jakub, Echeverría Aitken Colin, and Valášek Leoš S (2019) Yeast applied readthrough inducing system (YARIS): an *in vivo* assay for the comprehensive study of translational readthrough. *Nucleic Acids Res.* **47:** 6339–6350

Beznosková Petra, Wagner Susan, Jansen Myrte Esmeralda, von der Haar Tobias, and Valášek Leoš S (2015) Translation initiation factor eIF3 promotes programmed stop codon readthrough. *Nucleic Acids Res.* **43:** 5099–111

Bidou Laure, Allamand Valérie, Rousset Jean Pierre, and Namy Olivier (2012) Sense from nonsense: Therapies for premature stop codon diseases. *Trends Mol. Med.* **18:** 679–688

Blanchet Sandra, Cornu David, Argentini Manuela, and Namy Olivier (2014) New insights into the incorporation of natural suppressor tRNAs at stop codons in Saccharomyces cerevisiae. *Nucleic Acids Res.* **42:** 10061–10072

Britten Roy J, and Roberts Richard B (1960) High-resolution density gradient sedimentation analysis. *Science.* **131:** 32–33

Brown Alan, Shao Sichen, Murray Jason, Hegde Ramanujan S, and Ramakrishnan Ventrakraman (2015) Structural basis for stop codon recognition in eukaryotes. *Nature* **524:** 493–496

Buchan J Ross, Muhlrad Denise, and Parker Roy (2008) P bodies promote stress granule assembly in Saccharomyces cerevisiae. *J. Cell Biol.* **183:** 441–455

Bulygin Konstantin N, Graifer Dmitri M, Hountondji Codjo, Frolova Ludmila Y, and Karpova Galina (2017) Exploring contacts of eRF1 with the 3′-terminus of the P site tRNA and mRNA stop signal in the human ribosome at various translation termination steps. *Biochim. Biophys. Acta - Gene Regul. Mech.* **1860:** 782–793

Carnes Jason, Jacobson Marty, Leinwand Leslie, and Yarus Michael (2003) Stop codon suppression via inhibition of eRF1 expression. *RNA* **9:** 648–653

Cate Jamie HD (2017) Human eIF3: From 'blobology' to biological insight. *Philos. Trans. R. Soc. B Biol. Sci.* **372:** 20160176.

Chao Fu Chuan, and Schachman Howard K (1956) The isolation and characterization of a macromolecular ribonucleoprotein from yeast. *Arch. Biochem. Biophys.* **61:** 220–230

Chauvin Céline, Salhi Samia, Le Goff Catherine, Viranaicken Wildriss, Diop Dialo, and Jean Olivier (2005) Involvement of human release factors eRF3a and eRF3b in translation termination and regulation of the termination complex formation. *Mol. Cell. Biol.* **25:** 5801–11

Chew Guo Liang, Pauli Andrea, and Schier Alexander F (2016) Conservation of uORF repressiveness and sequence features in mouse, human and zebrafish. *Nat. Commun.* **7:** 1–10

Chiu Wen-Ling, Wagner Susan, Herrmannová Anna, Burela Laxminarayana, Zhang Fan, Saini Adesh K, Valášek Leoš, and Hinnebusch Alan G (2010) The C-terminal region of eukaryotic translation initiation factor 3a (eIF3a) promotes mRNA recruitment, scanning, and, together with eIF3j and the eIF3b RNA recognition motif, selection of AUG start codons. *Mol. Cell. Biol.* **30:** 4415–34

Cosson Bertrand, Couturier Anne, Chabelskaya Svetlana, Kiktev Denis, Inge-Vechtomov S, Philippe Michel, and Zhouravleva Galina (2002) Poly(A)-Binding Protein Acts in Translation Termination via Eukaryotic Release Factor 3 Interaction and Does Not Influence [PSI+] Propagation. *Mol. Cell. Biol.* **22:** 3301–3315

Cridge Andrew G, Crowe-Mcauliffe Caillan, Mathew Suneeth F, and Tate Warren P (2018) Eukaryotic translational termination efficiency is influenced by the 3′ nucleotides within the ribosomal mRNA channel. *Nucleic Acids Res.* **46:** 1927–1944

Cuchalová Lucie, Kouba Tomáš, Herrmannová Anna, Dányi István, Chiu Wen-Ling, and Valášek Leoš (2010) The RNA recognition motif of eukaryotic translation initiation factor 3g (eIF3g) is required for resumption of scanning of posttermination ribosomes for reinitiation on GCN4 and together with eIF3i stimulates linear scanning. *Mol. Cell. Biol.* **30:** 4671–86

Dabrowski Maciej, Bukowy-Bieryllo Zuzanna, and Zietkiewicz Ewa (2018) Advances in therapeutic use of a drug-stimulated translational readthrough of premature termination codons. *Mol. Med.* **24:**

Damoc Eugen, Fraser Christopher S, Zhou Min, Videler Hortense, Mayeur Greg L, Hershey John WB, Doudna Jennifer A, Robinson Carol V., and Leary Julie A (2007) Structural characterization of the human eukaryotic initiation factor 3 protein complex by mass spectrometry. *Mol. Cell. Proteomics* **6:** 1135–1146

Davies Julian, Gilbert Walter, and Gorini Luigi (1964) Streptomycin, suppression and the code. *Proc. Natl. Acad. Sci. United States* **51:** 883–890

Denisenko Oleg, and Bomsztyk Karol (2002) Yeast hnRNP K-Like Genes Are Involved in Regulation of the Telomeric Position Effect and Telomere Length. *Mol. Cell. Biol.* **22:** 286–297

Dong Jinsheng, Aitken Colin Echeverría, Thakur Anil, Shin Byung-Sik, Lorsch Jon R, and Hinnebusch Alan G (2017) Rps3/uS3 promotes mRNA binding at the 40S ribosome entry channel and stabilizes preinitiation complexes at start codons. *Proc. Natl. Acad. Sci.* **114:** E2126–E2135

Dong Zizheng, Qi Jing, Peng Hui, Liu Jianguo, and Zhang Jian Ting (2013) Spectrin domain of eukaryotic initiation factor 3a is the docking site for formation of the a:b:i:g subcomplex. *J. Biol. Chem.* **288:** 27951–27959

Donnelly Michelle L, Hughes Lorraine E, Luke Garry, Mendoza Heidi, Ten Dam Edwin, Gani David, and Ryan Martin D (2001) The 'cleavage' activities of foot-and-mouth disease virus 2A site-directed mutants and naturally occurring '2A-like' sequences. *J. Gen. Virol.* **82:** 1027–1041

Fang Nancy N, Chan Gerard T, Zhu Mang, Comyn Sophie A, Persaud Avinash, Deshaies Raymond J, Rotin Daniela, Gsponer Joerg, and Mayor Thibault (2014) Rsp5/Nedd4 is the main ubiquitin ligase that targets cytosolic misfolded proteins following heat stress. *Nat. Cell Biol.* **16:** 1227–1237

Ferreira-Cerca Sébastien, Pöll Gisela, Kühn Holger, Neueder Andreas, Jakob Steffen, Tschochner Herbert, and Milkereit Philipp (2007) Analysis of the In Vivo Assembly Pathway of Eukaryotic 40S Ribosomal Proteins. *Mol. Cell* **28:** 446–457

Ferretti Max B, Ghalei Homa, Ward Ethan A, Potts Elizabeth L, and Karbstein Katrin (2017) Rps26 directs mRNA-specific translation by recognition of Kozak sequence elements. *Nat. Struct. Mol. Biol.* **24:** 700–707

Firth Andrew E, and Brierley Ian (2012) Non-canonical translation in RNA viruses. *J. Gen. Virol.* **93:** 1385–1409

Flury Valentin, Restuccia Umberto, Bachi Angela, and Mühlemann Oliver (2014) Characterization of phosphorylation- and RNA-dependent UPF1 interactors by quantitative proteomics. *J. Proteome Res.* **13:** 3038–3053

Fourmy Dominique, Recht Michael I, Blanchard Scott C, and Puglisi Joseph D (1996) Structure of the A site of Escherichia coli 16S ribosomal RNA complexed with an aminoglycoside antibiotic. *Science.* **274:** 1367–1371

Gao Xiaofei, and Hardwidge Philip R (2011) Ribosomal protein S3: A multifunctional target of attaching/effacing bacterial pathogens. *Front. Microbiol.* **2:**137

Genuth Naomi R, and Barna Maria (2018) The Discovery of Ribosome Heterogeneity and Its Implications for Gene Regulation and Organismal Life. *Mol. Cell* **71:** 364–374

Des Georges Amedee, Dhote Vidya, Kuhn Lauriane, Hellen Christopher UT, Pestova Tatyana V., Frank Joachim, and Hashem Yaser (2015) Structure of mammalian eIF3 in the context of the 43S preinitiation complex. *Nature* **525:** 491–495

Gietz R Daniel, and Akio Sugino (1988) New yeast-Escherichia coli shuttle vectors constructed with in vitro mutagenized yeast genes lacking six-base pair restriction sites. *Gene* **74:** 527–534

Graifer Dmitri, Malygin Alexey, Zharkov Dmitry O, and Karpova Galina (2014) Eukaryotic ribosomal protein S3: A constituent of translational machinery and an extraribosomal player in various cellular processes. *Biochimie 77***:**197-205

Grentzmann Guido, Ingram Jennifer A, Kelly Paul J, Gesteland Raymond F, and Atkins John F (1998) A dual-luciferase reporter system for studying recoding signals. *RNA* **4:** 479–486

Grishin Nick V (2001) KH domain: one motif, two folds. *Nucleic Acids Res.* **29:** 638–643

Gruschke Steffi, and Ott Martin (2010) The polypeptide tunnel exit of the mitochondrial ribosome is tailored to meet the specific requirements of the organelle. *BioEssays* **32:** 1050–1057

Gunišová Stanislava, Hronová Vladislava, Mohammad Mahabub P, Hinnebusch Alan G, and Valášek Leoš S (2018) Please do not recycle! Translation reinitiation in microbes and higher eukaryotes. *FEMS Microbiol. Rev.* **42:** 165–192

Gunišova Stanislava, and Valašek Leoš S (2014) Fail-safe mechanism of GCN4 translational control-uORF2 promotes reinitiation by analogous mechanism to uORF1 and thus secures its key role in GCN4 expression. *Nucleic Acids Res.* **42:** 5880-5893.

von der Haar Tobias (2008) A quantitative estimation of the global translational activity in logarithmically growing yeast cells. *BMC Syst. Biol.* **2:**87

Haimov Ora, Sinvani Hadar, Martin Franck, Ulitsky Igor, Emmanuel Rafi, Tamarkin-Ben-Harush Ana, Vardy Assaf, and Dikstein Rivka (2017) Efficient and Accurate Translation Initiation Directed by TISU Involves RPS3 and RPS10e Binding and Differential Eukaryotic Initiation Factor 1A Regulation. *Mol. Cell. Biol.* **37:** e00150-17

Hašek Jiří, Kovařík Pavel, Valášek Leoš, Malínská Kateřina, Schneider J, Kohlwein Sepp D, and Ruis Helmut (2000) Rpg1p, the subunit of the Saccharomyces cerevisiae eIF3 core complex, is a microtubule-interacting protein. *Cell Motil. Cytoskeleton* **45:** 235–246

Hellen Christopher UT (2018) Translation termination and ribosome recycling in eukaryotes. *Cold Spring Harb. Perspect. Biol.* **10:** a032656

Hendrick James L, Wilson Patricia G, Edelman Irving I, Sandbaken Mark G, Ursic Doris, and Culbertson Michael R (2001) Yeast frameshift suppressor mutations in the genes coding for transcription factor Mbf1p and ribosomal protein S3: evidence for autoregulation of S3 synthesis. *Genetics* **157:** 1141–58

Herrmannová Anna, Daujotyte Dalia, Yang Ji-Chun, Cuchalová Lucie, Gorrec Fabrice, Wagner Susan, Danyi Istvan, Lukavský Peter J, and Valášek Leoš S (2011) Structural analysis of an eIF3 subcomplex reveals conserved interactions required for a stable and proper translation pre-initiation complex assembly. *Nucleic Acids Res.* **40:** 2294–311

Herrmannová Anna, Prilepskaja Terezie, Wagner Susan, Šikrová Darina, Zeman Jakub, Poncová Kristýna, and Valášek Leoš S (2019) Adapted formaldehyde gradient cross-linking protocol implicates human eIF3d and eIF3c, k and l subunits in the 43S and 48S pre-initiation complex assembly, respectively. *Nucleic Acids Res.* **48:**1969-1984

Hinnebusch Alan G (2005) Translational regulation of GCN4 and the general amino acid control of yeast. *Annu. Rev. Microbiol.* **59:** 407–50

Hinnebusch Alan G (2017) Structural Insights into the Mechanism of Scanning and Start Codon Recognition in Eukaryotic Translation Initiation. *Trends Biochem. Sci.* **42:** 589–611

Hinnebusch Alan G, Ivanov Ivaylo P, and Sonenberg Nahum (2016) Translational control by 5′-untranslated regions of eukaryotic mRNAs. *Science.* **352:** 1413–1416

Isken Olaf, Kim Yoon Ki, Hosoda Nao, Mayeur Greg L, Hershey John WB, and Maquat Lynne E (2008) Upf1 Phosphorylation Triggers Translational Repression during Nonsense-Mediated mRNA Decay. *Cell* **133:** 314–327

Jackson Richard J, Hellen Christopher UT, and Pestova Tatyana V. (2010) The mechanism of eukaryotic translation initiation and principles of its regulation. *Nat. Rev. Mol. Cell Biol.* **11:** 113–127

James Paula D, Raut Sanj, Rivard Georges E, Poon Man Chiu, Warner Margaret, McKenna Susan, Leggo Jayne, and Lillicrap David (2005) Aminoglycoside suppression of nonsense mutations in severe hemophilia. *Blood* **106:** 3043–3048

Jang Chang Young, Lee Jae Yung, and Kim Joon (2004) RpS3, a DNA repair endonuclease and ribosomal protein, is involved in apoptosis. *FEBS Lett.* **560:** 81–85

Janich Peggy, Arpat Alaaddin Bulak, Castelo-Szekely Violeta, Lopes Maykel, and Gatfield David (2015) Ribosome profiling reveals the rhythmic liver translatome and circadian clock regulation by upstream open reading frames. *Genome Res.* **25:** 1848–1859

Janzen Deanna M, and Geballe Adam P (2004) The effect of eukaryotic release factor depletion on translation termination in human cell lines. *Nucleic Acids Res.* **32:** 4491–4502

Jia Jieshuang, Werkmeister Elisabeth, Gonzalez-Hilarion Sara, Leroy Catherine, Gruenert Dieter C, Lafont Frank, Tulasne David, and Lejeune Fabrice (2017) Premature termination codon readthrough in human cells occurs in novel cytoplasmic foci and requires UPF proteins. *J. Cell Sci.* **130:** 3009–3022

Kar Debaleena, Sellamuthu Karthi, Kumar Sangeetha Devi, and Eswarappa Sandeep M (2019) Induction of translational readthrough across the thalassemia-causing premature stop codon in β-globin-encoding mRNA. *Biochemistry*. **59**:80-84

Karásková Martina, Gunišová Stanislava, Herrmannová Anna, Wagner Susan, Munzarová Vanda, and Valášek Leoš S (2012) Functional Characterization of the Role of the N-terminal Domain of the c/Nip1 Subunit of eIF3 in AUG recognition. *J. Biol. Chem.* **287:** 1–15

Keeling Kim M, and Bedwell David M (2011) Suppression of nonsense mutations as a therapeutic approach to treat genetic diseases. *Wiley Interdiscip. Rev. RNA* **2:** 837–52

Keeling Kim M, Lanier Jessica, Du Ming, Salas-Marco Joe, Gao Lin, Kaenjak-Angeletti Anisa, and Bedwell David M (2004a) Leaky termination at premature stop codons antagonizes nonsense-mediated mRNA decay in S. cerevisiae. *RNA* **10:** 691–703

Keeling Patrick J (2016) Genomics: Evolution of the Genetic Code. *Curr. Biol.* **26:** R851–R853

Khoshnevis Sohail, Gross Thomas, Rotte Carmen, Baierlein Claudia, Ficner Ralf, and Krebber Heike (2010) The iron–sulphur protein RNase L inhibitor functions in translation termination. *EMBO Rep.* **11:** 214–219

Khoshnevis Sohail, Gunišová Stanislava, Vlčková Vladislava, Kouba Tomáš, Neumann Piotr, Beznosková Petra, Ficner Ralf, and Valášek Leoš S (2014) Structural integrity of the PCI domain of eIF3a/TIF32 is required for mRNA recruitment to the 43S pre-initiation complexes. *Nucleic Acids Res.* **42**: 4123–4139

Khoshnevis Sohail, Hauer Florian, Milón Pohl, Stark Holger, and Ficner Ralf (2012) Novel insights into the architecture and protein interaction network of yeast eIF3. *RNA* **18:** 2306–19

Klein Dan J, Moore Peter B, and Steitz Thomas A (2004) The roles of ribosomal proteins in the structure assembly, and evolution of the large ribosomal subunit. *J. Mol. Biol.* **340:** 141–177

Kouba Tomáš, Danyi Istvan, Gunišová Stanislava, Munzarová Vanda, Vlčková Vladislava, Cuchalová Lucie, Neueder Andreas, Milkereit Philipp, and Valášek Leoš S (2012) Small Ribosomal Protein RPS0 Stimulates Translation Initiation by Mediating 40S-Binding of eIF3 via Its Direct Contact with the eIF3a/TIF32 Subunit. *PLoS One* **7:** e40464

Kovařík Pavel, Hašek Jiří, Valášek Leoš, and Ruis Helmut (1998) RPG1: An essential gene of Saccharomyces cerevisiae encoding a 110-kDa protein required for passage through the G1 phase. *Curr. Genet.* **33:** 100–109

Kulkarni Sucheta, Dolezal James M, Wang Huabo, Jackson Laura, Lu Jie, Frodey Brian P, Dosunmu-Ogunbi Atinuke, Li Youjun, Fromherz Marc, Kang Audry, Santana-Santos Lucas, Benos Panayiotis V., and Prochownik Edward V. (2017) Ribosomopathy-like properties of murine and human cancers. *PLoS One* **12:** e0182705

de la Cruz Jesús, Karbstein Katrin, and Woolford John L (2015) Functions of Ribosomal Proteins in Assembly of Eukaryotic Ribosomes In Vivo. *Annu. Rev. Biochem.* **84:** 93–129

Laletina Elena, Graifer Dmitri, Malygin Alexey, Ivanov Anton, Shatsky Ivan, and Karpova Galina (2006) Proteins surrounding hairpin IIIe of the hepatitis C virus internal ribosome entry site on the human 40S ribosomal subunit. *Nucleic Acids Res.* **34:** 2027–2036

Landry Dori M, Hertz Marla I, and Thompson Sunnie R (2009) RPS25 is essential for translation initiation by the Dicistroviridae and hepatitis C viral IRESs. *Genes Dev.* **23:** 2753–2764

Langkjær Rikke B, Cliften Paul F, Johnston Mark, and Piškur Jure (2003) Yeast genome duplication was followed by asynchronous differentiation of duplicated genes. *Nature* **421:** 848–852

Lawless Craig, Pearson Richard D, Selley Julian N, Smirnova Julia B, Grant Christopher M, Ashe Mark P, Pavitt Graham D, and Hubbard Simon J (2009) Upstream sequence elements direct post-transcriptional regulation of gene expression under stress conditions in yeast. *BMC Genomics* **10:7**

Li Zhihua, Lee Insuk, Moradi Emily, Hung Nai Jung, Johnson Arlen W, and Marcotte Edward M (2009) Rational extension of the ribosome biogenesis pathway using network-guided genetics. *PLoS Biol.* **7:** e1000213

Limoncelli Kelly A, Merrikh Christopher N, and Moore Melissa J (2017) ASC1 and RPS3: New actors in 18S nonfunctional rRNA decay. *RNA* **23:** 1946–1960

Llácer Jose L, Hussain Tanweer, Marler Laura, Aitken Colin Echeverría, Thakur Anil, Lorsch Jon R, Hinnebusch Alan G, and Ramakrishnan Ventrakraman (2015) Conformational Differences between Open and Closed States of the Eukaryotic Translation Initiation Complex. *Mol. Cell* **59:** 399–412

Llácer Jose Luis, Hussain Tanweer, Saini Adesh K, Nanda Jagpreet Singh, Kaur Sukhvir, Gordiyenko Yuliya, Kumar Rakesh, Hinnebusch Alan G, Lorsch Jon R, and Ramakrishnan Ventrakraman (2018) Translational initiation factor eIF5 replaces eIF1 on the 40S ribosomal subunit to promote start-codon recognition. *Elife* **7:** e39273

Loughran Gary, Howard Michael T, Firth Andrew E, and Atkins John F (2017) Avoidance of reporter assay distortions from fused dual reporters. *Rna* **23:** 1285–1289

Mager Willem H (1988) Control of ribosomal protein gene expression. *BBA - Gene Struct. Expr.* **949:** 1–15

Marintchev Assen, and Wagner Gerhard (2004) Translation initiation: Structures, mechanisms and evolution. *Q. Rev. Biophys.* **37:** 197–284

Marygold Steven J, Roote John, Reuter Gunter, Lambertsson Andrew, Ashburner Michael, Millburn Gillian H, Harrison Paul M, Yu Zhan, Kenmochi Naoya, Kaufman Thomas C, Leevers Sally J, and Cook Kevin R (2007) The ribosomal protein genes and Minute loci of Drosophila melanogaster. *Genome Biol.* **8:**R216

Matheisl Sarah, Berninghausen Otto, Becker Thomas, and Beckmann Roland (2015) Structure of a human translation termination complex. *Nucleic Acids Res.* **43:** 8615–8626

Melnikov Sergey, Ben-Shem Adam, Garreau De Loubresse Nicolas, Jenner Lasse, Yusupova Gulnara, and Yusupov Marat (2012) One core, two shells: Bacterial and eukaryotic ribosomes. *Nat. Struct. Mol. Biol.* **19:** 560–567

Meskauskas Arturas, Russ Johnathan R, and Dinman Jonathan D (2008) Structure/function analysis of yeast ribosomal protein L2. *Nucleic Acids Res.* **36:** 1826–1835

Mitterer Valentin, Murat Guillaume, Réty Stéphane, Blaud Magali, Delbos Lila, Stanborough Tamsyn, Bergler Helmut, Leulliot Nicolas, Kressler Dieter, and Pertschy Brigitte (2016) Sequential domain assembly of ribosomal protein S3 drives 40S subunit maturation. *Nat. Commun.* **7:** 10336

Mohammad Mahabub P, Munzarová Pondělíčková Vanda, Zeman Jakub, Gunišová Stanislava, and Valášek Leoš S (2017) *In vivo* evidence that eIF3 stays bound to ribosomes elongating and terminating on short upstream ORFs to promote reinitiation. *Nucleic Acids Res.* **45:** 2658-2674

Morris Christelle, Wittmann Jürgen, Jäck Hans Martin, and Jalinot Pierre (2007) Human INT6/eIF3e is required for nonsense-mediated mRNA decay. *EMBO Rep.* **8:** 596–602

Mottagui-Tabar Salim, Björnsson Asgeir, and Isaksson Leif A (1994) The second to last amino acid in the nascent peptide as a codon context determinant. *EMBO J.* **13:** 249–257

Mottagui-Tabar Salim, Tuite Mick F, and Isaksson Leif A (1998) The influence of 5' codon context on translation termination in Saccharomyces cerevisiae. *Eur. J. Biochem.* **257:** 249–54

Munzarová Vanda, Pánek Josef, Gunišová Stanislava, Dányi István, Szamecz Béla, and Valášek Leoš S (2011) Translation reinitiation relies on the interaction between eIF3a/TIF32 and progressively folded cis-acting mRNA elements preceding short uORFs. *PLoS Genet.* **7:** e1002137

Namy Olivier, Hatin Isabelle, and Rousset Jean P (2001) Impact of the six nucleotides downstream of the stop codon on translation termination. *EMBO Rep.* **2:** 787–793

Namy Olivier, Duchateau-Nguyen Guillemette, and Rousset Jean P (2002) Translational readthrough of the PDE2 stop codon modulates cAMP levels in Saccharomyces cerevisiae. *Mol. Microbiol.* **43:** 641–652

Neu-Yilik Gabriele, Raimondeau Etienne, Eliseev Boris, Yeramala Lahari, Amthor Beate, Deniaud Aurélien, Huard Karine, Kerschgens Kathrin, Hentze Matthias W, Schaffitzel Christiane, and Kulozik Andreas E (2017) Dual function of UPF3B in early and late translation termination. *EMBO J.* **36:** 2968–2986

Nguyen Tan-Trung, Stahl Guillaume, Déquard-Chablat Michelle, Contamine Véronique, and Denmat Sylvie Hermann-Le (2020) The eukaryotic ribosomal protein S15/uS19 is involved in fungal development and its C-terminal tail contributes to stop codon recognition. *bioRxiv***:** 2020.02.09.940346

Nonomura Yoshiaki, Blobel Günter, and Sabatini David (1971) Structure of liver ribosomes studied by negative staining. *J. Mol. Biol.* **60:** 303-23.

Obayashi Eiji, Luna Rafael E, Nagata Takashi, Martin-Marcos Pilar, Hiraishi Hiroyuki, Singh Chingakham Ranjit, Erzberger Jan Peter, Zhang Fan, Arthanari Haribabu, Morris Jacob, Pellarin Riccardo, Moore Chelsea, Harmon Ian, Papadopoulos Evangelos, Yoshida Hisashi, Nasr Mahmoud L, Unzai Satoru, Thompson Brytteny, Aube Eric, Hustak Samantha, Stengel Florian, Dagraca Eddie, Ananbandam Asokan, Gao Philip, Urano Takeshi, Hinnebusch Alan G, Wagner Gerhard, and Asano Katsura (2017) Molecular Landscape of the Ribosome Pre-initiation Complex during mRNA Scanning: Structural Role for eIF3c and Its Control by eIF5. *Cell Rep.* **18:** 2651–2663

Palade George E (1955) A small particulate component of the cytoplasm. *J. Biophys. Biochem. Cytol.* **1:** 59–68

Pánek Tomáš, Žihala David, Sokol Martin, Derelle Romain, Klimeš Vladimír, Hradilová Miluše, Zadrobílková Eliška, Susko Edward, Roger Andrew J, Čepička Ivan, and Eliáš Marek (2017) Nuclear genetic codes with a different meaning of the UAG and the UAA codon. *BMC Biol.* **15:** 8

Parenteau Julie, Durand Mathieu, Morin Genevive, Gagnon Jules, Lucier Jean Franois, Wellinger Raymund J, Chabot Benoit, and Elela Sherif Abou (2011) Introns within ribosomal protein genes regulate the production and function of yeast ribosomes. *Cell* **147:** 320–331

Parenteau Julie, Lavoie Mathieu, Catala Mathieu, Malik-Ghulam Mustafa, Gagnon Jules, Abou Sherif, and Correspondence Elela (2015) Preservation of Gene Duplication Increases the Regulatory Spectrum of Ribosomal Protein Genes and Enhances Growth under Stress. *Cell Rep.* **13:** 2516-2526

Passmore Lori A, Schmeing T Martin, Maag David, Applefield Drew J, Acker Michael G, Algire Mikkel AA, Lorsch Jon R, and Ramakrishnan Ventrakraman (2007) The Eukaryotic Translation Initiation Factors eIF1 and eIF1A Induce an Open Conformation of the 40S Ribosome. *Mol. Cell* **26:** 41–50

Peng Junmin, Schwartz Daniel, Elias Joshua E, Thoreen Carson C, Cheng Dongmei, Marsischky Gerald, Roelofs Jeroen, Finley Daniel, and Gygi Steven P (2003) A proteomics approach to understanding protein ubiquitination. *Nat. Biotechnol.* **21:** 921–926

Pertschy Brigitte (2017) When a ribosomal protein grows up - The ribosome assembly path of Rps3. *Microb. Cell* **4:** 140–143

Pestova Tatyana V., and Kolupaeva Victoria G (2002) The roles of individual eukaryotic translation initiation factors in ribosomal scanning and initiation codon selection. *Genes Dev.* **16:** 2906–2922

Pick Elah, Hofmann Kay, and Glickman Michael H (2009) PCI Complexes: Beyond the Proteasome, CSN, and eIF3 Troika. *Mol. Cell* **35:** 260–264

Pisarev Andrey V., Hellen Christopher UT, and Pestova Tatyana V. (2007) Recycling of Eukaryotic Posttermination Ribosomal Complexes. *Cell* **131:** 286–299

Poncová Kristýna, Wagner Susan, Jansen Myrte Esmeralda, Beznosková Petra, Gunišová Stanislava, Herrmannová Anna, Zeman Jakub, Dong Jinsheng, and Valášek Leoš S (2019) uS3/Rps3 controls fidelity of translation termination and programmed stop codon readthrough in co-operation with eIF3. *Nucleic Acids Res.* **47:** 11326–11343

Prokhorova Irina, Altman Roger B, Djumagulov Muminjon, Shrestha Jaya P, Urzhumtsev Alexandre, Ferguson Angelica, Chang Cheng Wei Tom, Yusupov Marat, Blanchard Scott C, Yusupova Gulnara, and Puglisi Joseph D (2017) Aminoglycoside interactions and impacts on the eukaryotic ribosome. *Proc. Natl. Acad. Sci. U. S. A.* **114:** E10899–E10908

Qu Xiaohui, Wen Jin Der, Lancaster Laura, Noller Harry F, Bustamante Carlos, and Tinoco Ignacio (2011) The ribosome uses two active mechanisms to unwind messenger RNA during translation. *Nature* **475:** 118–121

Rabl Julius, Leibundgut Marc, Ataide Sandro F, Haag Andrea, and Ban Nenad (2011) Crystal structure of the eukaryotic 40S ribosomal subunit in complex with initiation factor 1. *Science* **331:** 730–6

Ramakrishnan Ventrakraman, and Moore Peter B (2001) Atomic structures at last: The ribosome in 2000. *Curr. Opin. Struct. Biol.* **11:** 144–154

Riba Andrea, Nanni Noemi Di, Mittal Nitish, Arhné Erik, Schmidt Alexander, and Zavolan Mihaela (2019) Protein synthesis rates and ribosome occupancies reveal determinants of translation elongation rates. *Proc. Natl. Acad. Sci. U. S. A.* **116:** 15023–15032

Rodnina Marina V, Korniy Natalia, Klimova Mariia, Karki Prajwal, Peng Bee-Zen, Senyushkina Tamara, Belardinelli Riccardo, Maracci Cristina, Wohlgemuth Ingo, Samatova Ekaterina, and Peske Frank (2020) Translational recoding: canonical translation mechanisms reinterpreted. *Nucleic Acids Res.* ***48*:**1056-1067

Ruiz-Echevarría Maria J, and Peltz Stuart W (2000) The RNA binding protein Pub1 modulates the stability of transcripts containing upstream open reading frames. *Cell* **101:** 741–51

Salas-Marco Joe, and Bedwell David M (2005) Discrimination between defects in elongation fidelity and termination efficiency provides mechanistic insights into translational readthrough. *J. Mol. Biol.* **348:** 801–815

Schluenzen Frank, Tocilj Ante, Zarivach Raz, Harms Joerg, Gluehmann Marco, Janell Daniela, Bashan Anat, Bartels Heike, Agmon Ilana, Franceschi François, and Yonath Ada (2000) Structure of functionally activated small ribosomal subunit at 3.3 Å resolution. *Cell* **102:** 615–623

Schmidt Christian, Becker Thomas, Heuer André, Braunger Katharina, Shanmuganathan Vivekanandan, Pech Markus, Berninghausen Otto, Wilson Daniel N, and Beckmann Roland (2016) Structure of the hypusinylated eukaryotic translation factor eIF-5A bound to the ribosome. *Nucleic Acids Res.* **44:** 1944–1951

Schueren Fabian, and Thoms Sven (2016) Functional Translational Readthrough: A Systems Biology Perspective. *PLoS Genet.* **12:** e1006196

Schuller Anthony P, Wu Colin Chih-Chien, Dever Thomas E, Buskirk Allen R, and Green Rachel (2017) eIF5A Functions Globally in Translation Elongation and Termination. *Mol Cell* **66:** 194–205

Sehrawat Urmila, Koning Femke, Ashkenazi Shaked, Stelzer Gil, Leshkowitz Dena, and Dikstein Rivka (2018) Cancer-Associated Eukaryotic Translation Initiation Factor 1A Mutants Impair Rps3 and Rps10 Binding and Enhance Scanning of Cell Cycle Genes. *Mol. Cell. Biol.* **39:** e00441-18

Seong Ki Moon, Jung Sang-Oun, Kim Hag Dong, Kim Hee Ju, Jung You-Jin, Choi Soo-Young, and Kim Joon (2012) Yeast ribosomal protein S3 possesses a β-lyase activity on damaged DNA. *FEBS Lett.* **586:** 356–361

Serdar Lucas D, Whiteside Da Juan L, and Baker Kristian E (2016) ATP hydrolysis by UPF1 is required for efficient translation termination at premature stop codons. *Nat. Commun.* **7:** 14021

Sha Zhe, Brill Laurence M, Cabrera Rodrigo, Kleifeld Oded, Scheliga Judith S, Glickman Michael H, Chang Eric C, and Wolf Dieter A (2009) The eIF3 Interactome Reveals the Translasome, a Supercomplex Linking Protein Synthesis and Degradation Machineries. *Mol. Cell* **36:** 141–152

Sikorski Robert S, and Hieter Philip (1989) A system of shuttle vectors and yeast host strains designed for efficient manipulation of DNA in Saccharomyces cerevisiae. *Genetics* **122:** 19–27

Simms Carrie L, Kim Kyusik Q, Yan Liewei L, Qiu Jessica, and Zaher Hani S (2018) Interactions between the mRNA and Rps3/uS3 at the entry tunnel of the ribosomal small subunit are important for no-go decay. *PLOS Genet.* **14:** e1007818

Simoff Ivailo, Moradi Hossein, and Nygärd Odd (2009) Functional characterization of ribosomal protein L15 from Saccharomyces cerevisiae. *Curr. Genet.* **55:** 111–125

Singh Arjun, Ursic Doris, and Davies Julian (1979) Phenotypic suppression and misreading in Saccharomyces cerevisiae [20]. *Nature* **277:** 146–148

Singleton Rachelle S, Liu-Yi Phebee, Formenti Fabio, Ge Wei, Sekirnik Rok, Fischer Roman, Adam Julie, Pollard Patrick J, Wolf Alexander, Thalhammer Armin, Loenarz Christoph, Flashman Emily, Yamamoto Atsushi, Coleman Mathew L, Kessler Benedikt M, Wappner Pablo, Schofield Christopher J, Ratcliffe Peter J, and Cockman Matthew E (2014) OGFOD1 catalyzes prolyl hydroxylation of RPS23 and is involved in translation control and stress granule formation. *Proc. Natl. Acad. Sci. U. S. A.* **111:** 4031–4036

Siomi Haruhiko, Matunis Michael J, Michael W Matthew, and Dreyfuss Gideon (1993) The pre-mRNA binding K protein contains a novel evolutionary conserved motif. *Nucleic Acids Res.* **21:** 1193–1198

Skabkin Maxim A, Skabkina Olga V., Dhote Vidya, Komar Anton A, Hellen Christopher UT, and Pestova Tatyana V. (2010) Activities of Ligatin and MCT-1/DENR in eukaryotic translation initiation and ribosomal recycling. *Genes Dev.* **24:** 1787–1801

Skuzeski James M, Nichols Lindy M, Gesteland Raymond F, and Atkins John F (1991) The signal for a leaky UAG stop codon in several plant viruses includes the two downstream codons. *J. Mol. Biol.* **218:** 365–373

Smith Donald B, and Johnson Kevin S (1988) Single-step purification of polypeptides expressed in Escherichia coli as fusions with glutathione S-transferase. *Gene* **67:** 31–40

Song Haiwei, Mugnier Pierre, Das Amit K, Webb Helen M, Evans David R, Tuite Mick F, Hemmings Brian A, and Barford David (2000) The crystal structure of human eukaryotic release factor eRF1-mechanism of stop codon recognition and peptidyl-tRNA hydrolysis. *Cell* **100:** 311–21

Steel Laura F, and Jacobson Allan (1986) Ribosomal proteins are encoded by single copy genes in Dictyostelium discoideum. *Gene* **41:** 165–172

Steffen Kristan K, McCormick Mark A, Pham Kim M, Mackay Vivian L, Delaney Joe R, Murakami Christopher J, Kaeberlein Matt, and Kennedy Brian K (2012) Ribosome deficiency protects against ER stress in Saccharomyces cerevisiae. *Genetics* **191:** 107–118

Swart Estienne Carl, Serra Valentina, Petroni Giulio, and Nowacki Mariusz (2016) Genetic Codes with No Dedicated Stop Codon: Context-Dependent Translation Termination. *Cell* **166:** 691–702

Szamecz Béla, Rutkai Edit, Cuchalová Lucie, Munzarová Vanda, Herrmannová Anna, Nielsen Klaus H, Burela Laxminarayana, Hinnebusch Alan G, and Valášek Leoš (2008) eIF3a cooperates with sequences 5' of uORF1 to promote resumption of scanning by post-termination ribosomes for reinitiation on GCN4 mRNA. *Genes Dev.* **22:** 2414–25

Szick Kathleen, Springer Mark, and Bailey-Serres Julia (1998) Evolutionary analyses of the 12-kDa acidic ribosomal P-proteins reveal a distinct protein of higher plant ribosomes. *Proc. Natl. Acad. Sci. U. S. A.* **95:** 2378–2383

Takyar Seyedtaghi, Hickerson Robyn P, and Noller Harry F (2005) mRNA helicase activity of the ribosome. *Cell* **120:** 49–58

Taylor Derek, Unbehaun Anett, Li Wen, Das Sanchaita, Lei Jianlin, Liao Hstau Y, Grassucci Robert a, Pestova Tatyana V, and Frank Joachim (2012) Cryo-EM structure of the mammalian eukaryotic release factor eRF1-eRF3-associated termination complex. *Proc. Natl. Acad. Sci.* **109:** 18413–18418

Thompson Mary K, Rojas-Duran Maria F, Gangaramani Paritosh, and Gilbert Wendy V. (2016) The ribosomal protein Asc1/RACK1 is required for efficient translation of short mRNAs. *Elife* **5:** e11154

Tork Sanaa, Hatin Isabelle, Rousset Jean Pierre, and Fabret Céline (2004) The major 5′ determinant in stop codon read-through involves two adjacent adenines. *Nucleic Acids Res.* **32:** 415–421

Urakov Valery N, Mitkevich Olga V, Safenkova Irina V, and Ter-Avanesyan Michael D (2017) Ribosome-bound Pub1 modulates stop codon decoding during translation termination in yeast. *FEBS J.* **284:** 1914–1930

Valášek Leoš, Phan Lon, Schoenfeld Lori W, Valášková Věra, and Hinnebusch Alan G (2001) Related eIF3 subunits TIF32 and HCR1 interact with an RNA recognition motif in PRT1 required for eIF3 integrity and ribosome binding. *EMBO J.* **20:** 891–904

Valášek Leoš, Trachsel Hans, Hašek Jiří, and Ruis Helmut (1998) Rpg1, the Saccharomyces cerevisiae homologue of the largest subunit of mammalian translation initiation factor 3, is required for translational activity. *J. Biol. Chem.* **273:** 21253–21260

Valášek Leoš, Mathew Amy A, Shin Byung-Sik, Nielsen Klaus H, Szamecz Béla, and Hinnebusch Alan G (2003) The yeast eIF3 subunits TIF32/a, NIP1/c, and eIF5 make critical connections with the 40S ribosome in vivo. *Genes Dev.* **17:** 786–799

Valášek Leoš, Nielsen Klaus H, and Hinnebusch Alan G (2002) Direct eIF2-eIF3 contact in the multifactor complex is important for translation initiation in vivo. *EMBO J.* **21:** 5886–5898

Valášek Leoš, Nielsen Klaus H, Zhang Fan, Fekete Christie A, and Hinnebusch Alan G (2004) Interactions of Eukaryotic Translation Initiation Factor 3 (eIF3) Subunit NIP1/c with eIF1 and eIF5 Promote Preinitiation Complex Assembly and Regulate Start Codon Selection. *Mol. Cell. Biol.* **24:** 9437–9455

Valášek Leoš S (2012) 'Ribozoomin'--translation initiation from the perspective of the ribosome-bound eukaryotic initiation factors (eIFs). *Curr. Protein Pept. Sci.* **13:** 305–30

Valášek Leoš S, Zeman Jakub, Wagner Susan, Beznosková Petra, Pavlíková Zuzana, Mohammad Mahabub P Hronová Vladislava, Herrmannová Anna, Hashem Yaser, and Gunišová Stanislava (2017) Survey and summary: Embraced by eIF3: Structural and functional insights into the roles of eIF3 across the translation cycle. *Nucleic Acids Res.* **45:** 10948–10968

Vattem Krishna M, and Wek Ronald C (2004) Reinitiation involving upstream ORFs regulates ATF4 mRNA translation in mammalian cells. *Proc. Natl. Acad. Sci. U. S. A.* **101:** 11269–74

Voth Warren P, Jiang Yi Wei, and Stillman David J (2003) New 'marker swap' plasmids for converting selectable markers on budding yeast gene disruptions and plasmids. *Yeast* **20:** 985–93

Wach Achim, Brachat Arndt, Pöhlmann Rainer, and Philippsen Peter (1994) New heterologous modules for classical or PCR-based gene disruptions in Saccharomyces cerevisiae. *Yeast* **10:** 1793–1808

Wagner Susan, Herrmannová Anna, Malík Radek, Peclinovská Lucie, and Valášek Leoš S (2014) Functional and biochemical characterization of human eukaryotic translation initiation factor 3 in living cells. *Mol. Cell. Biol.* **34:** 3041–52

Wagner Susan, Herrmannová Anna, Šikrová Darina, and Valášek Leoš S (2016) Human eIF3b and eIF3a serve as the nucleation core for the assembly of eIF3 into two interconnected modules: The yeast-like core and the octamer. *Nucleic Acids Res.* **44:** 10772–10788

Wan Fengyi, Anderson D Eric, Barnitz Robert A, Snow Andrew, Bidere Nicolas, Zheng Lixin, Hegde Vijay, Lam Lloyd T, Staudt Louis M, Levens David, Deutsch Walter A, and Lenardo Michael J (2007) Ribosomal Protein S3: A KH Domain Subunit in NF-κB Complexes that Mediates Selective Gene Regulation. *Cell* **131:** 927–939

Wang Jiyu, Zhou Jie, Yang Qidi, and Grayhack Elizabeth J (2018) Multi-protein bridging factor 1(Mbf1), Rps3 and Asc1 prevent stalled ribosomes from frameshifting. *Elife* **7:** e39637

Wang W, Czaplinski K, Rao Y, and Peltz SW (2001) The role of Upf proteins in modulating the translation read-through of nonsense-containing transcripts. *EMBO J.* **20:** 880–90

Warner Jonathan R (1999) The economics of ribosome biosynthesis in yeast. *Trends Biochem. Sci.* **24**: 437-440.

Warner Jonathan R, and Mcintosh Kerri B (2009) Review How Common Are Extraribosomal Functions of Ribosomal Proteins ? *Mol. Cell* **34:** 3–11

Weinert Brian T, Schölz Christian, Wagner Sebastian A, Iesmantavicius Vytautas, Su Dan, Daniel Jeremy A, and Choudhary Chunaram (2013) Lysine succinylation is a frequently occurring modification in prokaryotes and eukaryotes and extensively overlaps with acetylation. *Cell Rep.* **4:** 842–851

Wittenstein Amnon, Caspi Michal, David Yifat, Shorer Yamit, Nadar-Ponniah Prathamesh T, and Rosin-Arbesfeld Rina (2019) Serum starvation enhances nonsense mutation readthrough. *J. Mol. Med.* **12**:1695-1710

Woolford John L, and Baserga Susan J (2013) Ribosome biogenesis in the yeast Saccharomyces cerevisiae. *Genetics* **195:** 643–681

Xue Xiaojiao, Mutyam Venkateshwar, Thakerar Amita, Mobley James, Bridges Robert J, Rowe Steven M, Keeling Kim M, and Bedwell David M (2017) Identification of the amino acids inserted during suppression of CFTR nonsense mutations and determination of their functional consequences. *Hum. Mol. Genet.* **26:** 3116–3129

Young David J, and Guydosh Nicholas R (2019) Hcr1/eIF3j Is a 60S Ribosomal Subunit Recycling Accessory Factor In Vivo. *Cell Rep.* **28:** 39-50

Yusupova Gulnara, and Yusupov Marat (2017) Crystal structure of eukaryotic ribosome and its complexes with inhibitors. *Philos. Trans. R. Soc. B Biol. Sci.* **372:** 1–9

Zeman Jakub, Itoh Yuzuru, Kukačka Zdeněk, Rosůlek Michal, Kavan Daniel, Kouba Tomáš, Jansen Myrte E, Mohammad Mahabub P, Novák Petr, and Valášek Leoš S (2019) Binding of eIF3 in complex with eIF5 and eIF1 to the 40S ribosomal subunit is accompanied by dramatic structural changes. *Nucleic Acids Res.* **47:** 8282–8300

Zhang Yan, Baranov Pavel V., Atkins John F, and Gladyshev Vadim N (2005) Pyrrolysine and selenocysteine use dissimilar decoding strategies. *J. Biol. Chem.* **280:** 20740–20751

Zhou Xiang, Liao Wen Juan, Liao Jun Ming, Liao Peng, and Lu Hua (2015) Ribosomal proteins: Functions beyond the ribosome. *J. Mol. Cell Biol.* **7:** 92–104

Zinoni Franz, Heider Johann, and Böck August (1990) Features of the formate dehydrogenase mRNA necessary for decoding of the UGA codon as selenocysteine. *Proc. Natl. Acad. Sci. U. S. A.* **87:** 4660–4664